An introduction to relativistic hydrodynamics: theory, numerics, and astrophysical applications.

José A. Font

Departamento de Astronomía y Astrofísica

Universitat de València

VII Mexican School on Gravitation and Mathematical Physics

"Relativistic Astrophysics and Numerical Relativity"

Playa del Carmen, Quintana Roo, Mexico
November 26 - December 2, 2006

Outline of the course

- ✓ Part 1: General relativistic hydrodynamics equations.
- ✓ Part 2: GR-MHD equations. Formulations of Einstein's equations.
- ✓ Part 3: Numerical methods for conservation laws.
- ✓ Part 4: Tests and applications in astrophysics.

Some bibliography:

A.M. Anile, "Relativistic fluids and magneto-fluids", Cambridge University Press (1989)

J.M. Ibáñez et al, "Riemann solvers in general relativistic hydrodynamics", Proc. Workshop "Godunov Methods: Theory and Applications", Ed. E.F. Toro, Kluwer Academic/Plenum Publishers, New York (2001)

J.M. Martí & E. Müller, "Numerical hydrodynamics in special relativity", Living Reviews in Relativity (2003) (www.livingreviews.org)

J.A. Font, "Numerical hydrodynamics in general relativity", Living Reviews in Relativity (2003) (www.livingreviews.org)

L. Antón et al, "Numerical 3+1 general relativistic magneto-hydrodynamics: a local characteristic approach" Astrophysical Journal, 637, 296 (2006)

R.J. LeVeque, "Numerical methods for conservation laws", Birkhäuser, Basel (1992)

E.F. Toro, "Riemann solvers and numerical methods for fluid dynamics", Springer Verlag, Berlin (1997)

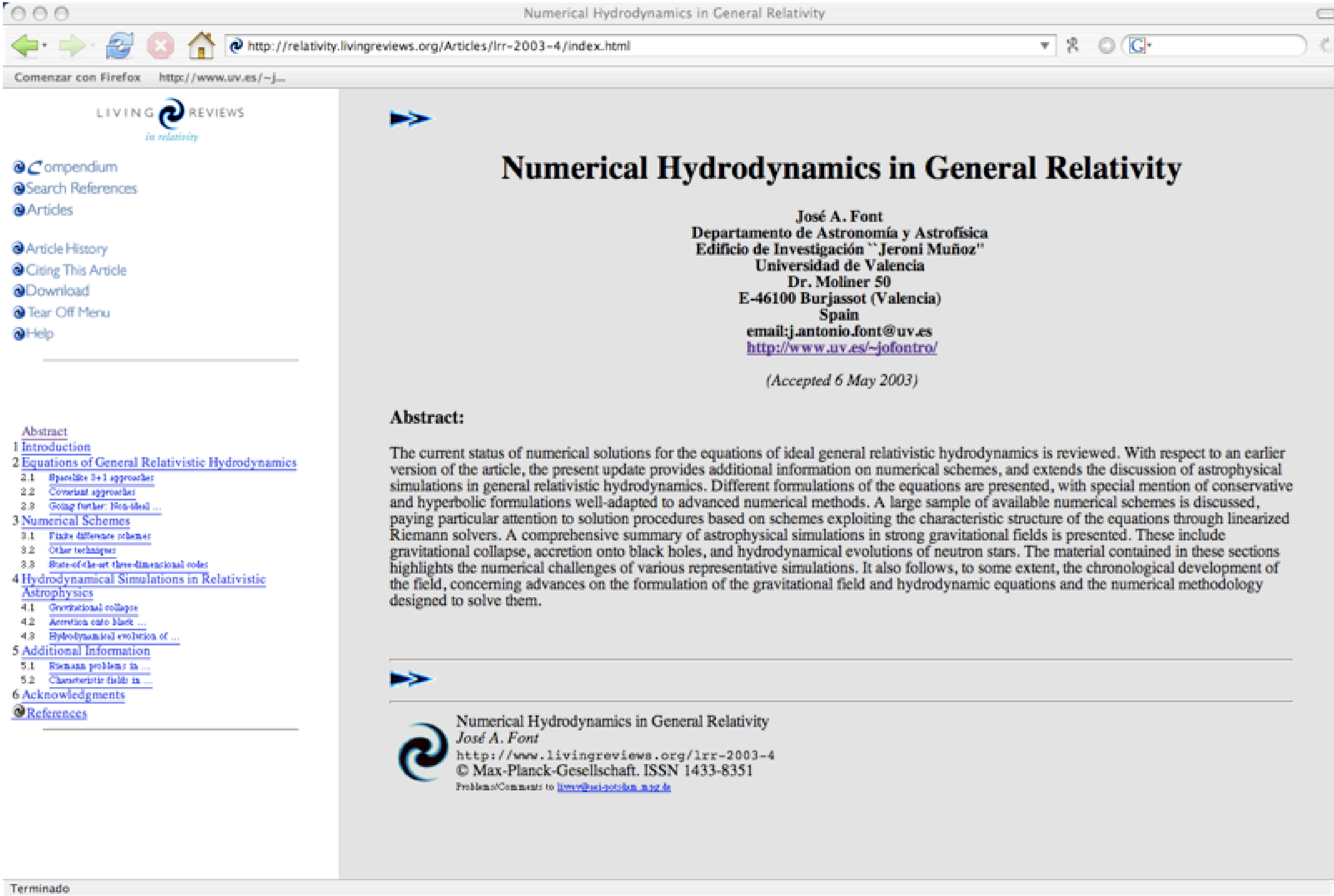

Numerical Hydrodynamics in General Relativity

http://relativity.livingreviews.org/Articles/lrr-2003-4/index.html

Comenzar con Firefox http://www.uv.es/~j...

LIVING REVIEWS in relativity

Compendium
Search References
Articles

Article History
Citing This Article
Download
Tear Off Menu
Help

Numerical Hydrodynamics in General Relativity

José A. Font
Departamento de Astronomía y Astrofísica
Edificio de Investigación ``Jeroni Muñoz''
Universidad de Valencia
Dr. Moliner 50
E-46100 Burjassot (Valencia)
Spain
email:j.antonio.font@uv.es
http://www.uv.es/~jofontro/

(Accepted 6 May 2003)

Abstract:

The current status of numerical solutions for the equations of ideal general relativistic hydrodynamics is reviewed. With respect to an earlier version of the article, the present update provides additional information on numerical schemes, and extends the discussion of astrophysical simulations in general relativistic hydrodynamics. Different formulations of the equations are presented, with special mention of conservative and hyperbolic formulations well-adapted to advanced numerical methods. A large sample of available numerical schemes is discussed, paying particular attention to solution procedures based on schemes exploiting the characteristic structure of the equations through linearized Riemann solvers. A comprehensive summary of astrophysical simulations in strong gravitational fields is presented. These include gravitational collapse, accretion onto black holes, and hydrodynamical evolutions of neutron stars. The material contained in these sections highlights the numerical challenges of various representative simulations. It also follows, to some extent, the chronological development of the field, concerning advances on the formulation of the gravitational field and hydrodynamic equations and the numerical methodology designed to solve them.

Numerical Hydrodynamics in General Relativity
José A. Font
`http://www.livingreviews.org/lrr-2003-4`

Terminado

Part 1
General relativistic hydrodynamics

The natural domain of applicability of general relativistic hydrodynamics (GRHD) and magneto-hydrodynamics (GRMHD) is in the field of relativistic astrophysics.

General relativity and relativistic (magneto-)hydrodynamics play a major role in the description of gravitational collapse leading to the formation of compact objects (neutron stars and black holes):

- Stellar core-collapse supernovae
- Black hole formation (and accretion)
- Coalescing compact binaries
- gamma-ray bursts
- jet formation (black hole plus disk)

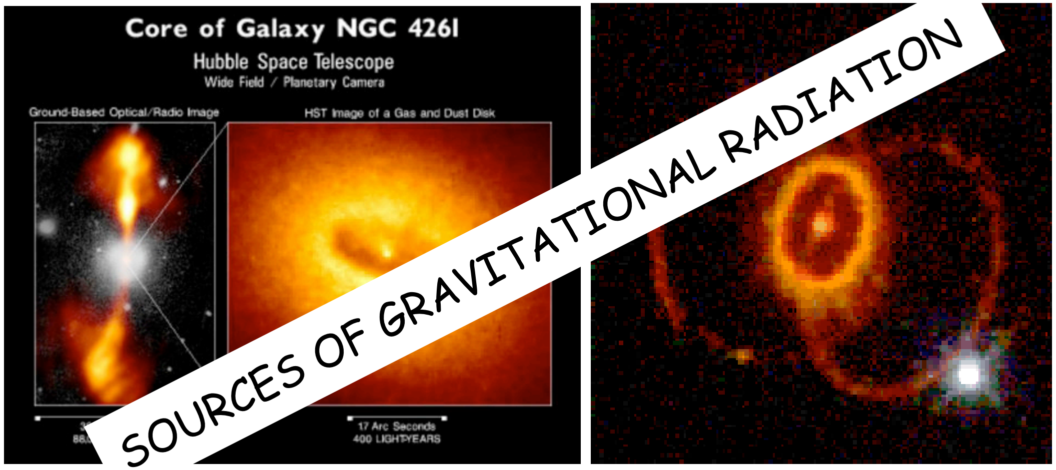

The natural domain of applicability of general relativistic hydrodynamics (GRHD) and magneto-hydrodynamics (GRMHD) is in the field of relativistic astrophysics.

General relativity and relativistic (magneto-)hydrodynamics play a major role in the description of gravitational collapse leading to the formation of compact objects (neutron stars and black holes):

- Stellar core-collapse supernovae
- Black hole formation (and accretion)
- Coalescing compact binaries
- gamma-ray bursts
- jet formation (black hole plus disk)

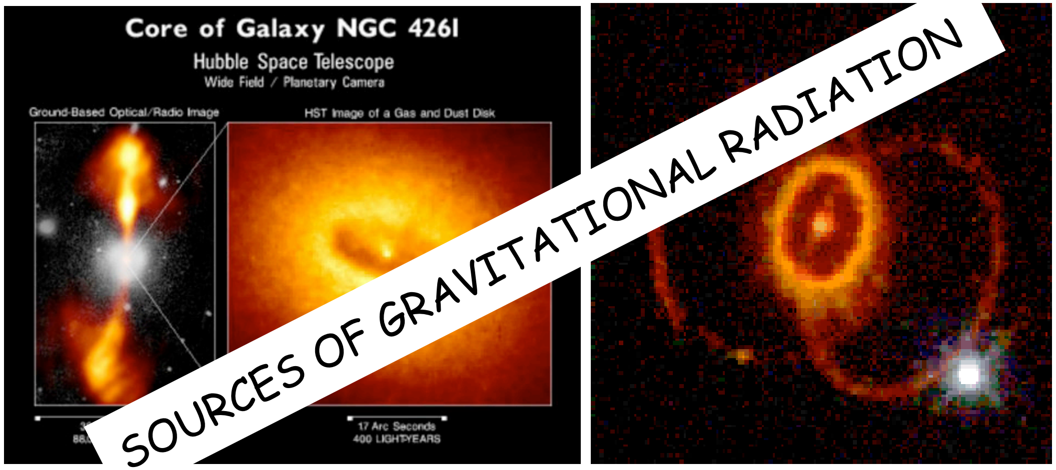

Time-dependent evolutions of fluid flow coupled to the spacetime geometry (Einstein's equations) only possible through accurate, large-scale numerical simulations.

Some scenarios can be described in the test-fluid approximation: GRHD/GRMHD computations in curved backgrounds (highly mature, particularly GRHD case).

The GRHD/GRMHD equations constitute nonlinear hyperbolic systems.

Solid mathematical foundations and accurate numerical methodology imported from CFD. A "preferred" choice: high-resolution shock-capturing schemes written in conservation form.

Motivation: intense work in recent years on formulating/solving the MHD equations in general relativistic spacetimes (either background or dynamical).

Pioneers: Wilson (1975), Sloan & Smarr (1985), Evans & Hawley (1988), Yokosawa (1993)

More recently: Koide et al (1998 …), De Villiers & Hawley (2003 …), Baumgarte & Shapiro (2003), Gammie et al (2003), Komissarov (2005), Duez et al (2005 …), Shibata & Sekiguchi (2005), Antón et al (2006), Neilsen et al (2006). Both, artificial viscosity and HRSC schemes developed.

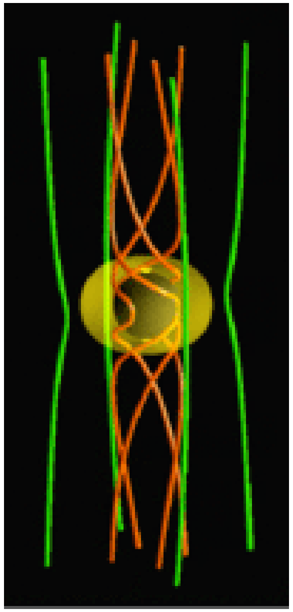

Most of the applications are in the field of black hole accretion and jet formation …

Development of the MRI in a magnetised torus around a Kerr black hole (Gammie, McKinney & Tóth 2003)

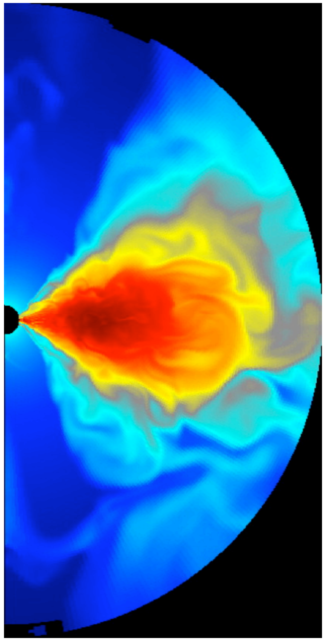

Jet formation: the twisting of magnetic field lines around a Kerr black hole. The yellow surface is the ergosphere (Koide et al 2002)

… many others under way (you name it!)

The number of groups working in special relativistic MHD is even larger: Komissarov; Balsara; Koldoba et al; Del Zanna et al; Leisman et al; …

Exact solution of the SRMHD Riemann problem found recently: Romero et al (2005) – particular case; Giacomazzo & Rezzolla (2005) – general case.

Fluid dynamics: introduction

The defining property of fluids (liquids and gases) lies in the ease with which they may be deformed.

A "simple fluid" may be defined as a material such that the relative positions of its constituent elements change by a large amount when suitable forces, however small in magnitude, are applied to the material.

The properties of solids and fluids are directly related to their molecular structure and to the nature of the forces between the molecules.

For most simple molecules, stable equilibrium between two molecules is achieved when their separation $d_0 \sim 3\text{-}4 \times 10^{-8}$ cm. The average spacing of the molecules in a gaseous phase at normal temperature and pressure is of the order of $10d_0$, while in liquids and solids is of the order of d_0.

Fluid dynamics deals with the behaviour of matter in the large (average quantities per unit volume), on a macroscopic scale large compared with the distance between molecules, $l \gg d_0$, not taking into account the molecular structure of fluids.

Even when considering an infinitesimal volume element it must be assumed that it is much smaller than the dimensions of the fluid, L, but much larger than the distance between molecules, i.e. $L \gg l \gg d_0$.

The macroscopic behaviour of fluids is assumed to be perfectly continuous in structure, and physical quantities such as mass, density, or momentum contained within a given small volume are regarded as uniformly spread over that volume.

Hence, the quantities which characterize a fluid (in the continuum limit) are functions of time and position:

$$\rho \ : \ (t,\vec{r}) \in \mathbb{R}^4 \rightarrow \rho(t,\vec{r}) \in \mathbb{R} \quad \text{density (scalar field)}$$

$$\vec{v} \ : \ (t,\vec{r}) \in \mathbb{R}^4 \rightarrow \vec{v}(t,\vec{r}) \in \mathbb{R}^3 \quad \text{velocity (vector field)}$$

$$\Pi \ : \ (t,\vec{r}) \in \mathbb{R}^4 \rightarrow \Pi(t,\vec{r}) \in \mathbb{R}^9 \quad \text{pressure tensor (tensor field)}$$

Eulerian description: time variation of the fluid properties in a fixed position in space.

Lagrangian description: variation of properties of a “fluid particle” along its motion.

Both descriptions are equivalent: there exists a change of variables between them which is related to the Jacobian of the so-called “flux function” which describes the trajectories of fluid particles.

Transport theorems:

Scalar field: $$\frac{d}{dt}\int_{V_t} f\,dV = \int_{V_t}\left[\frac{\partial f}{\partial t} + \nabla\cdot(f\vec{v})\right]dV, \qquad f = f(t,\vec{r})$$

Vector field: $$\frac{d}{dt}\int_{V_t} \vec{F}\,dV = \int_{V_t}\left[\frac{\partial \vec{F}}{\partial t} + (\vec{v}\cdot\nabla)\vec{F} + \vec{F}(\nabla\cdot\vec{v})\right]dV, \quad \vec{F} = \vec{F}(t,\vec{r})$$

V_t is a volume which moves with the fluid (Lagrangian description; image of V_0 by the difeomorphism given by the flux function).

(Perfect) fluid dynamics: equations (1)

Mass conservation (continuity equation)

Let V_t be a volume which moves with the fluid; its mass is given by:

$$m(V_t) = \int_{V_t} \rho(t,\vec{r})\, dV$$

The principle of conservation of mass enclosed within that volume reads:

$$\frac{d}{dt} m(V_t) = \frac{d}{dt}\int_{V_t} \rho(t,\vec{r})\, dV = 0$$

Applying the so-called transport theorem for the density (scalar field) we get:

$$0 = \frac{d}{dt}\int_{V_t} \rho(t,\vec{r})\, dV = \int_{V_t} \left[\frac{D\rho}{Dt} + \rho(\nabla\cdot\vec{v})\right] dV$$

where the convective derivative is defined as

$$\frac{D}{Dt} \equiv \frac{\partial}{\partial t} + \vec{v}\cdot\nabla$$

Since the above eq. must hold for any volume V_t, we obtain the continuity equation:

$$\frac{D\rho}{Dt} + \rho(\nabla\cdot\vec{v}) = 0 \Rightarrow \frac{D\log\rho}{Dt} = -\Theta \Rightarrow \frac{\partial\rho}{\partial t} + \nabla\cdot(\rho\vec{v}) = 0$$

Corolary:

$$-\frac{\partial}{\partial t}\int_V \rho\, dV = \int_{\partial V} \rho\vec{v}\cdot d\vec{\Sigma}$$

the variation of the mass enclosed in a fixed volume V is equal to the flux of mass across the surface at the boundary of the volume.

Incompressible fluid:

$$\nabla\cdot\vec{v} = 0 \Leftrightarrow \frac{D\rho}{Dt} = 0$$

(Perfect) fluid dynamics: equations (2)

Momentum balance (Euler's equation)

"the variation of momentum of a given portion of fluid is equal to the net force (stresses plus external forces) exerted on it" (Newton's 2nd law):

$$\frac{d}{dt}\int_{V_t} \rho\vec{v}\, dV = -\int_{\partial V_t} p\, d\vec{\Sigma} + \int_{V_t} \vec{G}\, dV = \int_{V_t} [\vec{G} - \nabla p]\, dV$$

Applying the transport theorem on the l.h.s. of the above eq. we get

$$\int_{V_t} \left[\frac{\partial}{\partial t}(\rho\vec{v}) + (\vec{v}\cdot\nabla)(\rho\vec{v}) + \rho\vec{v}(\nabla\cdot\vec{v})\right] dV = \int_{V_t} [\vec{G} - \nabla p]\, dV$$

which must be valid for any volume V_t, hence:

$$\frac{\partial}{\partial t}(\rho\vec{v}) + (\vec{v}\cdot\nabla)(\rho\vec{v}) + \rho\vec{v}(\nabla\cdot\vec{v}) = \vec{G} - \nabla p$$

After some algebra and using the equation of continuity we obtain Euler's equation:

$$\boxed{\rho\frac{D\vec{v}}{Dt} = \vec{G} - \nabla p \Leftrightarrow \rho\vec{a} = \vec{G} - \nabla p}$$

(Perfect) fluid dynamics: equations (3)

Energy conservation

Let E be the total energy of the fluid, sum of its kinetic energy and internal energy:

$$E = E_{\rm K} + E_{\rm int} = \frac{1}{2}\int_{V_t} \rho \vec{v}^2 \, dV + \int_{V_t} \rho\varepsilon \, dV$$

Principle of energy conservation: “the variation in time of the total energy of a portion of fluid is equal to the work done per unit time over the system by the stresses (internal forces) and the external forces”.

$$\frac{dE}{dt} = \frac{d}{dt}\int_{V_t}\left(\frac{1}{2}\rho\vec{v}^2 + \rho\varepsilon\right) dV = -\int_{\partial V_t} p\vec{v}\cdot d\vec{\Sigma} + \int_{V_t} \vec{G}\cdot\vec{v}\, dV$$

After some algebra (transport theorem, divergence theorem) we obtain:

$$\int_{V_t}\left(\frac{\partial}{\partial t}\left(\frac{1}{2}\rho\vec{v}^2 + \rho\varepsilon\right) + \nabla\cdot\left[\left(\frac{1}{2}\rho\vec{v}^2 + \rho\varepsilon + p\right)\vec{v}\right]\right) dV = \int_{V_t} \rho\vec{g}\cdot\vec{v}\, dV \qquad \vec{g} = \frac{\vec{G}}{\rho}$$

which, as must be satisfied for any given volume, implies:

$$\boxed{\frac{\partial}{\partial t}\left(\frac{1}{2}\rho\vec{v}^2 + \rho\varepsilon\right) + \nabla\cdot\left[\left(\frac{1}{2}\rho\vec{v}^2 + \rho\varepsilon + p\right)\vec{v}\right] = \rho\vec{g}\cdot\vec{v}}$$

Fluid dynamics equations as a hyperbolic system of conservation laws

The equations of perfect fluid dynamics are a nonlinear hyperbolic system of conservation laws:

$$\frac{\partial \vec{u}}{\partial t} + \frac{\partial \vec{f}^i}{\partial x^i} = \vec{s}(\vec{u})$$

$$\begin{aligned}
\vec{u} &= (\rho, \rho v^j, e) && \text{state vector} \\
\vec{f}^i &= (\rho v^i . \rho v^i v^i + p\delta^{ij}, (e+p)v^i) && \text{fluxes} \\
\vec{s} &= \left(0, -\rho\frac{\partial \Phi}{\partial x^j} + Q_M^j, -\rho v^i \frac{\partial \Phi}{\partial x^i} + Q_E + v^i Q_M^i\right) && \text{sources}
\end{aligned}$$

$\vec{g}$ is a conservative external force field (e.g. the gravitational field): $\vec{g} = -\vec{\nabla}\Phi$

$$\Delta\Phi = 4\pi G\rho$$

Q_M^i, Q_E are source terms in the momentum and energy equations, respectively, due to coupling between matter and radiation (when transport phenomena are also taken into account).

Hyperbolic equations have finite propagation speed: information can travel with speed at most that given by the largest characteristic curves of the system.

The range of influence of the solution is bounded by the eigenvalues of the Jacobian matrix of the system.

$$A = \frac{\partial \vec{f}^i}{\partial \vec{u}} \Rightarrow \lambda_0 = v_i, \lambda_\pm = v_i \pm c_s$$

A bit on viscous fluids

A perfect fluid can be defined as that for which the force across the surface separating two fluid particles is normal to that surface.

Kinetic theory tells us that the existence of velocity gradients implies the appearance of a force tangent to the surface separating two fluid layers (across which there is molecular difusion).

$$d\vec{F} = -p\,d\vec{\Sigma} \Rightarrow \boxed{d\vec{F} = -\Pi\, d\vec{\Sigma}}$$

where Π is the pressure tensor which depends on the pressure and on the velocity gradients.

$\Pi = p\mathrm{I} - \mathrm{S}$ where S is the **stress tensor** given by:

$$\mathcal{S} = 2\mu\underbrace{\left(D - \frac{1}{3}\Theta\mathbb{I}\right)}_{\text{distortion}} + \xi\Theta\mathbb{I}$$

expansion

shear and bulk viscosities

Using the pressure tensor in the previous derivation of the Euler equation and of the energy equation yields the viscous version of those equations:

$$\rho\frac{D\vec{v}}{Dt} = \vec{G} - \nabla p + \mu\Delta\vec{v} + \left(\xi + \frac{1}{3}\mu\right)\nabla\cdot(\nabla\cdot\vec{v})$$

Navier-Stokes equation

$$\rho\frac{D\left(\frac{1}{2}\vec{v}^2 + \varepsilon\right)}{Dt} = \rho\vec{g}\cdot\vec{v} - \nabla\cdot(p\vec{v}) + \nabla\cdot(\mathcal{S}\cdot\vec{v}) - \nabla\cdot\vec{Q}$$

Energy equation

General relativistic hydrodynamics equations

The general relativistic hydrodynamics equations are obtained from the local conservation laws of the stress-energy tensor, $T^{\mu\nu}$ (the Bianchi identities), and of the matter current density J^μ (the continuity equation):

$$\nabla_\mu(\rho u^\mu) = 0 \qquad \nabla_\mu T^{\mu\nu} = 0$$

Equations of motion

As usual ∇_μ stands for the covariant derivative associated with the four dimensional spacetime metric $g_{\mu\nu}$. The density current is given by $J^\mu=\rho u^\mu$, u^μ representing the fluid 4-velocity and ρ the rest-mass density in a locally inertial reference frame.

The stress-energy tensor for a non-perfect fluid is defined as:

$$T^{\mu\nu} = \rho(1+\varepsilon)u^\mu u^\nu + (p - \mu\Theta)h^{\mu\nu} - 2\xi\sigma^{\mu\nu} + q^\mu u^\nu + q^\nu u^\mu$$

where ε is the rest-frame specific internal energy density of the fluid, p is the pressure, and $h^{\mu\nu}$ is the spatial projection tensor, $h^{\mu\nu}=u^\mu u^\nu+g^{\mu\nu}$.

In addition, μ and ξ are the shear and bulk viscosity coefficients. The expansion, Θ, describing the divergence or convergence of the fluid world lines is defined as $\Theta=\nabla_\mu u^\nu$. The symmetric, trace-free, and spatial shear tensor $\sigma^{\mu\nu}$ is defined by:

$$\sigma^{\mu\nu} = \frac{1}{2}(\nabla_\alpha u^\mu h^{\alpha\nu} + \nabla_\alpha u^\nu h^{\alpha\mu}) - \frac{1}{3}\Theta h^{\mu\nu}$$

Finally q^μ is the energy flux vector.

In the following we will neglect non-adiabatic effects, such as viscosity or heat transfer, assuming the stress-energy tensor to be that of a perfect fluid:

$$T^{\mu\nu} \equiv \rho h u^{\mu} u^{\nu} + p g^{\mu\nu}$$

where we have introduced the relativistic specific enthalpy, h, defined as:

$$h = 1 + \varepsilon + \frac{p}{\rho}$$

Introducing an explicit coordinate chart the previous conservation equations read:

$$\boxed{\begin{aligned} &\frac{\partial}{\partial x^{\mu}}\left(\sqrt{-g}\,\rho u^{\mu}\right) = 0 \\ &\frac{\partial}{\partial x^{\mu}}\left(\sqrt{-g}\,T^{\mu\nu}\right) = \sqrt{-g}\,\Gamma^{\nu}_{\mu\lambda} T^{\mu\lambda} \end{aligned}}$$

where the scalar x^0 represents a foliation of the spacetime with hypersurfaces (coordinatised by x^i). Additionally, $\sqrt{-g}$ is the volume element associated with the 4-metric $g_{\mu\nu}$, with $g=\det(g_{\mu\nu})$, and $\Gamma^{\nu}_{\mu\lambda}$ are the 4-dimensional Christoffel symbols.

The system formed by the equations of motion and the continuity equation must be supplemented with an equation of state (EOS) relating the pressure to some fundamental thermodynamical quantities, e.g.

$$p = p(\rho, \varepsilon)$$

- Ideal fluid EOS: $p = (\Gamma - 1)\rho\varepsilon$
- Polytropic EOS: $p = \kappa \rho^{\Gamma}, \quad \left(\Gamma = 1 + 1/n\right)$

In the "test-fluid" approximation (fluid's self-gravity neglected), the dynamics of the matter fields is fully described by the previous conservation laws and the EOS.

When such approximation does not hold, the previous equations must be solved in conjunction with Einstein's equations for the gravitational field which describe the evolution of a dynamical spacetime:

$$\nabla_\mu(\rho u^\mu) = 0 \qquad [1]$$
$$\nabla_\mu T^{\mu\nu} = 0 \qquad [4]$$
$$p = p(\rho,\varepsilon) \qquad [1]$$

$$R_{\mu\nu} - \frac{1}{2} g_{\mu\nu} R = 8\pi T_{\mu\nu}$$

Einstein's equations

(Newtonian analogy: Euler's equation + Poisson's equation)

The most widely used approach to solve Einstein's equations in Numerical Relativity is the so-called Cauchy or 3+1 formulation (IVP).

Spacetime is foliated with a set of non-intersecting spacelike hypersurfaces Σ. Within each surface distances are measured with the spatial 3-metric γ_{ij}.

There are two kinematical variables which describe the evolution between each hypersurface: the lapse function α, and the shift vector β^i

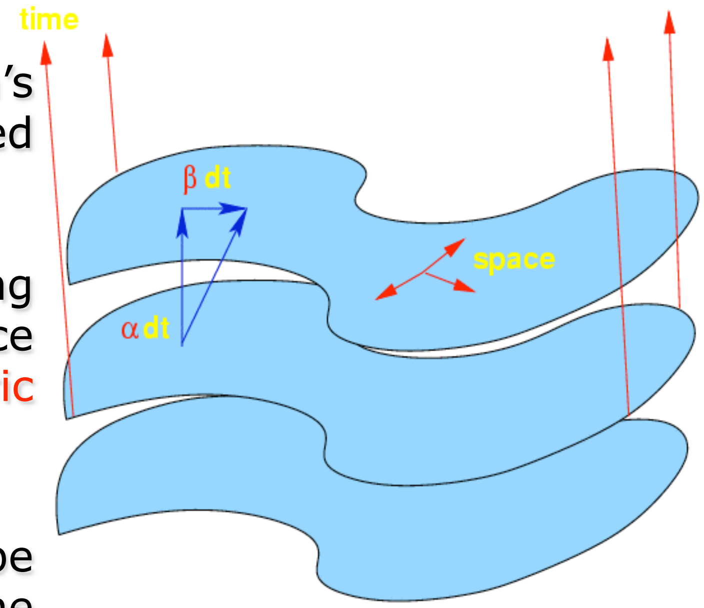

$$ds^2 = -(\alpha^2 - \beta_i\beta^i)dt^2 + 2\beta_i dx^i dt + \gamma_{ij} dx^i dx^j$$

(Numerical) General Relativity: Which portion of spacetime shall we foliate?

(original formulation of the 3+1 equations)

$$\partial_t \gamma_{ij} = -2\alpha K_{ij} + \nabla_i \beta_j + \nabla_j \beta_i$$

$$\partial_t K_{ij} = -\nabla_i \nabla_j \alpha + \alpha\left(R_{ij} + KK_{ij} - 2K_{im}K^m_j\right) + \beta^m \nabla_m K_{ij} + K_{im}\nabla_j \beta^m + K_{jm}\nabla_i \beta^m - 8\pi T_{ij}$$

$$R + K^2 - K_{ij}K^{ij} - 16\pi\alpha^2 T^{00} = 0$$

$$\nabla_i\left(K^{ij} - \gamma^{ij}K\right) - 8\pi S^j = 0$$

Reformulating these equations to achieve numerical stability is one of the arts of numerical relativity.

(Numerical) General Relativity: Which portion of spacetime shall we foliate?

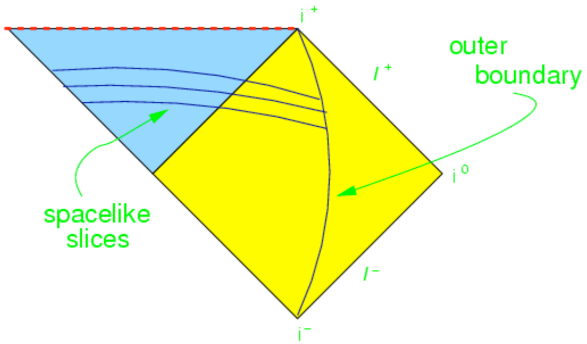

3+1 (Cauchy) formulation

Lichnerowicz (1944); Choquet-Bruhat (1962); Arnowitt, Deser & Misner (1962); York (1979)

Standard choice for most Numerical Relativity groups.
Spatial hypersurfaces have a finite extension.

$$\partial_t \gamma_{ij} = -2\alpha K_{ij} + \nabla_i \beta_j + \nabla_j \beta_i$$

(original formulation of the 3+1 equations)

$$\partial_t K_{ij} = -\nabla_i \nabla_j \alpha + \alpha\left(R_{ij} + K K_{ij} - 2 K_{im} K^m_j\right) + \beta^m \nabla_m K_{ij} + K_{im} \nabla_j \beta^m + K_{jm} \nabla_i \beta^m - 8\pi T_{ij}$$

$$R + K^2 - K_{ij} K^{ij} - 16\pi\alpha^2 T^{00} = 0$$

$$\nabla_i \left(K^{ij} - \gamma^{ij} K\right) - 8\pi S^j = 0$$

Reformulating these equations to achieve numerical stability is one of the arts of numerical relativity.

Conformal formulation: Spatial hypersurfaces have infinite extension (Friedrich et al).

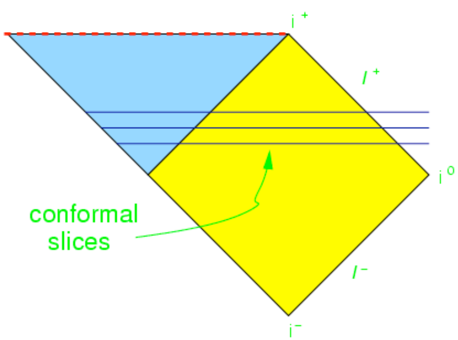

Characteristic formulation (Winicour et al).

Hypersuperfaces are light cones (incoming/outgoing) with infinite extension.

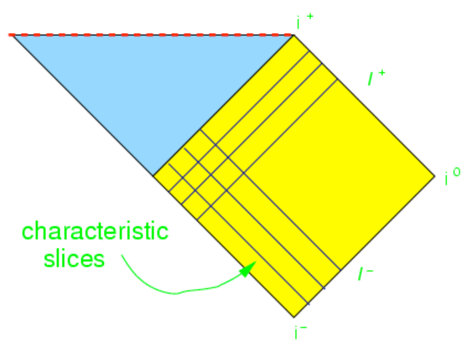

3+1 GR Hydro equations: formulations

$$\nabla_\mu(\rho u^\mu) = 0 \qquad [1]$$
$$\nabla_\mu T^{\mu\nu} = 0 \qquad [4]$$
$$p = p(\rho, \varepsilon) \qquad [1]$$

Equations of motion:

local conservation laws of density current (continuity equation) and stress-energy (Bianchi identities)

$$\frac{\partial}{\partial x^\mu}(\sqrt{-g}\rho u^\mu) = 0$$
$$\frac{\partial}{\partial x^\mu}(\sqrt{-g}T^{\mu\nu}) = \sqrt{-g}\Gamma^\nu_{\mu\lambda}T^{\mu\lambda}$$

Perfect fluid stress-energy tensor

$$T^{\mu\nu} \equiv \rho h u^\mu u^\nu + p g^{\mu\nu}$$

Introducing an explicit coordinate chart:

Different formulations exist depending on:

1. Choice of slicing: level surfaces of x^0 can be spatial (3+1) or null (characteristic)

2. Choice of physical (primitive) variables (ρ, ε, u^i …)

Wilson (1972) wrote the system as a set of advection equation within the 3+1 formalism. Non-conservative.

Conservative formulations well-adapted to numerical methodology are more recent:

- Martí, Ibáñez & Miralles (1991): 1+1, general EOS
- Eulderink & Mellema (1995): covariant, perfect fluid
- Banyuls et al (1997): 3+1, general EOS
- Papadopoulos & Font (2000): covariant, general EOS

Wilson's formulation (1972)

The use of Eulerian coordinates in multidimensional numerical relativistic hydrodynamics started with the seminal work of J. Wilson (1972).

Introducing the basic dynamical variables D, S_μ, and E, i.e. the relativistic density, momenta, and energy, respectively, defined as:

$$D = \rho u^0, \qquad S_\mu = \rho h u_\mu u^0, \qquad E = \rho \varepsilon u^0$$

the equations of motion in Wilson's formulation are:

$$\boxed{\begin{aligned}
&\frac{1}{\sqrt{-g}}\frac{\partial}{\partial x^0}\left(\sqrt{-g}\,D\right)+\frac{1}{\sqrt{-g}}\frac{\partial}{\partial x^i}\left(\sqrt{-g}\,DV^i\right)=0\\
&\frac{1}{\sqrt{-g}}\frac{\partial}{\partial x^0}\left(\sqrt{-g}\,S_\mu\right)+\frac{1}{\sqrt{-g}}\frac{\partial}{\partial x^i}\left(\sqrt{-g}\,S_\mu V^i\right)+\frac{\partial p}{\partial x^\mu}+\frac{1}{2}\frac{\partial g^{\alpha\beta}}{\partial x^\mu}\frac{S_\alpha S_\beta}{S^0}=0\\
&\frac{\partial}{\partial x^0}\left(\sqrt{-g}\,E\right)+\frac{\partial}{\partial x^i}\left(\sqrt{-g}\,EV^i\right)+p\frac{\partial}{\partial x^\mu}\left(\sqrt{-g}\,u^0V^\mu\right)=0
\end{aligned}}$$

with the "transport velocity" given by $V^\mu = u^\mu/u^0$.

Note that the momentum density equation is only solved for the three spatial components, S_i, and S_0 is obtained through the normalization condition $u_\mu u^\mu = -1$.

A direct inspection of the system shows that the equations are written as a coupled set of advection equations.

Conservation of mass:

$$\boxed{\frac{\partial \rho}{\partial t}+\frac{\partial(\rho u)}{\partial x}=0, \quad \text{if } u(x,t)=a \Rightarrow \frac{\partial \rho}{\partial t}+a\frac{\partial \rho}{\partial x}=0}$$

(linear advection eq.)

This approach sidesteps an important guideline for the formulation of nonlinear hyperbolic systems of equations, namely the preservation of their conservation form.

This is a necessary feature to guarantee correct evolution in regions of entropy generation (i.e. shocks). As a result, some amount of numerical dissipation (artificial viscosity) must be used to stabilize the numerical solution across discontinuities.

Wilson's formulation showed some limitations in dealing with situations involving ultrarelativistic flows, as first pointed out by Centrella & Wilson (1984).

Norman & Winkler, in their 1986 paper *"Why ultrarelativistic hydrodynamics is difficult?"* performed a comprehensive numerical study of such formulation in the special relativistic limit.

Relativistic shock reflection

The relativistic shock reflection problem was among the 1D tests considered by Norman & Winkler (1986).

This is a demanding test involving the heating of a cold gas which impacts at relativistic speed with a solid wall creating a shock which propagates off the wall.

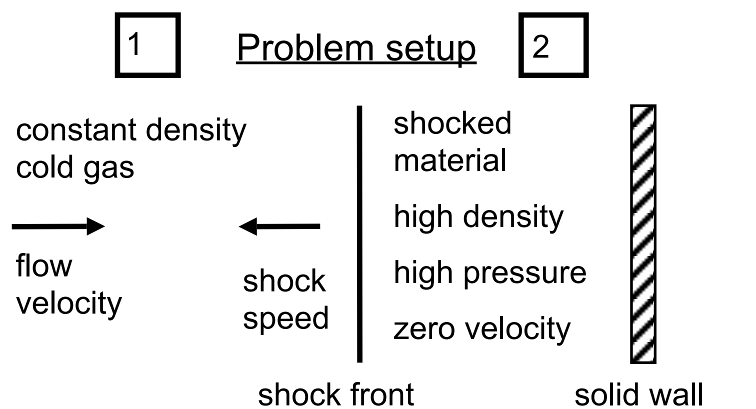

Analytic solution: $\frac{\rho_2}{\rho_1} = \frac{\gamma+1}{\gamma-1} + \frac{\gamma}{\gamma-1}\varepsilon_2, \quad \varepsilon_2 = W_1 - 1$

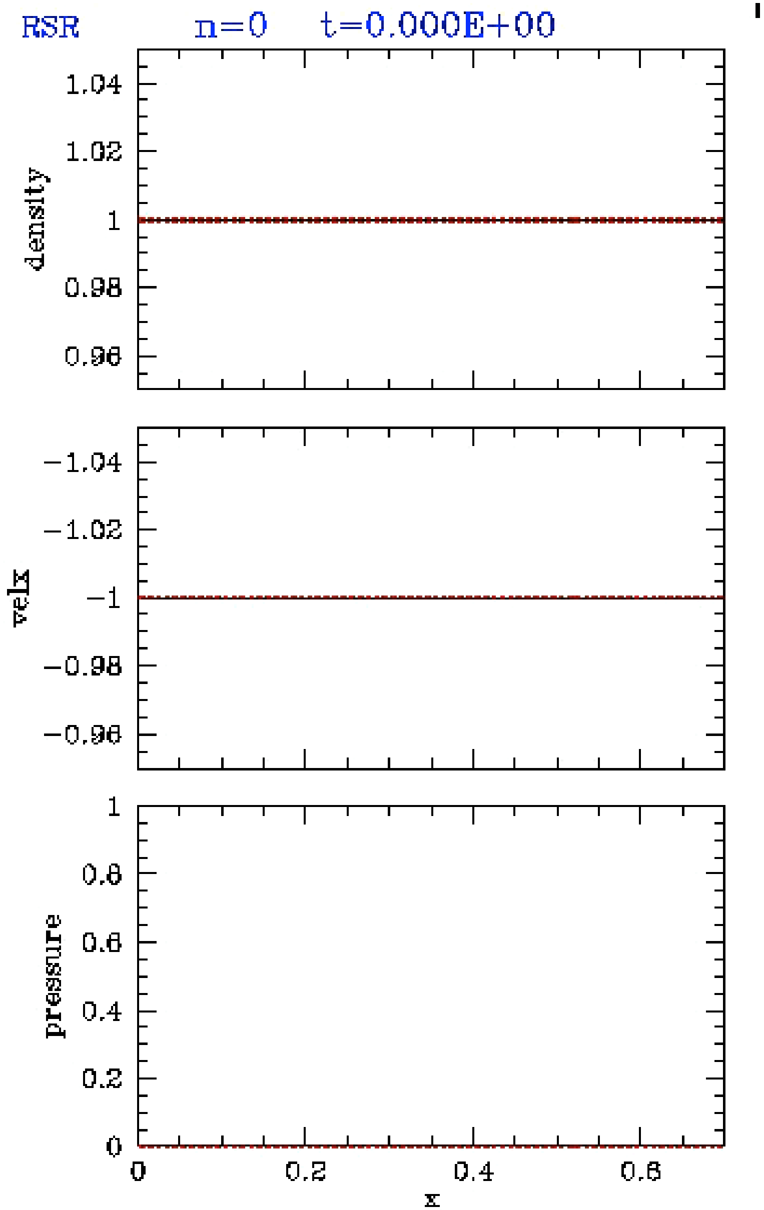

(from Martí & Müller, 2003)

Limitations to handle ultrarelativistic flows (Centrella & Wilson 1984, Norman & Winkler 1986).

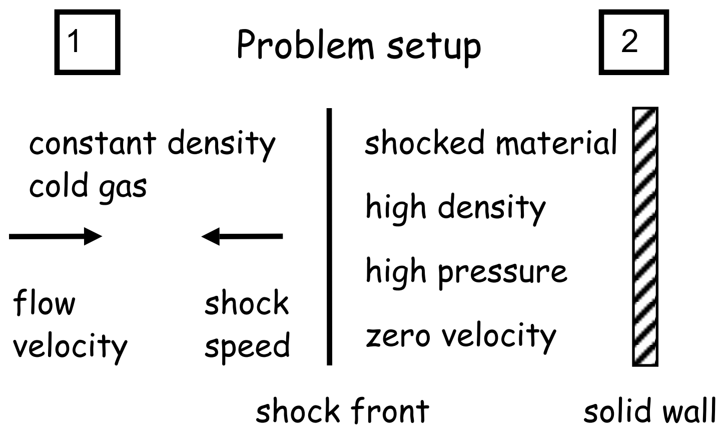

Analytic solution: $\frac{\rho_2}{\rho_1} = \frac{\gamma+1}{\gamma-1} + \frac{\gamma}{\gamma-1}\varepsilon_2, \quad \varepsilon_2 = W_1 - 1$

Relativistic shock reflection test: Relative errors of the numerical solution as a function of the Lorentz factor W of the incoming gas.

For $W \approx 2$ ($v \approx 0.86c$), errors are 5-7% (depending on the adiabatic index of the ideal fluid EOS), showing a linear growth with W.

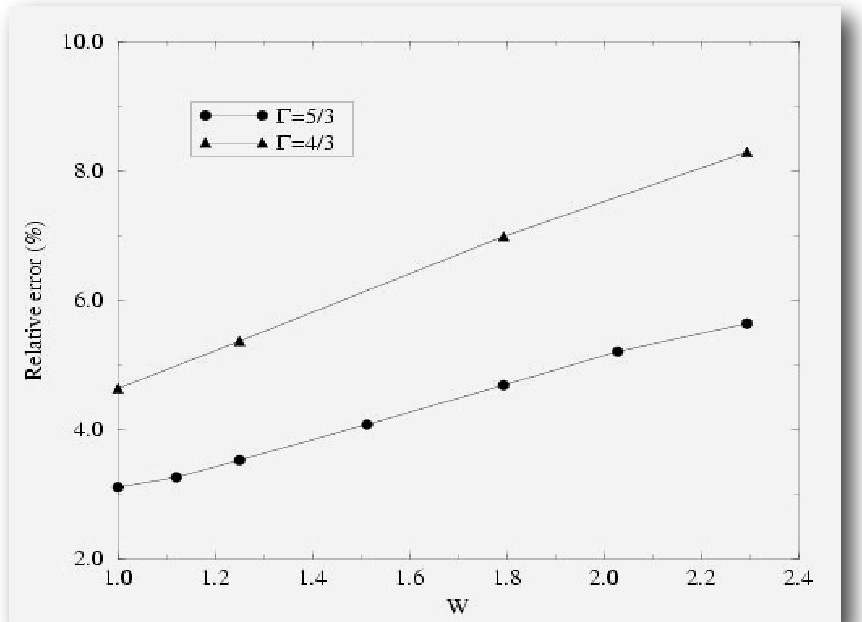

Presence of Lorentz factor in the convective terms of the hydrodynamic equations (and of the pressure in the specific enthalpy) make the relativistic equations much more coupled than their Newtonian counterparts.

Norman & Winkler (1986) proposed the use of implicit schemes to capture more accurately such coupling. Limitation: $W \approx 10$

Ultrarelativistic flows could only be handled (with explicit schemes) once conservative formulations were adopted (Martí, Ibáñez & Miralles 1991; Marquina et al 1992)

Norman & Winkler (1986) concluded that those errors were due to the way in which the artificial viscosity terms Q are included in the numerical scheme in Wilson's formulation.

These terms are added to the pressure terms only in some cases (at the pressure gradient in the source of the momentum equation and at the divergence of the velocity in the source of the energy equation), and not to all terms.

However, Norman & Winkler (1986) proposed to add the viscosity terms Q globally, in order to consider the artificial viscosity as a real viscosity. Hence, the equations of motion should be rewritten for a modified stress-energy tensor of the form:

$$T^{\mu\nu} = \rho\left(1 + \varepsilon + \frac{p+Q}{\rho}\right)u^{\mu}u^{\nu} + (p+Q)g^{\mu\nu}$$

In this way, in flat spacetime, the Euler (momentum) equations take the form:

$$\frac{\partial}{\partial x^0}\left((\rho h + Q)W^2 V_j\right) + \frac{\partial}{\partial x^i}\left((\rho h + Q)W^2 V_j V^i\right) + \frac{\partial (p+Q)}{\partial x^{\mu}} = 0$$

where $W = \alpha u^0$ is the Lorentz factor, α being the lapse function.

In Wilson's formulation Q is omitted in the two terms containing quantity ρh. Q is in general a nonlinear function of the velocity and, hence, the quantity QW^2V in the momentum density equation is a highly nonlinear function of the velocity and its derivatives.

Despite the nonconservative nature of the formulation and the limitations to handle ultrarelativistic flows, Wilson's approach has been widely used by many groups in relativistic astrophysics and numerical relativity along the years, e.g.:

1. Axisymmetric stellar collapse: Wilson 1979, Dykema 1980, Nakamura et al 1980, Nakamura 1981, Nakamura & Sato 1982, Bardeen & Piran 1983, Evans 1984, 1986, Stark & Piran 1985, Piran & Stark 1986, Shibata 2000, Shibata & Shapiro 2002.
2. Instabilities in rotating relativistic stars: Shibata, Baumgarte & Shapiro, 2000.
3. Numerical cosmology: Centrella & Wilson 1983, 1984, Anninos 1998.
4. Accretion on to black holes: Hawley, Smarr & Wilson 1984, Petrich et al 1989, Hawley 1991.
5. Heavy ion collisions (SR limit): Wilson & Mathews 1989.
6. Binary neutron star mergers: Wilson, Mathews & Marronetti 1995, 1996, 2000, Nakamura & Oohara 1998, Shibata 1999, Shibata & Uryu 2000, 2002.
7. GRMHD simulations of BH accretion disks: Yokosawa 1993, 1995, Igumenshchev & Belodorov 1997, De Villiers & Hawley 2003, Hirose et al 2004.

Recently, Anninos & Fragile (2003) have compared state-of-the-art AV schemes and high-order non-oscillatory central schemes using Wilson's formulation and a conservative formulation. Ultrarelativistic flows could only be handled in the latter case.

This highlights the importance of the conservative character of the formulation of the equations to the detriment of the particular numerical scheme employed.

… but this was known long ago …

Conservative formulations - Ibáñez et al (1991, 1997)

Numerically, the hyperbolic and conservative nature of the GRHD equations allows to design a solution procedure based on the characteristic speeds and fields of the system, translating to relativistic hydrodynamics existing tools of CFD.

This procedure departs from earlier approaches, most notably in avoiding the need for artificial dissipation terms to handle discontinuous solutions as well as implicit schemes as proposed by Norman & Winkler (1986).

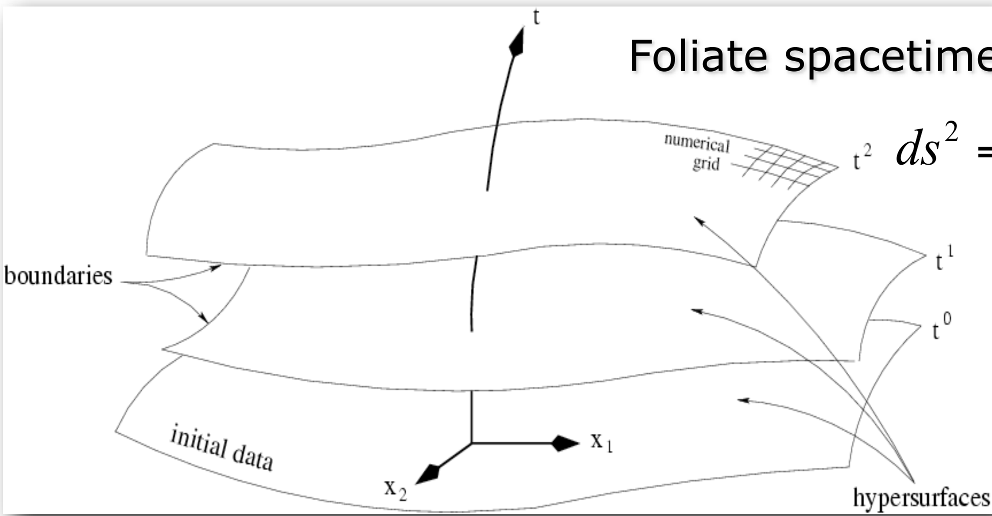

Foliate spacetime with t=const spatial hypersurfaces Σ_t

$$ds^2 = -(\alpha^2 - \beta_i\beta^i)dt^2 + 2\beta_i dx^i dt + \gamma_{ij} dx^i dx^j$$

Let n be the unit timelike 4-vector orthogonal to Σ_t such that

$$n = \frac{1}{\alpha}(\partial_t - \beta^i \partial_i)$$

Eulerian observer: at rest in a given hypersurface, moves from Σ_t to $\Sigma_{t+\Delta t}$ along the normal to the slice:

$$\mathbf{v} = -\frac{\mathbf{n}\cdot\partial_i}{\mathbf{n}\cdot\mathbf{u}} \qquad v^i = \frac{1}{\alpha}\left(\frac{u^i}{u^t} + \beta^i\right)$$

Definitions: u : fluid's 4-velocity, p : isotropic pressure, ρ : rest-mass density

ε : specific internal energy density, $e = \rho(1+\varepsilon)$: energy density

The extension of modern high-resolution shock-capturing (HRSC) schemes from classical fluid dynamics to relativistic hydrodynamics was accomplished in three steps:

1. Casting the GRHD equations as a system of conservation laws.
2. Identifying the suitable vector of unknowns.
3. Building up an approximate Riemann solver (or high-order symmetric scheme).

The associated numerical scheme had to meet a key prerequisite – being written in conservation form, as this automatically guarantees the correct propagation of discontinuities as well as the correct Rankine-Hugoniot (jump) conditions across discontinuities (the shock-capturing property).

In 1991 Martí, Ibáñez, and Miralles presented a new formulation of the general relativistic hydrodynamics equations, in 1+1, aimed at taking advantage of their hyperbolic character.

The corresponding 3+1 extension of the 1991 formulation was presented in Font et al (1994) in special relativity, and in Banyuls et al (1997) in general relativity.

Replace the "primitive variables" in terms of the "conserved variables" :

$$\vec{w} = (\rho, \varepsilon, v^i) \Rightarrow \begin{aligned} D &= \rho W \\ S_j &= \rho h W^2 v_j \\ \tau &= \rho h W^2 - p - D \end{aligned}$$

$$W^2 = \frac{1}{1 - v^j v_j}$$

Lorentz factor

$$h = 1 + \varepsilon + \frac{p}{\rho}$$

specific enthalpy

Conservative formulations well-adapted to numerical methodology:

- Banyuls et al (1997); Font et al (2000): 3+1, general EOS

Hyperbolic system:

$$\frac{1}{\sqrt{-g}}\left(\frac{\partial\sqrt{\gamma}\mathbf{U}}{\partial x^0}+\frac{\partial\sqrt{-g}\mathbf{F}^i}{\partial x^i}\right)=\mathbf{S}$$

$$\begin{aligned}
\mathbf{U} &= (D, S_j, \tau) \\
\mathbf{F}^i &= \left(D\left(v^i-\frac{\beta^i}{\alpha}\right), S_j\left(v^i-\frac{\beta^i}{\alpha}\right)+p\delta^i_j, \tau\left(v^i-\frac{\beta^i}{\alpha}\right)+pv^i\right) \\
\mathbf{S} &= \left(0, T^{\mu\nu}\left(\frac{\partial g_{\nu j}}{\partial x^\mu}-\Gamma^\delta_{\nu\mu}g_{\delta j}\right), \alpha\left(T^{\mu 0}\frac{\partial \ln\alpha}{\partial x^\mu}-T^{\mu\nu}\Gamma^0_{\nu\mu}\right)\right)
\end{aligned}$$

First-order flux-conservative hyperbolic system

$$\begin{aligned}
D &= \rho W \\
S_j &= \rho h W^2 v_j \\
\tau &= \rho h W^2 - p - D
\end{aligned}$$

Solved using HRSC schemes

(either upwind or central)

Recovering special relativistic and Newtonian limits

Full GR

$$\frac{1}{\sqrt{-g}}\left(\frac{\partial\sqrt{\gamma}\rho W}{\partial t}+\frac{\partial\sqrt{-g}\rho W v^i}{\partial x^i}\right)=0$$

$$\frac{1}{\sqrt{-g}}\left(\frac{\partial\sqrt{\gamma}\rho h W^2 v^j}{\partial t}+\frac{\partial\sqrt{-g}(\rho h W^2 v^i v^j+p\delta^{ij})}{\partial x^i}\right)=T^{\mu\nu}\left(\frac{\partial g_{\nu j}}{\partial x^\mu}-\Gamma^{\delta}_{\nu\mu}g_{\delta j}\right)$$

$$\frac{1}{\sqrt{-g}}\left(\frac{\partial\sqrt{\gamma}(\rho h W^2-p-\rho W)}{\partial t}+\frac{\partial\sqrt{-g}(\rho h W^2-\rho W)v^i}{\partial x^i}\right)=\alpha\left(T^{\mu 0}\frac{\partial \ln\alpha}{\partial x^\mu}-T^{\mu\nu}\Gamma^{0}_{\nu\mu}\right)$$

$\Downarrow$

Minkowski

$$\frac{\partial\rho W}{\partial t}+\frac{\partial\rho W v^i}{\partial x^i}=0$$

$$\frac{\partial\rho h W^2 v^j}{\partial t}+\frac{\partial(\rho h W^2 v^i v^j+p\delta^{ij})}{\partial x^i}=0$$

$$\frac{\partial(\rho h W^2-p-\rho W)}{\partial t}+\frac{\partial(\rho h W^2-\rho W)v^i}{\partial x^i}=0$$

Newton

$$\frac{\partial\rho}{\partial t}+\frac{\partial\rho v^i}{\partial x^i}=0$$

$$\frac{\partial\rho v^j}{\partial t}+\frac{\partial(\rho v^i v^j+p\delta^{ij})}{\partial x^i}=0$$

$$\frac{\partial\left(\rho\varepsilon+\frac{1}{2}\rho v^2\right)}{\partial t}+\frac{\partial\left(\rho\varepsilon+\frac{1}{2}\rho v^2+p\right)v^i}{\partial x^i}=0$$

HRSC schemes based on approximate Riemann solvers use the local characteristic structure of the hyperbolic system of equations. For the previous system, this information was presented in Banyuls et al (1997).

The eigenvalues (characteristic speeds) are all real (but not distinct, one showing a threefold degeneracy), and a complete set of right-eigenvectors exists. The above system satisfies, hence, the definition of hiperbolicity.

Eigenvalues (along the x direction)

$$\lambda_0 = \alpha v^x - \beta^x \quad \text{(triple)}$$

$$\lambda_\pm = \frac{\alpha}{1 - v^2 c_s^2}\left\{ v^x(1-c_s^2) \pm c_s\sqrt{(1-v^2)[\gamma^{xx}(1-v^2c_s^2) - v^x v^x(1-c_s^2)]}\right\} - \beta^x$$

Right-eigenvectors

$$\mathbf{r}_{0,1} = \begin{bmatrix} \dfrac{\mathcal{K}}{hW} \\ v_x \\ v_y \\ v_z \\ 1 - \dfrac{\mathcal{K}}{hW} \end{bmatrix} \quad \mathbf{r}_{0,2} = \begin{bmatrix} Wv_y \\ h\left(\gamma_{xy} + 2W^2 v_x v_y\right) \\ h\left(\gamma_{yy} + 2W^2 v_y v_y\right) \\ h\left(\gamma_{zy} + 2W^2 v_z v_y\right) \\ Wv_y(2hW - 1) \end{bmatrix} \quad \mathbf{r}_{0,3} = \begin{bmatrix} Wv_z \\ h\left(\gamma_{xz} + 2W^2 v_x v_z\right) \\ h\left(\gamma_{yz} + 2W^2 v_y v_z\right) \\ h\left(\gamma_{zz} + 2W^2 v_z v_z\right) \\ Wv_z(2hW - 1) \end{bmatrix} \quad \mathbf{r}_\pm = \begin{bmatrix} 1 \\ hW\left(v_x - \dfrac{v^x - \Lambda_\pm^x}{\gamma^{xx} - v^x\Lambda_\pm^x}\right) \\ hWv_y \\ hWv_z \\ \dfrac{hW(\gamma^{xx} - v^x v^x)}{\gamma^{xx} - v^x \Lambda_\pm^x} - 1 \end{bmatrix}$$

Special relativistic limit (along x-direction)

$$\lambda_0 = v^x \quad \text{(triple)}$$

$$\lambda_\pm = \frac{1}{1 - v^2 c_s^2}\left(v^x\left(1 - c_s^2\right) \pm c_s \sqrt{\left(1 - v^2\right)\left[1 - v^x v^x - \left(v^2 - v^x v^x\right)c_s^2\right]}\right)$$

coupling with transversal components of the velocity (important difference with Newtonian case)

Even in the purely 1D case: $\vec{v} = \left(v^x, 0, 0\right) \Rightarrow \lambda_0 = v^x, \ \lambda_\pm = \dfrac{v^x \pm c_s}{1 \pm v^x c_s}$

For causal EOS the sound cone lies within the light cone

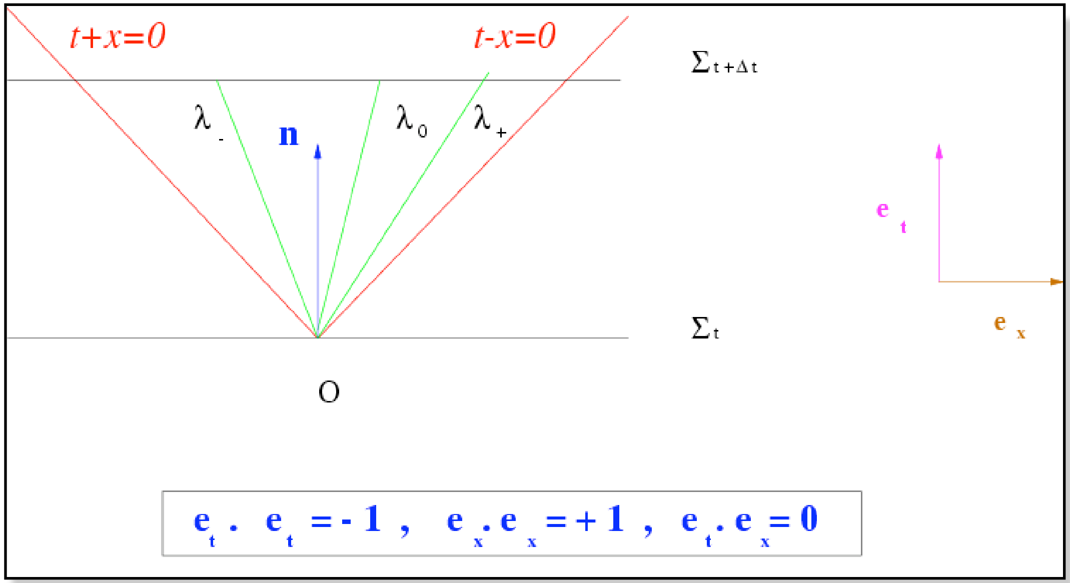

Recall Newtonian (1D) case:

$$\lambda_0 = v^x, \lambda_\pm = v^x \pm c_s$$

$$\lambda_0 = \alpha v^x - \beta^x \quad \text{(triple)}$$

$$\lambda_\pm = \frac{\alpha}{1 - v^2 c_s^2}\left(v^x\left(1 - c_s^2\right) \pm c_s \sqrt{\left(1 - v^2\right)\left[\gamma^{xx}\left(1 - v^2 c_s^2\right) - v^x v^x\left(1 - c_s^2\right)\right]}\right) - \beta^x$$

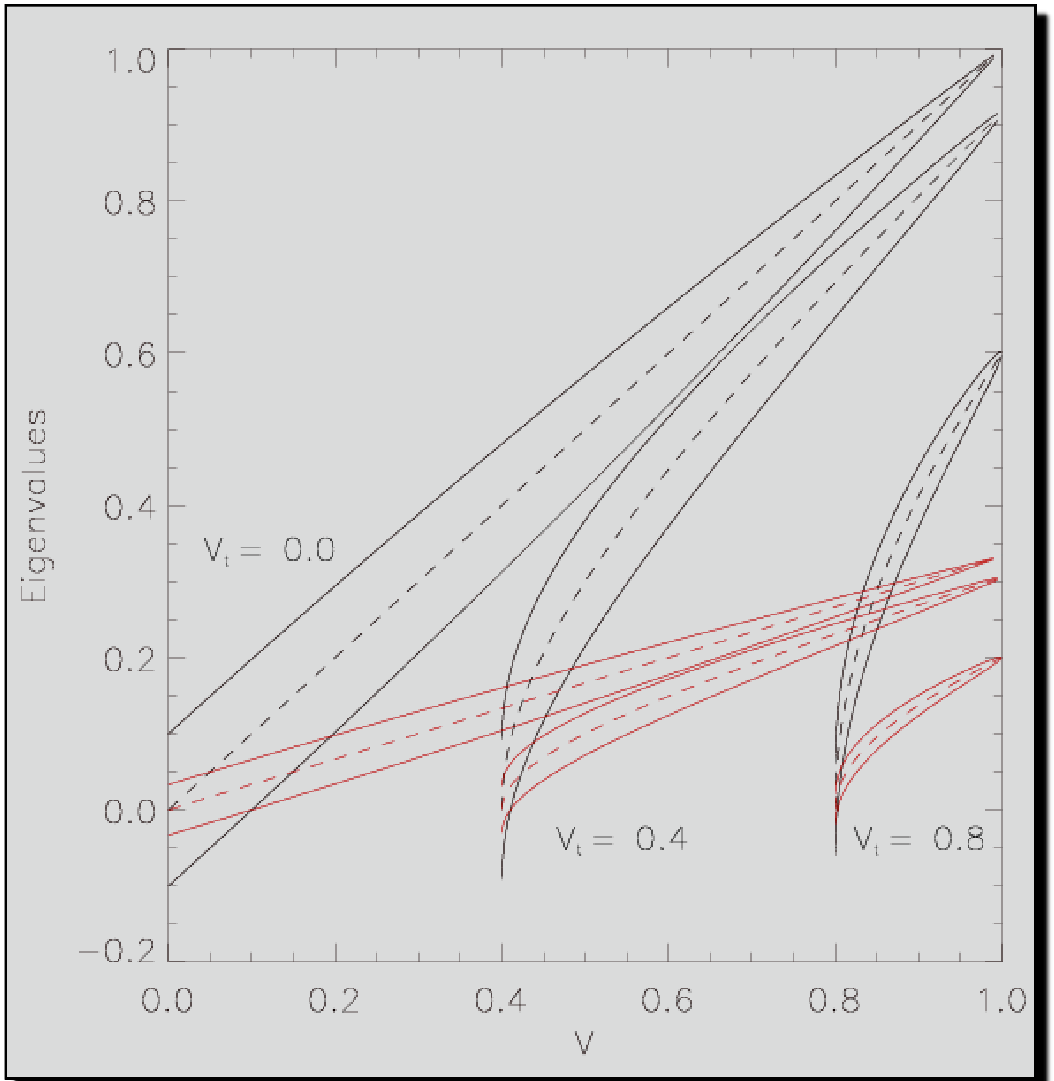

Black lines: SRHD

Red lines: GRHD

Relativistic effects:

- Tangential component of the flow velocity (v_t=0, 0.4, 0.8)
- Gravitational field (r=1.5 Schwarzschild radius)

Degeneracies in the eigenvalues occur as the flow speed reaches the speed of light and when the lapse function goes to zero (gauge effect), i.e. at the black hole horizon (sonic sphere).

Recovering primitive variables from state vector

A distinctive feature of the numerical solution of the relativistic hydrodynamics equations is that while the numerical algorithm updates the vector of conserved quantities, the numerical code makes extensive use of the primitive variables.

Those would appear repeatedly in the solution procedure, e.g. in the characteristic fields, in the solution of the Riemann problem, and in the computation of the numerical fluxes.

For spacelike foliations of the spacetime (3+1) the relation between the two sets of variables is implicit.

Hence, iterative (root-finding) algorithms are required. Those have been developed for all existing formulations (Eulderink & Mellema 1995; Banyuls et al 1997, Papadopoulos & Font 2000)

This feature, which is distinctive of the equations of general (and special) relativistic hydrodynamics (and also in GRMHD) – not existing in the Newtonian case – may lead to accuracy losses in regions of low density and small velocities, apart from being computationally inefficient.

For null foliations of the spacetime, the procedure of connecting primitive and conserved variables is explicit for a perfect fluid EOS, a direct consequence of the particular form of the Bondi-Sachs metric.

Recovering primitive variables: expressions

Newtonian hydrodynamics: fully explicit to obtain "primitive" variables from state vector.

3+1 general relativistic hydrodynamics: root-finding procedure. The expressions relating the primitive variables to the state vector depend explicitely on the EOS p(ρ,ε). Simple expressions are only obtained for simple EOS, i.e. ideal gas.

One can build a function of pressure whose zero represents the pressure in the physical state (other choices possible):

$$\vec{w} = (\rho, \varepsilon, v^i) \Rightarrow \begin{aligned} D &= \rho W \\ S_j &= \rho h W^2 v_j \\ \tau &= \rho h W^2 - p - D \end{aligned}$$

$$\boxed{f(\bar{p}) = p(\rho_*(\bar{p}), \varepsilon_*(\bar{p})) - \bar{p}}$$

$$\rho_*(\bar{p}) = \frac{D}{W_*(\bar{p})} \qquad \varepsilon_*(\bar{p}) = \frac{\tau + D[1 - W_*(\bar{p})] + \bar{p}[1 - W_*(\bar{p})^2]}{D W_*(\bar{p})}$$

$$W_*(\bar{p}) = \frac{1}{\sqrt{1 - v_*^i(\bar{p})\, v_{*i}(\bar{p})}} \qquad v_*^i(\bar{p}) = \frac{S^i}{\tau + D + \bar{p}}$$

The root of the above function can be obtained by means of a nonlinear root-finder (e.g. a Newton-Raphson method).

Astrophysical applications of Banyuls et al formulation

1. Simulations of relativistic jets (SR): Martí et al 1994, 1995, 1997, Gómez et al 1995, 1997, 1998, Aloy et al 1999, 2003, Scheck et al 2002.
2. Gamma-ray burst models: Aloy et al 2000, Aloy, Janka & Müller 2004.
3. Core collapse supernovae and GWs: Dimmelmeier, Font & Müller 2001, 2002a,b, Dimmelmeier et al 2004, Cerdá-Durán et al 2004, Shibata & Sekiguchi 2004.
4. QNM of rotating relativistic stars: Font, Stergioulas & Kokkotas 2000, Font et al 2001, 2002, Stergioulas & Font 2001, Stergioulas, Apostolatos & Font 2004, Shibata & Sekiguchi 2003.
5. Black hole formation: Baiotti et al 2004, 2006.
6. Accretion on to black holes: Font & Ibáñez 1998a,b, Font, Ibáñez & Papadopoulos 1999, Brandt et al 1998, Papadopoulos & Font 1998a,b, Nagar et al 2004.
7. Disk accretion: Font & Daigne 2002a,b, Daigne & Font 2004, Zanotti, Rezzolla & Font 2003, Rezzolla, Zanotti & Font 2003.
8. Binary neutron star mergers: Miller, Suen & Tobias 2001, Shibata, Taniguchi & Uryu 2003, Evans et al 2003, Miller, Gressman & Suen 2004.

Eulderink & Mellema formulation (1995)

Eulderink & Mellema (1995) derived a covariant formulation of the general relativistic hydrodynamic equations taking special care in the conservative form of the system.

Additionally they developed a numerical method to solve them based on a generalisation of Roe's approximate Riemann solver for the non relativistic Euler equations in Cartesian coordinates. Their procedure was specialized for a perfect fluid EOS.

After the appropriate choice of the state vector variables, the conservation laws are rewritten in flux-conservative form. The flow variables are expressed in terms of a parameter vector ω as:

$$\vec{F}^{\alpha} = \left(\left[k - \frac{\Gamma}{\Gamma - 1} w^4\right] w^{\alpha}, w^{\alpha} w^{\beta} + K w^4 g^{\alpha\beta}\right)$$

where $\omega^{\alpha} \equiv K u^{\alpha}$, $\omega^{4} \equiv K \dfrac{p}{\rho h}$, $K^2 \equiv \sqrt{-g}\,\rho h = -g_{\alpha\beta}\omega^{\alpha}\omega^{\beta}$

The vector $\vec{F}^{0}$ represents the state vector (the unknowns) and each vector $\vec{F}^{i}$ is the corresponding flux in the coordinate direction x^i

Eulderink and Mellema computed the appropriate "Roe matrix" for the above vector and obtained the corresponding spectral decomposition. This information is used to solve the system numerically using Roe's generalised approximate Riemann solver.

Formulation and numerical approach tested in 1D (shock tubes, spherical accretion onto a Schwarzschild black hole). In SR employed to study the confinement properties of relativistic jets. No astrophysical application in GR attempted yet.

Papadopoulos & Font formulation (2000)

Papadopoulos and Font (2000) derived another conservative formulation of the relativistic hydrodynamic equations form-invariant with respect to the nature of the spacetime foliation (spacelike, lightlike).

In this formulation the spatial components of the 4-velocity, together with the rest-frame density and internal energy, provide a unique description of the state of the fluid and are taken as the primitive variables

$$\vec{w} = \left(\rho, u^i, \varepsilon\right)$$

The initial value problem for the conservation laws is defined in terms of another vector in the same fluid state space, namely the conserved variables:

$$\vec{U} = (D, S^i, E) \qquad \begin{aligned} D &= J^0 = \rho u^0 \\ S^i &= T^{0i} = \rho h u^0 u^i + p g^{0i} \\ E &= T^{00} = \rho h u^0 u^0 + p g^{00} \end{aligned} \longrightarrow \boxed{\frac{\partial \sqrt{-g}\,\vec{U}^A}{\partial x^0} + \frac{\partial \sqrt{-g}\,\vec{F}^i}{\partial x^i} = \vec{S} \qquad (A = 0, i, 4)}$$

The flux vectors and the source terms (which depend only on the metric, its derivatives, and the undifferentiated stress energy tensor) are given by:

$$\vec{F}^j = \left(J^j, T^{ji}, T^{j0}\right) = \left(\rho u^j, \rho h u^i u^j + p g^{ij}, \rho h u^0 u^j + p g^{0j}\right)$$

$$\vec{S} = \left(0, -\sqrt{-g}\,\Gamma^i_{\mu\lambda} T^{\mu\lambda}, -\sqrt{-g}\,\Gamma^0_{\mu\lambda} T^{\mu\lambda}\right)$$

Characteristic structure of the above equations

Eigenvalues (along direction 1)

$$\lambda_0^1 = v^1 \quad \text{(triple)}$$

$$\lambda_\pm^1 = \frac{1}{1 - c_s^2(1 - L)}\left(Mc_s^2 + v^1(1 - c_s^2) \mp c_s\sqrt{c_s^2 M^2 + v^1(1 - c_s^2)(2M - Lv^1) + N(1 - c_s^2(1 - L))}\right)$$

$$v^1 \equiv \frac{u^1}{u^0}, \qquad L \equiv -\frac{g^{00}}{(u^0)^2}, \qquad M \equiv -\frac{g^{01}}{(u^0)^2}, \qquad N \equiv -\frac{g^{11}}{(u^0)^2}$$

Right-eigenvectors

$$\vec{r}_{0,1} = u^0 \begin{bmatrix} 1 \\ u^1 \\ u^2 \\ u^3 \\ u^0 \end{bmatrix} \quad \vec{r}_{0,2} = \begin{bmatrix} u^0 + \rho\mu_{13} \\ u^0 u^1 + \rho h(u^1\mu_{13} + u^0) \\ u^0 u^2 + \rho h u^2 \mu_{13} \\ u^0 u^3 + \rho h(u^3\mu_{13} - u^0) \\ (u^0)^2 + 2\rho h u^0 \mu_{13} \end{bmatrix} \quad \vec{r}_{0,3} = \begin{bmatrix} u^0 + \rho\mu_{31} \\ u^0 u^1 + \rho h(u^1\mu_{31} - u^0) \\ u^0 u^2 + \rho h u^2 \mu_{31} \\ u^0 u^3 + \rho h(u^3\mu_{31} + u^0) \\ (u^0)^2 + 2\rho h u^0 \mu_{31} \end{bmatrix} \quad \vec{r}_\pm = \begin{bmatrix} -\frac{\rho}{\varepsilon}u^0 B + \frac{\rho\Gamma}{h}K \\ -\frac{\rho}{\varepsilon}u^0 B u^1 h + \rho\Gamma\left[A(u^0 c^1 - a g^{01}) + u^1 K\right] \\ -\frac{\rho}{\varepsilon}u^0 B u^2 h + \rho\Gamma\left[A(u^0 c^2 - a g^{02}) + u^2 K\right] \\ -\frac{\rho}{\varepsilon}u^0 B u^3 h + \rho\Gamma\left[A(u^0 c^3 - a g^{03}) + u^3 K\right] \\ -\frac{\rho}{\varepsilon}(u^0)^2 \tilde{B} + \rho\Gamma\left[2u^0 K - aAg^{00}\right] \end{bmatrix}$$

with the definitions:

$$a \equiv u^1 - \lambda^1 u^0,\ c^i \equiv g^{k1} - \lambda^1 g^{0k},\ d \equiv g^{01} - \lambda^1 g^{00},\ \mu_i \equiv -\frac{u_i}{u_0},\ \mu_{ij} \equiv \mu_i - \mu_j$$

$$A \equiv \frac{u^0 - u^i\mu_i}{d - c^i\mu_i},\quad \tilde{A} \equiv \frac{\Gamma a A}{\Gamma - 1},\quad B \equiv 1 + \tilde{A},\quad \tilde{B} \equiv 1 + h\tilde{A},\quad K \equiv \mu_i(Ac^i - u^i)$$

Recovering primitive variables

For null foliations of the spacetime, the procedure of connecting primitive and conserved variables is explicit for a perfect fluid EOS, a direct consequence of the particular form of the Bondi-Sachs metric ($g^{00}=0$).

For the formulation of Papadopoulos & Font:

$$\varepsilon = \frac{\Lambda^2}{D^2 + D\sqrt{D^2 + \Gamma(2-\Gamma)\Lambda^2}}$$

$$\Lambda^2 = -D^2 - g_{00}E^2 - 2g_{0i}S^iE - g_{ij}S^iS^j$$

$$\Longrightarrow$$

$$h = 1 + \Gamma\varepsilon$$

$$\rho = \frac{D^2 h}{E}$$

$$u^i = \frac{S^i - p g^{oi}}{D(1+\Gamma\varepsilon)}$$

Lightcone hydrodynamics and characteristic numerical relativity

The formulation was tested in 1D relativistic flows (comparing with exact solutions in some cases) on null (lightlike) spacetime foliations (Papadopoulos & Font 1999):

- Shock tube tests in Minkowski spacetime (advanced and retarded time).
- Perfect fluid accretion on to a Schwarzschild black hole (ingoing null EF coordinates).
- Dynamical spacetime evolutions of polytropes (TOV) sliced along the radial null cones.
- Accretion of self-gravitating matter on a dynamic black hole.

Existing applications in relativistic astrophysics include:

- Accreting dynamic black holes and quasi-normal modes (Papadopoulos & Font, PRD, 63, 044016, 2001).
- Gravitational collapse of supermassive stars (GRB model) (Linke et al, A&A, 376, 568, 2001).
- Interaction of scalar fields with relativistic stars (Siebel, Font & Papadopoulos, PRD, 65, 024021, 2002).
- Nonlinear pulsations of axisymmetric neutron stars (Siebel, Font, Müller & Papadopoulos, PRD, 65, 064038, 2002).
- Axisymmetric core collapse and gravitational radiation (Bondi news) (Siebel, Font, Müller & Papadopoulos, PRD, 67, 124018, 2003).

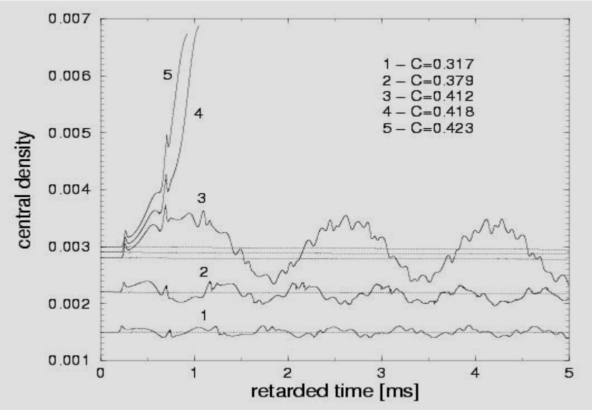

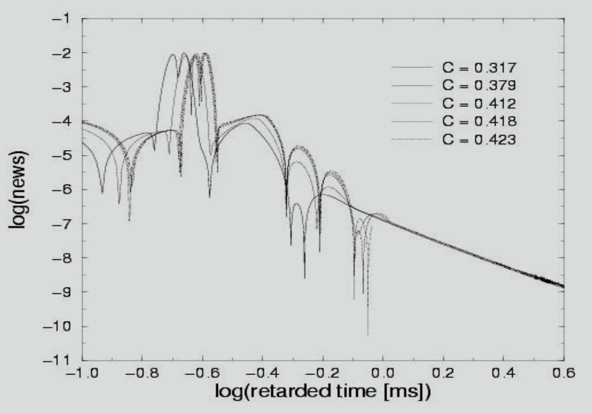

Part 2

a) General relativistic magneto-hydrodynamics

General Relativistic Magneto-Hydrodynamics (1)

GRMHD: Dynamics of relativistic, electrically conducting fluids in the presence of magnetic fields.

Ideal GRMHD: Absence of viscosity effects and heat conduction in the limit of infinite conductivity (perfect conductor fluid).

The stress-energy tensor includes contribution from the perfect fluid and from the magnetic field b^μ measured by observer comoving with the fluid.

$$T^{\mu\nu} = T^{\mu\nu}_{\mathrm{PF}} + T^{\mu\nu}_{\mathrm{EM}} \longrightarrow \boxed{T^{\mu\nu} = \rho h^* u^\mu u^\nu + p^* g^{\mu\nu} - b^\mu b^\nu}$$

$$T^{\mu\nu}_{\mathrm{PF}} = \rho h u^\mu u^\nu + p g^{\mu\nu}$$

with the definitions:

$$T^{\mu\nu}_{\mathrm{EM}} = F^{\mu\lambda} F^{\nu}_{\lambda} - \frac{1}{4} g^{\mu\nu} F^{\lambda\delta} F_{\lambda\delta} = \left(u^\mu u^\nu + \frac{1}{2} g^{\mu\nu}\right) b^2 - b^\mu b^\nu$$

$$F^{\mu\nu} = -\eta^{\mu\nu\lambda\delta} u_\lambda b_\delta$$

$$\begin{aligned} b^2 &= b^\nu b_\nu \\ p^* &= p + \frac{b^2}{2} \\ h^* &= h + \frac{b^2}{\rho} \end{aligned}$$

Ideal MHD condition: electric four-current must be finite.

$$F^{\mu\nu} u_\nu = 0$$

$$J^\mu = \rho_{\mathrm{q}} u^\mu + \sigma F^{\mu\nu} u_\nu \quad \sigma \longrightarrow \infty$$

General Relativistic Magneto-Hydrodynamics (2)

Conservation of mass: $\nabla_\mu(\rho u^\mu) = 0$

Conservation of energy and momentum: $\nabla_\mu T^{\mu\nu} = 0$

Maxwell's equations: $\nabla_\mu {}^*F^{\mu\nu} = 0$ $\qquad {}^*F^{\mu\nu} = \frac{1}{W}(u^\mu B^\nu - u^\nu B^\mu)$

- Divergence-free constraint: $\vec{\nabla} \cdot \vec{B} \ = \ 0$
- Induction equation: $\dfrac{1}{\sqrt{\gamma}}\dfrac{\partial}{\partial t}\left(\sqrt{\gamma}\vec{B}\right) \ = \ \vec{\nabla} \times \left[\left(\alpha\vec{v} - \vec{\beta}\right) \times \vec{B}\right]$

Adding all up: first-order, flux-conservative, hyperbolic system + constraint

$$\frac{1}{\sqrt{-g}}\left(\frac{\partial\sqrt{\gamma}\mathbf{U}}{\partial t} + \frac{\partial\sqrt{-g}\mathbf{F}^i}{\partial x^i}\right) = \mathbf{S} \qquad \frac{\partial(\sqrt{\gamma}B^i)}{\partial x^i} = 0$$

Antón et al. (2006)

$$\mathbf{U} = \begin{bmatrix} D \\ S_j \\ \tau \\ B^k \end{bmatrix} \quad \mathbf{F}^i = \begin{bmatrix} D\tilde{v}^i \\ S_j\tilde{v}^i + p^*\delta^i_j - b_j B^i/W \\ \tau\tilde{v}^i + p^* v^i - \alpha b^0 B^i/W \\ \tilde{v}^i B^k - \tilde{v}^k B^i \end{bmatrix} \quad \mathbf{S} = \begin{bmatrix} 0 \\ T^{\mu\nu}\left(\frac{\partial g_{\nu j}}{\partial x^\mu} - \Gamma^\delta_{\nu\mu} g_{\delta j}\right) \\ \alpha\left(T^{\mu 0}\frac{\partial \ln\alpha}{\partial x^\mu} - T^{\mu\nu}\Gamma^0_{\nu\mu}\right) \\ 0^k \end{bmatrix}$$

RMHD: some issues on hyperbolic structure (I)

Wave structure classical MHD (Brio & Wu 1988): 7 physical waves

Two ALFVEN WAVES: $\lambda_{a_\pm} \Longrightarrow \lambda_a = v_x \pm v_a$

Two FAST MAGNETOSONIC WAVES: $\lambda_{f_\pm} \Longrightarrow \lambda_{f_\pm} = v_x \pm v_f$

Two SLOW MAGNETOSONIC WAVES: $\lambda_{s_\pm} \Longrightarrow \lambda_{s_\pm} = v_x \pm v_s$

One ENTROPY WAVE: $\lambda_e \Longrightarrow \lambda_e = v_x$

$$\boxed{\lambda_{f_-} \le \lambda_{a_-} \le \lambda_{s_-} \le \lambda_e \le \lambda_{s_+} \le \lambda_{a_+} \le \lambda_{f_+}}$$

$$\boxed{v_{f,s}^2 = \frac{1}{2}\left\{c_s^2 + \frac{B_x^2+B_y^2+B_z^2}{\rho} \pm \sqrt{\left(c_s^2 + \frac{B_x^2+B_y^2+B_z^2}{\rho}\right)^2 - 4\left(\frac{B_x^2}{\rho}\right)c_s^2}\right\}, \quad v_a = \sqrt{\frac{B_x^2}{\rho}}}$$

Anile & Pennisi (1987), Anile (1989) (see also van Putten 1991) have studied the characteristic structure of the equations (eigenvalues, right/left eigenvectors) in the space of covariant variables (u^μ,b^μ,p,s).

Wave structure for relativistic MHD (Anile 1989): roots of the characteristic equation.

Only entropic waves and Alfvén waves are explicit.

Magnetosonic waves are given by the numerical solution of a quartic equation.

Augmented system of equations: Unphysical eigenvalues/eigenvectors (entropy & Alfvén) which must be removed numerically (Anile 1989, Komissarov 1999, Balsara 2001, Koldoba et al 2002).

RMHD: some issues on hyperbolic structure (II)

Degeneracy in eigenvalues (wave speeds coincidence) as for classical MHD.

The wave propagation velocity depends on the relative orientation of the magnetic field, θ.

As in classical MHD there are two types of degeneracies:

- Degeneracy I: $b^\mu{}_n=0$
- Degeneracy II: $b^\mu{}_t=0$

Implications:

- Physically two or more wave speeds become equal (compound waves).
- Numerically the spectral decomposition (needed in upwind HRSC schemes) blows up.

Wavefront diagrams in the fluid rest frame (Jeffrey & Taniuti 1964).

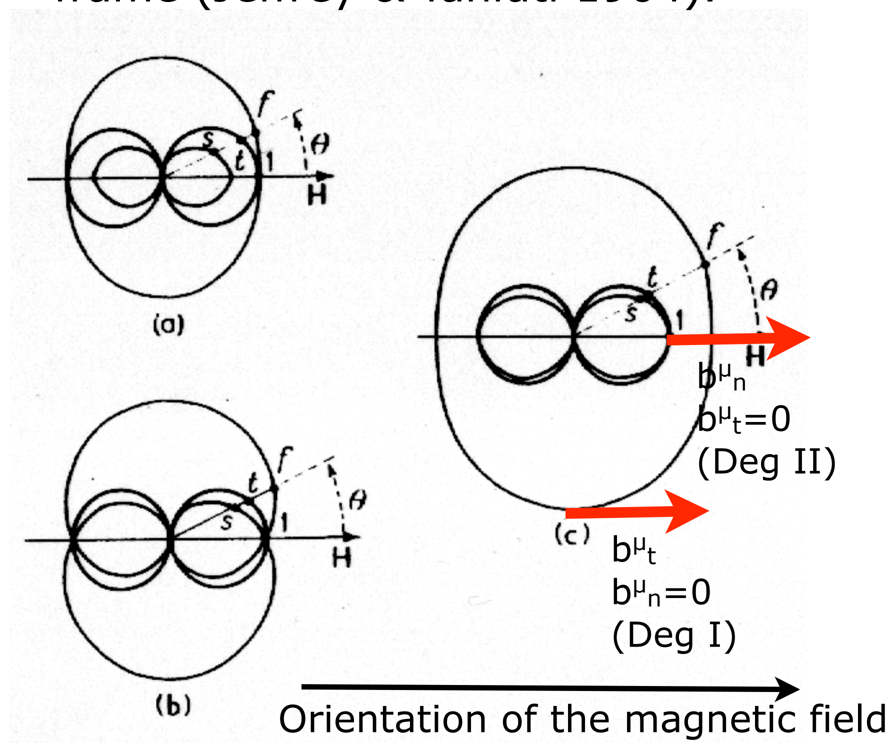

Breakup of hyperbolicity (Komissarov 1999; degeneracy characterisation).

Eigenvectors renormalization needed: Brio & Wu 1988 for classical MHD. Extended to RMHD for a Roe-type solver by Antón (PhD thesis, University of Valencia 2006).

Particular case: Minkowski + transverse B-field

$$\boxed{u^\mu = W(1, v^x, 0, v^z) \;\; , \;\; b^\mu = (0, 0, b, 0)}$$

$$\lambda_0 = v^x \quad \text{(triple)}$$

$$\lambda_\pm = \frac{v^x(1-\omega^2) \pm \omega\sqrt{(1-v^2)[1-(v^x)^2-(v^2-(v^x)^2)\omega^2]}}{1-v^2\omega^2}$$

$$\omega^2 = c_s^2 + \mathbf{v_a}^2 - c_s^2 \mathbf{v_a}^2$$

c_s (*local sound velocity*) : $hc_s^2 = \chi + \frac{p}{\rho^2}\kappa \;\; , \;\; \chi = \left(\frac{\partial p}{\partial \rho}\right)_\varepsilon \;\; , \;\; \kappa = \left(\frac{\partial p}{\partial \varepsilon}\right)_\rho$

v_a (*relativistic Alfven velocity*): $v_a^2 = \frac{|b|^2}{\rho h^*}$

1D $\Longrightarrow$ $v^z = 0 \rightarrow v = v^x$: $\lambda_0 = v \;\; , \;\; \lambda_\pm = \frac{v \pm \omega}{1 \pm v\omega}$

Exact solutions of the Riemann problem in SRHD & SRMHD have recently been obtained:

- SRHD: Martí & Müller 1996; Pons et al 2000; Rezzolla & Zanotti 2002; Rezzolla et al 2003.
- SRMHD: Romero et al 2005, particular case; Giacomazzo & Rezzolla 2006, general orientations).

Important tool for code validation.

Recovering primitive variables in RMHD

In RMHD the recovery of primitive variables more involved than in RHD.
(see e.g. Noble et al 2006 for a comparison of methods.
Antón et al 2006 find the roots of an 8-th order polynomial using a 2d Newton-Raphson.

See PhD thesis of L. Antón (2006), University of Valencia, for details.

$$D = \rho W$$

$$S^i = \rho h^* W^2 v^i - b^i b^0$$

$$\tau = \rho h^* W^2 - D - p^* - (b^0)^2$$

$$H^i = W(b^i - v^i b^0)$$

$$\mathbf{U} = (D, S^i, \tau, H^i) \rightarrow (\rho, v^i, \varepsilon, B^i)$$

$$P_8 = \sum_{n=0}^{8} A_n Z^n \ , \ Z \equiv \rho h W^2$$

Unknowns: Z and W.

$$\left(\tau - Z - \mathbf{B}^2 + \frac{(\mathbf{BS})^2}{2Z^2}\right) W^2 + \left(\frac{\gamma - 1}{\gamma}\right)(Z - DW) + \frac{\mathbf{B}^2}{2} = 0$$

$$\left((Z + \mathbf{B}^2)^2 - \mathbf{S}^2 - \frac{(\mathbf{BS})^2}{Z^2}(2Z + \mathbf{B}^2)\right) W^2 - (Z + \mathbf{B}^2)^2 = 0$$

Part 2

b) (Some) formulations of Einstein's equations

(Numerical) General Relativity:
Which portion of spacetime shall we foliate?

(original formulation of the 3+1 equations)

$$\partial_t \gamma_{ij} = -2\alpha K_{ij} + \nabla_i \beta_j + \nabla_j \beta_i$$

$$\partial_t K_{ij} = -\nabla_i \nabla_j \alpha + \alpha\left(R_{ij} + K K_{ij} - 2 K_{im} K^m_j\right) + \beta^m \nabla_m K_{ij} + K_{im} \nabla_j \beta^m + K_{jm} \nabla_i \beta^m - 8\pi T_{ij}$$

$$R + K^2 - K_{ij} K^{ij} - 16\pi\alpha^2 T^{00} = 0$$

$$\nabla_i\left(K^{ij} - \gamma^{ij} K\right) - 8\pi S^j = 0$$

Reformulating these equations to achieve numerical stability is one of the arts of numerical relativity.

(Numerical) General Relativity: Which portion of spacetime shall we foliate?

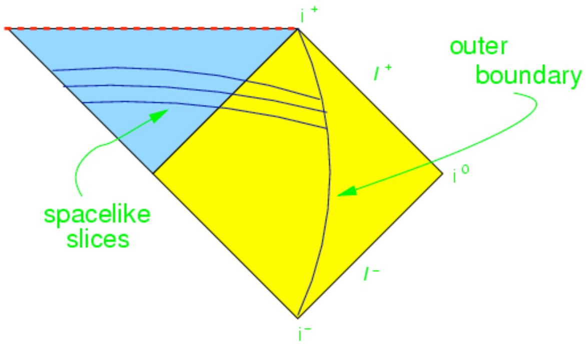

3+1 (Cauchy) formulation

Lichnerowicz (1944); Choquet-Bruhat (1962); Arnowitt, Deser & Misner (1962); York (1979)

Standard choice for most Numerical Relativity groups.
Spatial hypersurfaces have a finite extension.

(original formulation of the 3+1 equations)

$$\partial_t \gamma_{ij} = -2\alpha K_{ij} + \nabla_i \beta_j + \nabla_j \beta_i$$

$$\partial_t K_{ij} = -\nabla_i \nabla_j \alpha + \alpha\left(R_{ij} + K K_{ij} - 2K_{im} K^m_j\right) + \beta^m \nabla_m K_{ij} + K_{im} \nabla_j \beta^m + K_{jm} \nabla_i \beta^m - 8\pi T_{ij}$$

$$R + K^2 - K_{ij} K^{ij} - 16\pi\alpha^2 T^{00} = 0$$

$$\nabla_i \left(K^{ij} - \gamma^{ij} K\right) - 8\pi S^j = 0$$

Reformulating these equations to achieve numerical stability is one of the arts of numerical relativity.

Conformal formulation: Spatial hypersurfaces have infinite extension (Friedrich et al).

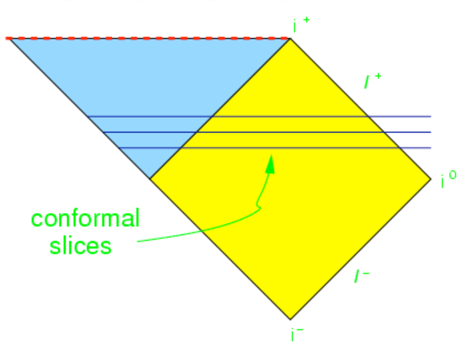

Characteristic formulation (Winicour et al).

Hypersuperfaces are light cones (incoming/outgoing) with infinite extension.

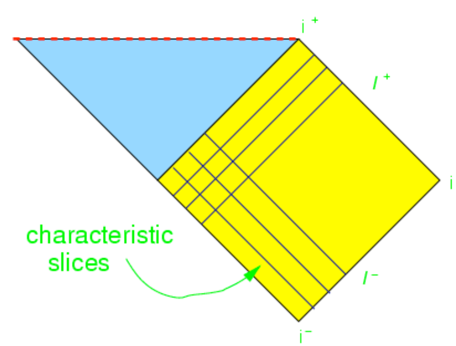

Gravity: CFC metric equations

In the CFC approximation (Isenberg 1985; Wilson & Mathews 1996) the ADM 3+1 equations

$$
\begin{aligned}
\partial_t \gamma_{ij} &= -2\alpha K_{ij} + \nabla_i \beta_j + \nabla_j \beta_i \\
\partial_t K_{ij} &= -\nabla_i \nabla_j \alpha + \alpha \left(R_{ij} + K\ K_{ij} - 2 K_{im} K^m_j \right) + \beta^m \nabla_m K_{ij} \\
&\quad + K_{im} \nabla_j \beta^m + K_{mj} \nabla_i \beta^m - 8\pi\alpha \left(T_{ij} - \frac{1}{2}\gamma_{ij} T^m_m + \frac{1}{2}\rho\gamma_{ij} \right)
\end{aligned}
$$

$$
\begin{aligned}
R + K^2 - K^{ij} K_{ij} &= 16\pi\rho \\
\nabla_i \left(K^{ij} - \gamma^{ij} K \right) &= 8\pi S^j
\end{aligned}
$$

reduce to a system of five coupled, nonlinear elliptic equations for the lapse function, conformal factor, and the shift vector:

CFC approximation

$$\gamma_{ij} = \phi^4 \delta_{ij}$$

$$
\boxed{
\begin{aligned}
\hat{\Delta}\phi &= -2\pi\phi^5 \left(\rho h W^2 - P + \frac{K_{ij} K^{ij}}{16\pi} \right) \\
\hat{\Delta}(\alpha\phi) &= 2\pi\alpha\phi^5 \left(\rho h (3W^2 - 2) + 5P + \frac{7 K_{ij} K^{ij}}{16\pi} \right) \\
\hat{\Delta}\beta^i &= 16\pi\alpha\phi^4 S^i + 2\phi^{10} K^{ij} \hat{\nabla}_j \left(\frac{\alpha}{\phi^6} \right) - \frac{1}{3} \hat{\nabla}^i \hat{\nabla}_k \beta^k
\end{aligned}
}
$$

Gravity: CFC+ metric equations

Cerdá-Duran, Faye, Dimmelmeier, Font, Ibáñez, Müller & Schäfer (2005)

CFC+ metric: $\gamma_{ij} = \phi^4 \hat{\gamma}_{ij} + h_{ij}^{\mathrm{TT}}$ (ADM gauge)

The second post-Newtonian deviation from isotropy is given by:

$$
\begin{aligned}
h_{ij}^{\mathrm{TT}} = \; & \frac{1}{2}\mathcal{S}_{ij} - 3x^k \hat{\nabla}_{(i}\mathcal{S}_{j)k} + \frac{5}{4}\hat{\gamma}_{jm}x^m \hat{\nabla}_i \left(\hat{\gamma}^{kl}\mathcal{S}_{kl}\right) + \frac{1}{4}x^k x^l \hat{\nabla}_i \hat{\nabla}_j \mathcal{S}_{kl} \\
& + 3\hat{\nabla}_{(i}\mathcal{S}_{j)} - \frac{1}{2}x^k \hat{\nabla}_i \hat{\nabla}_j \mathcal{S}_k + \frac{1}{4}\hat{\nabla}_i \hat{\nabla}_j \mathcal{S} - \frac{5}{4}\hat{\nabla}_i \mathcal{T}_j - \frac{1}{4}\hat{\nabla}_i \mathcal{R}_j \\
& + \hat{\gamma}_{ij}\left[\frac{1}{4}\hat{\gamma}^{kl}\mathcal{S}_{kl} + x^k \hat{\gamma}^{lm}\hat{\nabla}_m \mathcal{S}_{kl} - \hat{\gamma}^{kl}\hat{\nabla}_k \mathcal{S}_l\right]
\end{aligned}
$$

$$
\begin{aligned}
\hat{\Delta}\phi &= -2\pi\phi^5 \left(\rho h W^2 - P + \frac{K_{ij}K^{ij}}{16\pi}\right) \\
\hat{\Delta}(\alpha\phi) &= 2\pi\alpha\phi^5 \left(\rho h (3W^2 - 2) + 5P + \frac{7K_{ij}K^{ij}}{16\pi}\right) - \frac{1}{c^2}\hat{\gamma}^{ik}\hat{\gamma}^{jl}\, h_{ij}^{\mathrm{TT}} \hat{\nabla}_k \hat{\nabla}_l U \\
\hat{\Delta}\beta^i &= 16\pi\alpha\phi^4 S^i + 2\phi^{10}K^{ij}\hat{\nabla}_j \left(\frac{\alpha}{\phi^6}\right) - \frac{1}{3}\hat{\nabla}^i \hat{\nabla}_k \beta^k
\end{aligned}
$$

Modified equations with respect to CFC

Gravity: CFC+ metric equations (cont'd)

The required intermediate potentials satisfy 16 elliptic **linear** equations:

$$
\begin{aligned}
\hat{\Delta} U &= -4\pi G D^* \\
\hat{\Delta} \mathcal{S} &= -4\pi \frac{S_i^* S_j^*}{D^*} x^i x^j \\
\hat{\Delta} \mathcal{S}_i &= \left[-4\pi \frac{S_i^* S_j^*}{D^*} - \hat{\nabla}_i U \hat{\nabla}_j U\right] x^j \\
\hat{\Delta} \mathcal{T}_i &= \left[-4\pi \frac{S_j^* S_k^*}{D^*} - \hat{\nabla}_j U \hat{\nabla}_k U\right] \hat{\gamma}^{jk} \hat{\gamma}_{il} x^l \\
\hat{\Delta} \mathcal{R}_i &= \hat{\nabla}_i (\hat{\nabla}_j U \hat{\nabla}_k U x^j x^k) \\
\hat{\Delta} \mathcal{S}_{ij} &= -4\pi \frac{S_i^* S_j^*}{D^*} - \hat{\nabla}_i U \hat{\nabla}_j U
\end{aligned}
$$

Linear solver: LU decomposition using standard LAPACK routines

$$
\begin{aligned}
\mathcal{M}(\mathcal{S}) &= \frac{1}{r} \int \mathrm{d}^3\boldsymbol{x} \sqrt{\hat{\gamma}} \left(\frac{S_k^* S_l^*}{D^*} x^k x^l \right) \\
\mathcal{M}(\mathcal{S}_i) &= \frac{1}{r} \int \mathrm{d}^3\boldsymbol{x} \sqrt{\hat{\gamma}} D^* \left(\frac{S_i^* S_k^*}{D^{*2}} x^k + \hat{\gamma}_{ij} x^j (U + x^k \hat{\nabla}_k U) \right) + \frac{M^2}{2r} \hat{\gamma}_{ij} n^j \\
\mathcal{M}(\mathcal{T}_i) &= \frac{1}{r} \int \mathrm{d}^3\boldsymbol{x} \sqrt{\hat{\gamma}} D^* \left(\frac{\hat{\gamma}^{kl} S_k^* S_l^*}{D^{*2}} + U \right) \hat{\gamma}_{ij} x^j + \frac{M^2}{2r} \hat{\gamma}_{ij} n^j \\
\mathcal{M}(\mathcal{R}_i) &= \frac{M^2 \hat{\gamma}_{ij} n^j}{r} \\
\mathcal{M}(\mathcal{S}_{ij}) &= \frac{1}{r} \int \mathrm{d}^3\boldsymbol{x} \sqrt{\hat{\gamma}} D^* \left(\frac{S_i^* S_j^*}{D^{*2}} + \frac{1}{2} \hat{\gamma}_{ij} U + \hat{\gamma}_{ik} x^k \partial_j U \right)
\end{aligned}
$$

Boundary conditions: Multipole development in compact-supported integrals

Gravity: BSSN metric equations

Kojima, Nakamura & Oohara (1987); Shibata & Nakamura (1995); Baumgarte & Shapiro (1999)

Idea: Remove mixed second derivatives in the Ricci tensor by introducing auxiliary variables. Evolution equations start to look like wave equations for 3-metric and extrinsic curvature (idea goes back to De Donder 1921; Choquet-Bruhat 1952; Fischer & Marsden 1972).

- Conformal decomposition of the 3-metric:

$$\tilde{\gamma}_{ij} = \psi^4 \gamma_{ij} \qquad \det \tilde{\gamma}_{ij} = 1$$

- BSSN evolution variables (trace of extrinsic curvature is a separate variable):

$$\phi = \frac{1}{4} \log \psi \qquad \tilde{\gamma}_{ij} = e^{-4\phi} \gamma_{ij}$$

$$K = \gamma^{ij} K_{ij} \qquad \tilde{A}_{ij} = e^{-4\phi} \left(K_{ij} - \frac{1}{3} \gamma_{ij} K \right)$$

- Introduce evolution variables (gauge source functions):

$$\tilde{\Gamma}^a = \tilde{\gamma}^{ij} \tilde{\Gamma}^a_{ij} = -\partial_i \tilde{\gamma}^{ai}$$

BSSN metric evolution equations

Kojima, Nakamura & Oohara (1987); Shibata & Nakamura (1995); Baumgarte & Shapiro (1999)

$$
\begin{aligned}
(\partial_t - \mathcal{L}_\beta)\tilde{\gamma}_{ij} &= -2\alpha \tilde{A}_{ij} \\
(\partial_t - \mathcal{L}_\beta)\phi &= -\frac{1}{6}\alpha K \\
(\partial_t - \mathcal{L}_\beta)K &= -\gamma^{ij} D_i D_j \alpha + \alpha \left[\tilde{A}_{ij}\tilde{A}^{ij} + \frac{1}{3}K^2 + \frac{1}{2}(\rho + S)\right] \\
(\partial_t - \mathcal{L}_\beta)\tilde{A}_{ij} &= e^{-4\phi}\left[-D_i D_j \alpha + \alpha\left(R_{ij} - S_{ij}\right)\right]^{\mathrm{TF}} + \alpha\left(K\tilde{A}_{ij} - 2\tilde{A}_{il}\tilde{A}^l_j\right) \\
(\partial_t - \mathcal{L}_\beta)\tilde{\Gamma}^i &= -2\tilde{A}^{ij}\partial_j \alpha + 2\alpha\left(\tilde{\Gamma}^i_{jk}\tilde{A}^{kj} - \frac{2}{3}\tilde{\gamma}^{ij}\partial_j K - \tilde{\gamma}^{ij} S_j + 6\tilde{A}^{ij}\partial_j \phi\right) \\
&\quad + \partial_j\left(\beta^l \tilde{\partial}_l \gamma^{ij} - 2\tilde{\gamma}^{m(j}\partial_m \beta^{i)} + \frac{2}{3}\tilde{\gamma}^{ij}\partial_l \beta^l\right)
\end{aligned}
$$

BSSN is currently the standard 3+1 formulation in Numerical Relativity. Long-term stable applications include strongly-gravitating systems such as neutron stars (isolated and binaries) and single and binary black holes!

Part 3
Numerical methods for conservation laws

Linear hyperbolic systems of conservation laws

A one-dimensional linear hyperbolic system of PDEs is: $\boxed{\dfrac{\partial \vec{u}}{\partial t} + A\dfrac{\partial \vec{u}}{\partial x} = 0}$

where A is a constant coefficient pxp matrix with real eigenvalues $\lambda_i \left(i = 1,\cdots,p\right)$

By introducing the characteristic variables $\vec{w} = R^{-1}\vec{u}$ the above system can be written:

$$\frac{\partial \vec{w}}{\partial t} + \Lambda \frac{\partial \vec{w}}{\partial x} = 0$$

where $\Lambda = R^{-1}AR,\ \Lambda = \mathrm{diag}\left(\lambda_1 \cdots \lambda_p\right)$ and R is the right-eigenvectors matrix.

Since Λ is diagonal, the system of PDEs for the characteristic variables decouples into p independent scalar equations:

$$\frac{\partial w_i}{\partial t} + \lambda_i \frac{\partial w_i}{\partial x} = 0 \quad \left(i = 1\cdots p\right)$$

This is a system of constant coefficient linear advection equations whose solution is:

$w_i\left(x,t\right) = w_i\left(x - \lambda_i t, 0\right)$ And for the original system: $\boxed{\vec{u}\left(x,t\right) = R\vec{w}\left(x,t\right)}$

In a few slides we will link this with quasi-linear systems …

Numerical schemes

There exists a large variety of numerical schemes to solve the scalar advection equation.

Finite-difference schemes are based on a discretization of the x-t plane with a mesh of discrete points (x_j,t^n): $x_j = (j - 1/2)\Delta x, \quad t^n = n\Delta t, \quad j = 1, 2, \cdots \quad n = 0, 1, 2, \cdots$

where Δx and Δt stand for the cell width and time step.

A finite-difference scheme is a time-marching procedure which permits to obtain approximations to the solution in the mesh points w_j^{n+1} from the approximations in the previous time steps w_j^n

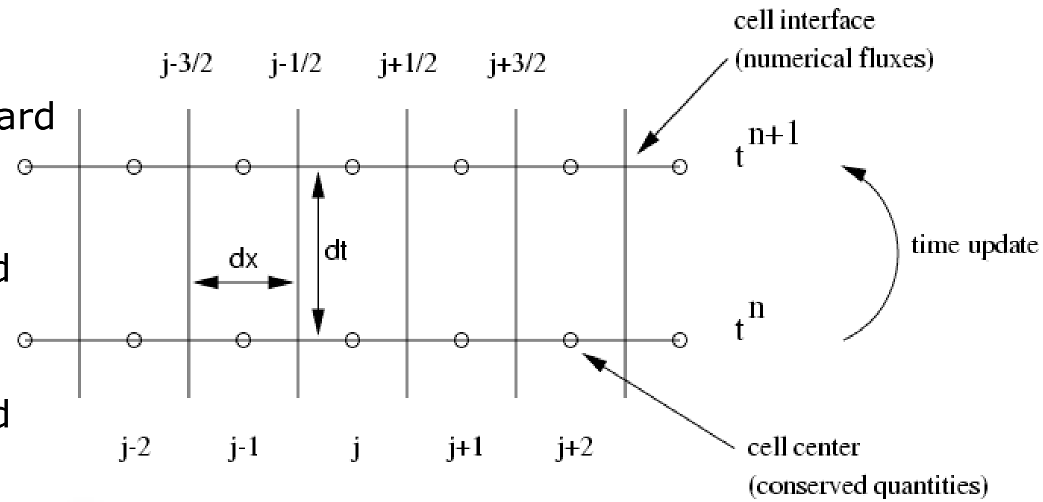

$$w_j^{n+1} = w_j^n - \frac{\Delta t}{2\Delta x}\lambda\left(w_{j+1}^n - w_{j-1}^n\right)$$ backward Euler

$$w_j^{n+1} = w_j^n - \frac{\Delta t}{\Delta x}\lambda\left(w_j^n - w_{j-1}^n\right)$$ one sided

$$w_j^{n+1} = w_j^n - \frac{\Delta t}{\Delta x}\lambda\left(w_{j+1}^n - w_j^n\right)$$ one sided

$$w_j^{n+1} = \frac{1}{2}\left(w_{j-1}^n + w_{j+1}^n\right) - \frac{\Delta t}{2\Delta x}\lambda\left(w_{j+1}^n - w_{j-1}^n\right)$$ Lax-Friedrichs

$$w_j^{n+1} = w_j^{n-1} - \frac{\Delta t}{2\Delta x}\lambda\left(w_{j+1}^n - w_{j-1}^n\right)$$ leapfrog

First-order accurate schemes

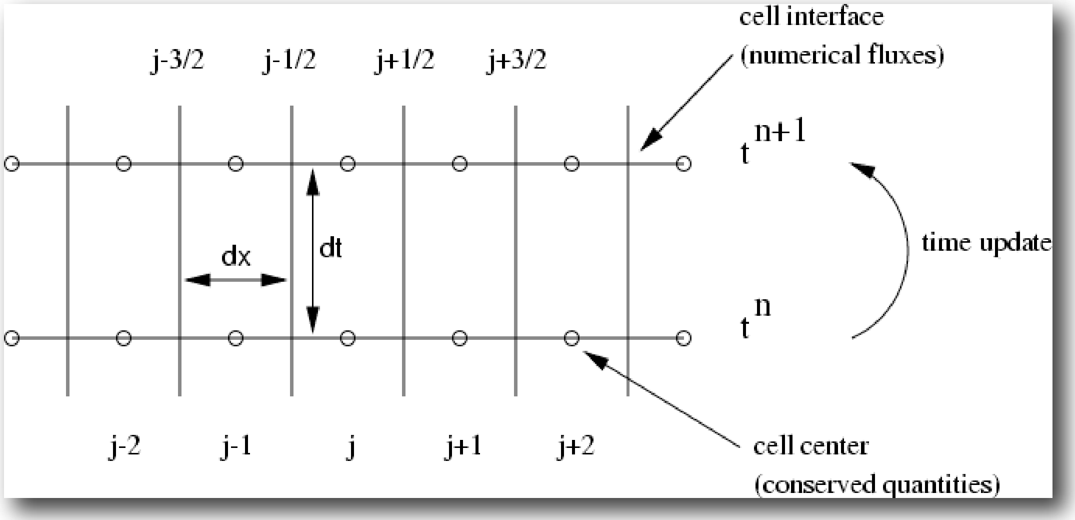

Second-order accurate schemes

Lax-Wendroff

$$w_j^{n+1} = w_j^n - \frac{\Delta t}{2\Delta x}\lambda\left(w_{j+1}^n - w_{j-1}^n\right) + \frac{(\Delta t)^2}{2(\Delta x)^2}\lambda^2\left(w_{j+1}^n - 2w_j^n + w_{j-1}^n\right)$$

$$w_j^{n+1} = w_j^n - \frac{\Delta t}{2\Delta x}\lambda\left(3w_j^n - 4w_{j-1}^n + w_{j-2}^n\right) + \frac{(\Delta t)^2}{2(\Delta x)^2}\lambda^2\left(w_j^n - 2w_{j-1}^n + w_{j-2}^n\right)$$

Beam-Warming

Some definitions:

- Global error: difference between exact solution and numerical solution.
- Convergence: a finite-difference scheme is convergent if the global error goes to zero as the computational grid is refined.
- Global order of accuracy: a scheme has global order p if the global error is $O(\Delta t^p + \Delta x^p)$ when $\Delta t, \Delta x \to 0$.
- Local truncation error (LTE): measures how well the finite-difference equations approximate the partial differential equations locally. It is defined by inserting the exact solution in the finite-difference equations for an arbitrary point of the computational grid.

For smooth functions Taylor expansion can be applied to obtain the local order of the scheme.

If the LTE goes to zero as $O(\Delta t^p + \Delta x^p)$ then the scheme has, locally, p-th order accuracy.

If the LTE goes to zero as the computational grid is refined, the numerical scheme is said to be consistent.

Some more definitions:

- An explicit scheme gives explicit expressions for each w_j^{n+1} from known values at the previous time-step t^n.
- An implicit scheme couples values from different spatial cells at time t^{n+1}, so that an algebraic system of equations needs to be solved at each time-step to update the solution.

Explicit schemes are, in general, preferred, as long as they can be used with reasonable (efficiency-wise) time-stepping.

- CFL condition: a numerical scheme can only be convergent if its (discrete) domain of dependence contains the corresponding domain of dependence of the PDE, at least in the limit Δt, $\Delta x \to 0$.

For hyperbolic systems with eigenvalues λ, the CFL condition implies $|\lambda \Delta t/\Delta x| \leq 1$ as a necessary condition for numerical stability.

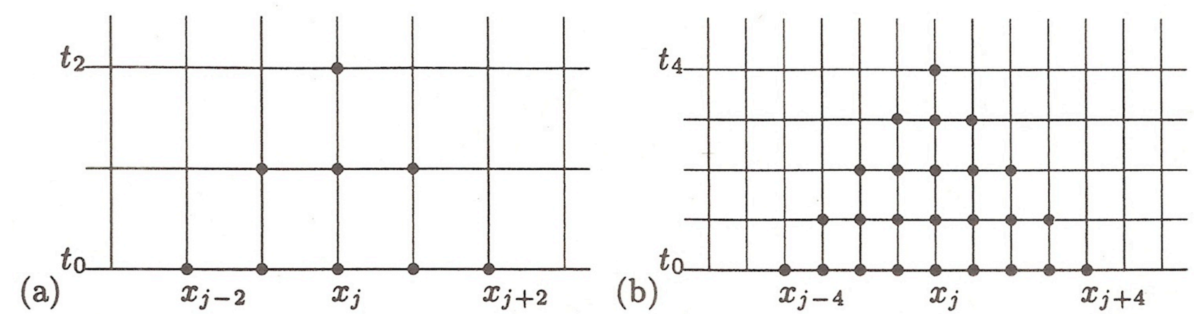

Fig. 4.2. (a) Numerical domain of dependence of a grid point when using a 3-point explicit method. (b) On a finer grid.

Standard finite difference schemes applied to linear systems work generally well for smooth solutions.

Q: What happens if the initial data are discontinuous?

A: The numerical scheme may have difficulties near the discontinuity.

Example: $$\frac{\partial u}{\partial t} + a\frac{\partial u}{\partial x} = 0 \qquad -\infty < x < \infty \qquad t \geq 0$$

$$u_0(x) = \begin{cases} 1 & \text{si} \quad x < 0 \\ 0 & \text{si} \quad x > 0 \end{cases}$$

First-order schemes: diffusion.

Second-order schemes: spurious oscillations.

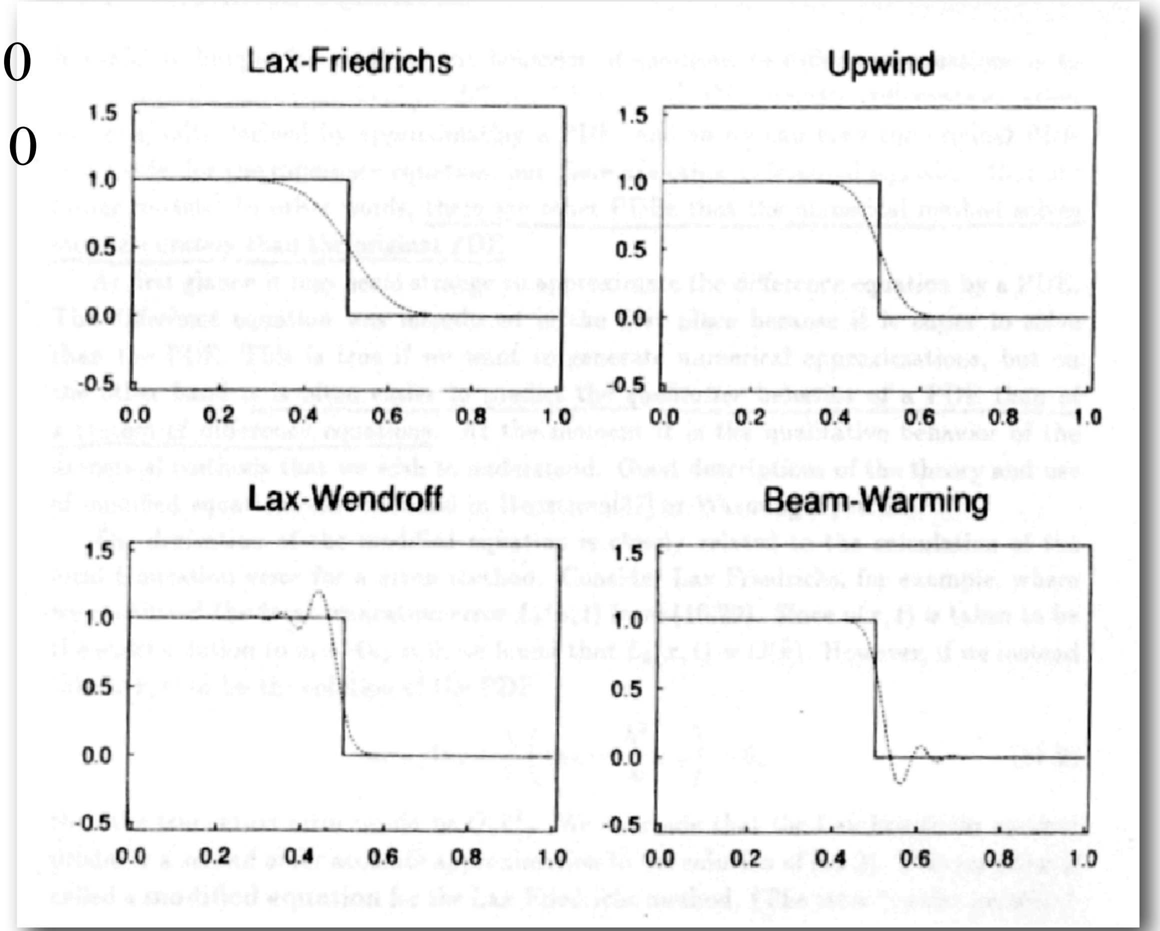

Nonlinear hyperbolic systems of CL (1)

Let us consider the system of *p* equations of conservation laws

$$\boxed{\begin{array}{l} \dfrac{\partial \vec{u}}{\partial t} + \displaystyle\sum_{j=1}^{d} \dfrac{\partial \vec{f}_j(\vec{u})}{\partial x_j} = 0 \quad (\vec{s}(\vec{u})) \\ \vec{u} = (u_1, \cdots, u_p) \quad \text{state vector} \\ \vec{f}_j(\vec{u}) = (f_{1j}, \cdots, f_{pj}) \quad \text{fluxes} \end{array}}$$

Formally, this system expresses the conservation of the state vector. Let D be an arbitrary domain of R_d and let $\vec{n} = (n_1, \cdots, n_d)$ be the outward unit normal to the boundary of D. Then,

$$\frac{d}{dt}\int_D \vec{u}\, d\vec{x} + \sum_{j=1}^{d} \int_{\partial D} \vec{f}_j(\vec{u}) n_j\, d\vec{S} = 0$$

In most situations one considers the so-called initial value problem (IVP), i.e. the solution of the above system with the initial condition

$$\vec{u}(\vec{x},0) = \vec{u}_0(\vec{x})$$

A key property of hyperbolic systems is that features in the solution propagate at the characteristic speeds given by the eigenvalues of the Jacobian matrices.

The characteristic variables are constant along the characteristic curves

$$\frac{dx}{dt} = \lambda_k(\vec{u}(x,t)), \; k = 1, \cdots, p$$

These curves give information about the propagation of the initial data, which formally permits to reconstruct the future solution for the IVP.

Nonlinear hyperbolic systems of CL (2)

Continuous and differentiable solutions that satisfy the IVP pointwise are called classical solutions.

For nonlinear systems classical solutions do not exist in general even for smooth initial data. Discontinuities develop after a finite time.

We seek generalized solutions that satisfy the integral form of the conservation system, which are classical solutions where they are continuous and have a finite number of discontinuities: weak solutions.

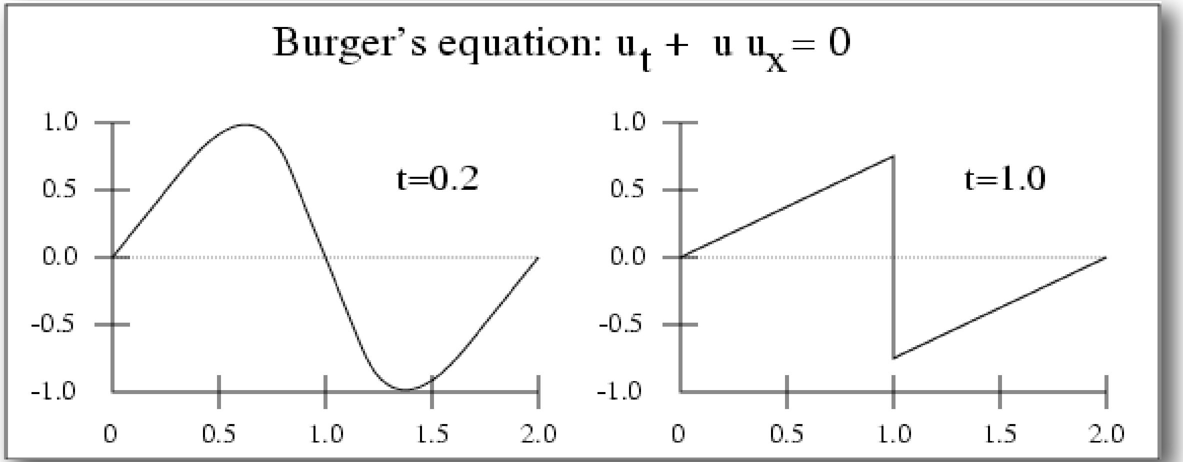

The class of all weak solutions is too wide in the sense that there is no uniqueness for the IVP.

A numerical scheme should guarantee convergence to the physically admissible solution: limit solution when $\varepsilon \to 0$ of the "viscous version" of the IVP:

$$\boxed{\frac{\partial \vec{u}}{\partial t} + \sum_{j=1}^{d} \frac{\partial \vec{f}_j(\vec{u})}{\partial x_j} = \varepsilon \sum_{j=1}^{d} \frac{\partial^2 \vec{u}}{\partial x_j^2}}$$

Nonlinear hyperbolic problems and classical solutions

$$\frac{\partial z}{\partial t} + \left(1 + \frac{3}{2}z\right)\frac{\partial z}{\partial x} = 0, \qquad z_0(x) = \begin{cases} \varepsilon(1+\cos x) & \text{if} |x| < \pi \\ 0 & \text{if} |x| > \pi \end{cases} \qquad 0 < \varepsilon \ll 1$$

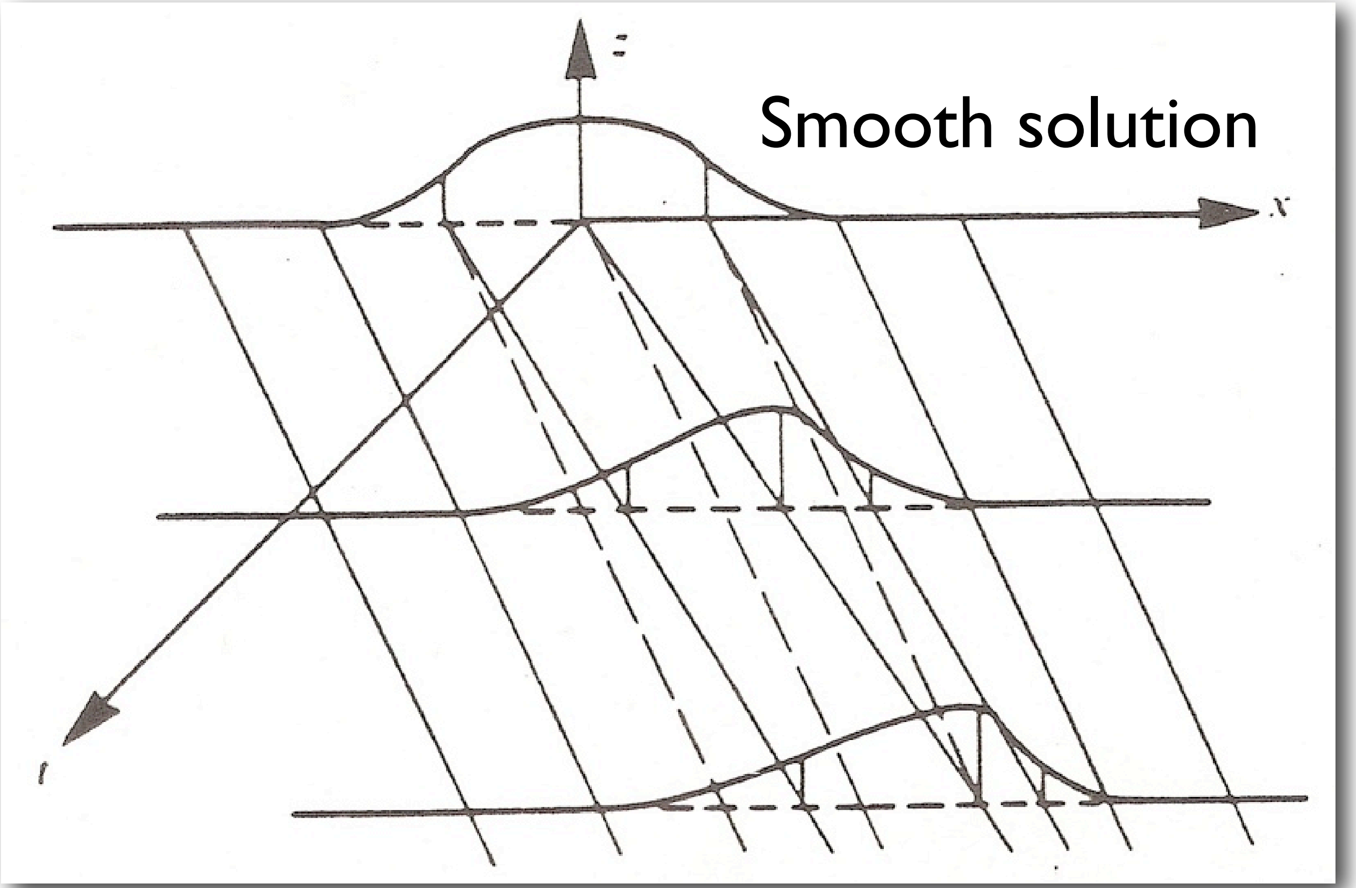

time

Discontinuous solution

Cross of characteristics

back

Weak solutions

Conservation law: $\frac{\partial \vec{u}}{\partial t} + \frac{\partial \vec{f}(\vec{u})}{\partial x} = 0$

Test function: $\Phi(x,t) \in C_0^1(R \times R)$

(space of continuously differentiable functions with compact support).

Multiplying the conservation law by the test function, integrating over space and time, and integrating by parts, we get:

$$\int_0^{\infty}\int_{-\infty}^{+\infty}\left(\Phi_t \vec{u} + \Phi_x \vec{f}(\vec{u})\right)dx\,dt = -\int_{-\infty}^{+\infty}\Phi(x,0)\vec{u}(x,0)\,dx$$

Definition: the function $\vec{u}(x,t)$ is a weak solution of the conservation law if the previous integral form holds for all functions $\Phi(x,t) \in C_0^1(R \times R)$

Theorem: let $\vec{u}(x,t)$ be a piecewise smooth function. Then, it is a solution of the integral form of the conservation system if and only if the two following conditions are satisfied:

1. $\vec{u}(x,t)$ is a classical solution in the domains where it is continuous.

2. Across a given surface of discontinuity it satisfies the jump (Rankine-Hugoniot) conditions:

$$\left(\vec{u}_R - \vec{u}_L\right)n_t + \sum_{j=1}^{d}\left(\vec{f}_j(\vec{u}_R) - \vec{f}_j(\vec{u}_L)\right)n_{xj} = 0$$

For 1D systems the RH conditions read:

$$s(\vec{u}_R - \vec{u}_L) = \vec{f}(\vec{u}_R) - \vec{f}(\vec{u}_L)$$

where s is the propagation speed of the discontinuity.

Shock-tracking techniques: use the RH conditions in combination with standard finite difference methods for the smooth regions and special procedures for tracking the location of discontinuities. This allows to solve the conservation law in the presence of shocks.

In 1D it is a viable approach. In multidimensions more complicated as discontinuities lie along curves (2D) or surfaces (3D) and there may be many such discontinuities interacting.

Vanishing viscosity approach: an example

Inviscid Burger's equation: $u_t + uu_x = 0$ (hyperbolic)

Viscous Burger's equation: $u_t + uu_x = \varepsilon u_{xx}$ (parabolic)

The correct physical behaviour is determined adopting the vanishing viscosity approach.

The inviscid equation is a model of the viscous one only for small ε and smooth u.

If the initial data are smooth and ε very small the term εu_{xx} is negligible before the wave begins to break. The solution to both PDEs look identical.

As the wave begins to break the u_{xx} term grows much faster than the u_x term, and the right-hand-side begins to play a dominant role. This term keeps the solution smooth at all times, thus preventing the breakdown of solutions which occurs for the hyperbolic problem.

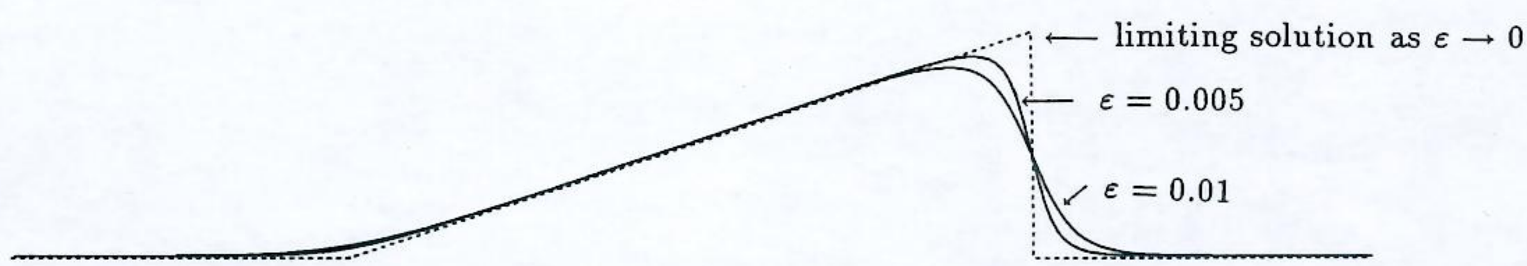

Figure 3.7. Solution to the viscous Burgers' equation for two different values of ε.

Nonlinear hyperbolic systems of CL (3)

A numerical scheme should guarantee convergence to the physically admissible solution: limit solution when ε→0 of the "viscous version" of the IVP:

$$\frac{\partial \vec{u}}{\partial t} + \sum_{j=1}^{d} \frac{\partial \vec{f}_j(\vec{u})}{\partial x_j} = \varepsilon \sum_{j=1}^{d} \frac{\partial^2 \vec{u}}{\partial x_j^2}$$

Mathematically, physical solutions are characterized by the so-called entropy condition (the entropy of any fluid element should increase when running into a discontinuity)

The characterization of the entropy-satisfying solutions for scalar equations follows Oleinik (1963), whereas for systems of conservation laws was developed by Lax (1972).

Entropy condition (for scalar equations): u(x,t) is the entropy solution if all discontinuities have the property that:

$$\boxed{\frac{f(u)-f(u_L)}{u-u_L} \geq s \geq \frac{f(u)-f(u_R)}{u-u_R}}$$

$$u_L \leq u \leq u_R$$

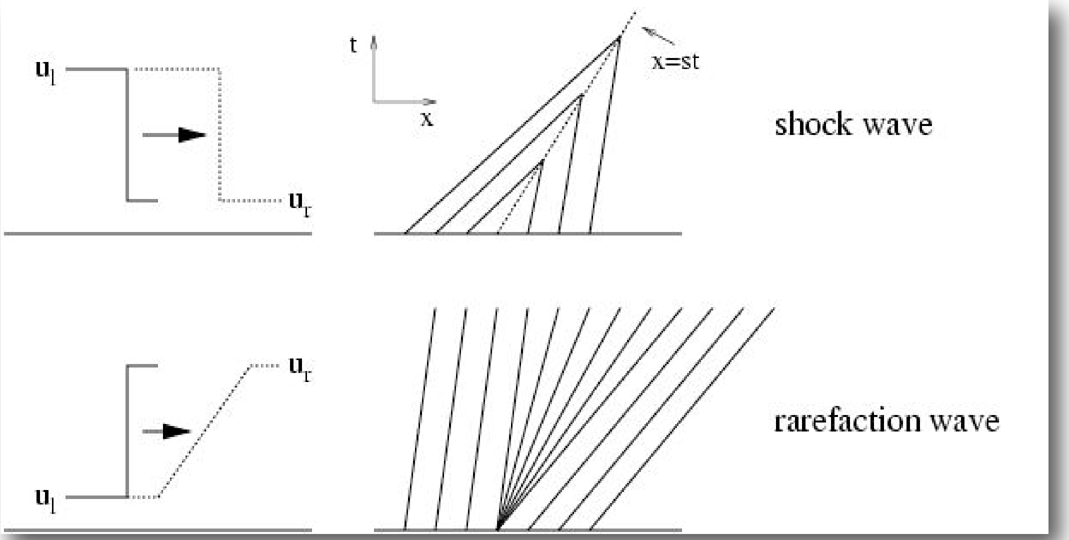

Nonlinear hyperbolic systems of CL (4)

High-resolution methods: modified high-order finite-difference methods with appropriate amount of numerical dissipation in the vicinity of a discontinuity.

A finite-difference scheme is a time-marching procedure which permits to obtain approximations to the solution in the mesh points $\vec{u}_j^n$ from the approximations in the previous time steps $\vec{u}_j^{n+1}$

Quantity $\vec{u}_j^n$ is an approximation to $\vec{u}(x_j, t^n)$ but in the case of a conservation law it is often preferable to view it as an approximation to the average of within the numerical cell $[x_{j-1/2}, x_{j+1/2}]\,(x_{j\pm 1/2} \equiv (x_j + x_{j\pm 1})/2)$

$$\boxed{\vec{u}_j^n \approx \frac{1}{\Delta x}\int_{x_{j-1/2}}^{x_{j+1/2}} \vec{u}(x, t^n)\,dx}$$

consistent with the integral form of the conservation law

For hyperbolic systems of conservation laws, schemes written in conservation form guarantee that the convergence (if it exists) is to one of the weak solutions of the original system of equations (Lax-Wendroff theorem 1960).

A scheme written in conservation form reads:

$$\boxed{\vec{u}_j^{n+1} = \vec{u}_j^n - \frac{\Delta t}{\Delta x}\left(\hat{\vec{f}}(\vec{u}_{j-r}^n, \vec{u}_{j-r+1}^n, \cdots, \vec{u}_{j+q}^n) - \hat{\vec{f}}(\vec{u}_{j-r-1}^n, \vec{u}_{j-r}^n, \cdots, \vec{u}_{j+q-1}^n)\right)}$$

where $\hat{\vec{f}}$ is a consistent numerical flux function:

$$\hat{\vec{f}}(\vec{u}, \vec{u}, \cdots, \vec{u}) = \vec{f}(\vec{u})$$

Nonlinear hyperbolic systems of CL (5)

Example: Burger's equation with discontinuous initial data

$$\frac{\partial u}{\partial t} + \frac{\partial (u^2/2)}{\partial x} = 0$$

can be e.g. discretized using a conservative upwind scheme:

$$u_j^{n+1} = u_j^n - \frac{\Delta t}{\Delta x}\left(\frac{1}{2}(u_j^n)^2 - \frac{1}{2}(u_{j-1}^n)^2\right)$$

or using a non-conservative upwind scheme:

$$u_j^{n+1} = u_j^n - \frac{\Delta t}{\Delta x} u_j^n (u_j^n - u_{j-1}^n)$$

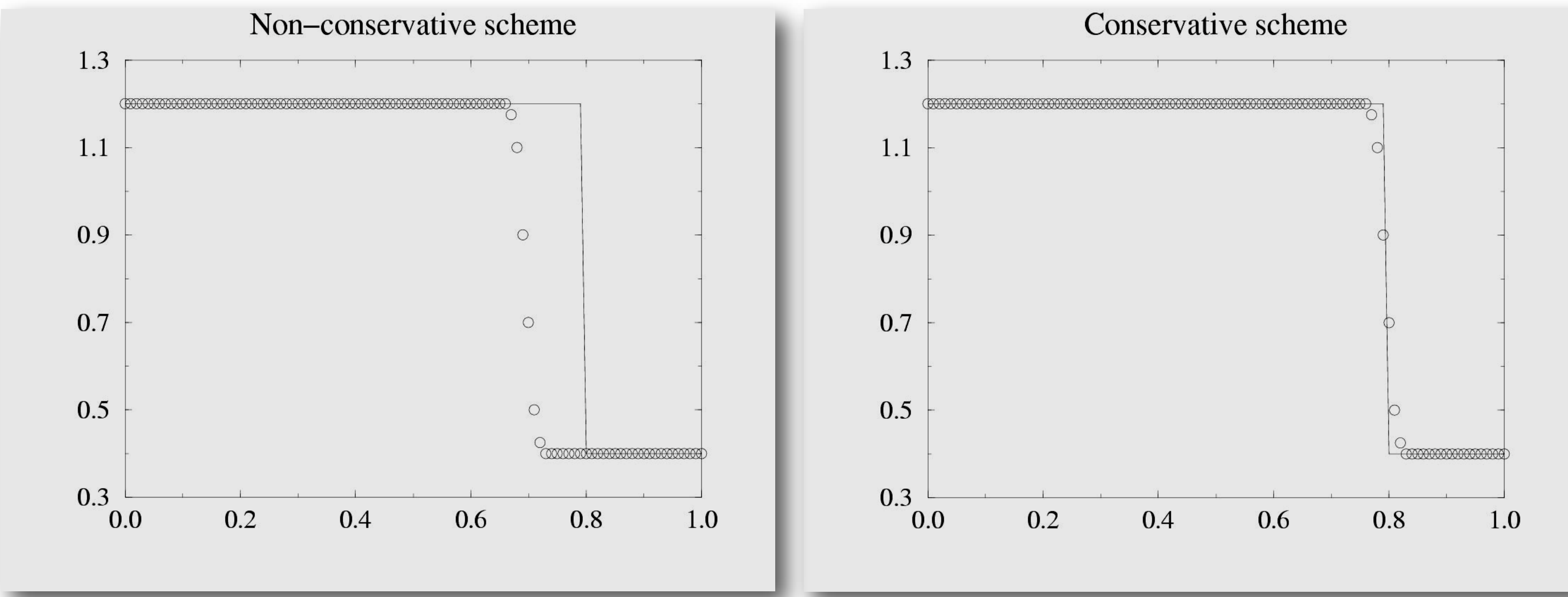

Nonlinear hyperbolic systems of CL (6)

The Lax-Wendroff theorem does not state whether the method converges. Some form of stability is required to guarantee convergence, as for linear problems (Lax equivalence theorem 1956).

The notion of total-variation stability has proved very successful. Powerful results have only been obtained for scalar conservation laws.

The conservation form of the scheme is ensured by starting with the integral version of the PDE in conservation form. By integrating the PDE within a spacetime computational cell $[x_{j-1/2}, x_{j+1/2}] \times [t^n, t^{n+1}]$ the numerical flux function is an approximation to the time-averaged flux across the interface:

$$\boxed{\hat{\vec{f}}_{j+1/2} \approx \frac{1}{\Delta t}\int_{t^n}^{t^{n+1}} \vec{f}(\vec{u}(x_{j+1/2}, t))dt}$$

The flux integral depends on the solution at the numerical interfaces during the time step $\vec{u}(x_{j+1/2}, t)$

Key idea: a possible procedure is to calculate $\vec{u}(x_{j+1/2}, t)$ by solving Riemann problems at every cell interface (Godunov)

$$\vec{u}(x_{j+1/2}, t) = \vec{u}(0; \vec{u}_j^n, \vec{u}_{j+1}^n)$$

Riemann solution for the left and right states along the ray x/t=0.

The Riemann problem

A Riemann problem is an IVP with discontinuous initial data:

$$\vec{u}_0 = \begin{cases} \vec{u}_L & \text{if } x < 0 \\ \vec{u}_R & \text{if } x > 0 \end{cases}$$

The Riemann problem is invariant under similarity transformations:

$$(x, t) \;\rightarrow\; (ax, at) \qquad\qquad a > 0$$

The solution is constant along the straight lines x/t=constant, and, hence, self-similar. It consists of constant states separated by rarefaction waves (continuous self-similar solutions of the differential equations), shock waves, and contact discontinuities (Lax 1972).

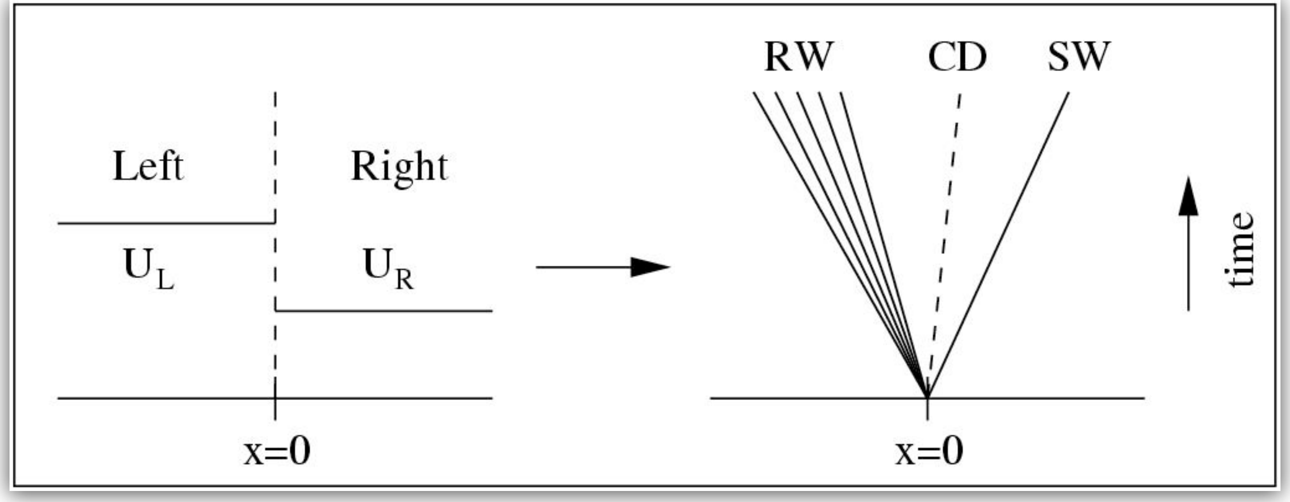

The incorporation of the exact solution of Riemann problems to compute the numerical fluxes is due to **Godunov** (1959)

Godunov's method (in a nutshell)

S. Godunov developed his method to solve the Euler equations of classical gas dynamics in the presence of shock waves. (In 1959 as part of his PhD)

1. Piecewise constant initial data: $$u_j^n \approx \frac{1}{\Delta x}\int_{x_{j-1/2}}^{x_{j+1/2}} u(x,t^n)\,dx$$

2. Solve exactly the conservation law over the time interval $[t^n, t^{n+1}]$ with initial data u_j^n (family of local Riemann problems) ⇒ $u(x_{j+1/2}, t),\ t \in [t^n, t^{n+1}]$

   The solution to the Riemann problem at $x_{j+1/2}$ is a self-similar solution, which is constant along each ray $$\frac{x - x_{j+1/2}}{t} = \text{const.}$$

   $u^*(u_L, u_R)$ is the exact solution along the ray x/t=0 with data: $u(x,0) = \begin{cases} u_L & \text{if } x < 0 \\ u_R & \text{if } x > 0 \end{cases}$

   Then, we have $u(x_{j+1/2}, t) = u^*(u_j^n, u_{j+1}^n)$

   To compute $u^*(u_j^n, u_{j+1}^n)$ the full wave structure and wave speeds must be determined in order to find where it lies in state space (computationally expensive procedure!). Δt must be small enough so that waves from Riemann problem do not travel farther than distance Δx in this time step (CFL condition).

3. Compute the numerical flux function: $$\hat{f}_{j+1/2} \approx \frac{1}{\Delta t}\int_{t^n}^{t^{n+1}} f(u(x_{j+1/2}, t))\,dt$$

When a Cauchy problem described by a set of continuous PDEs is solved in a discretized form the numerical solution is piecewise constant (collection of local Riemann problems).

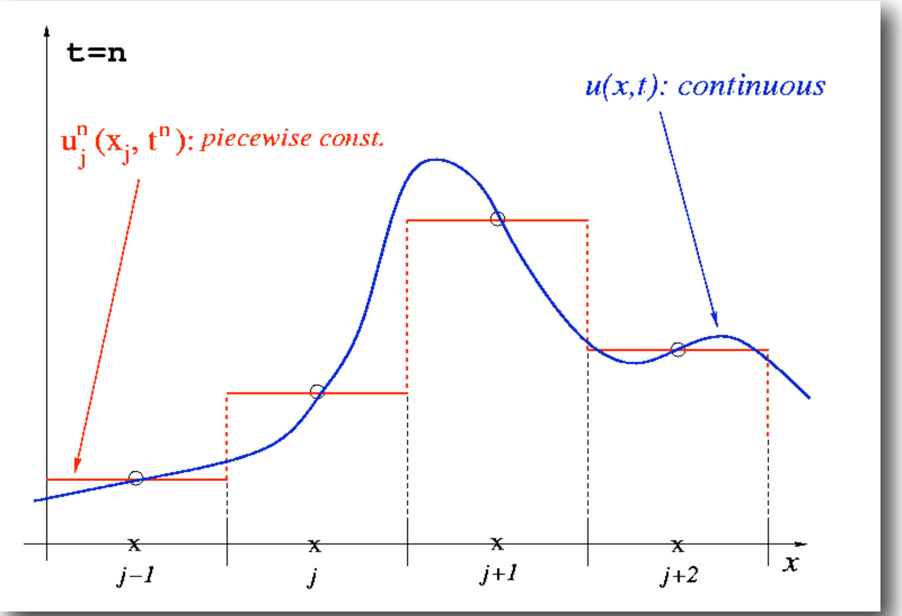

This is particularly problematic when solving the hydrodynamic equations (either Newtonian or relativistic) for compressible fluids.

Their hyperbolic, nonlinear character produces discontinuous solutions in a finite time (shock waves, contact discontinuities) even from smooth initial data!

Any FD scheme must be able to handle discontinuities in a satisfactory way.

1. **1st order accurate schemes (Lax-Friedrich):** Non-oscillatory but inaccurate across discontinuities (excessive diffusion)
2. **(standard) 2nd order accurate schemes (Lax-Wendroff):** Oscillatory across discontinuities
3. 2nd order accurate schemes with artificial viscosity
4. Godunov-type schemes (upwind High Resolution Shock Capturing schemes)

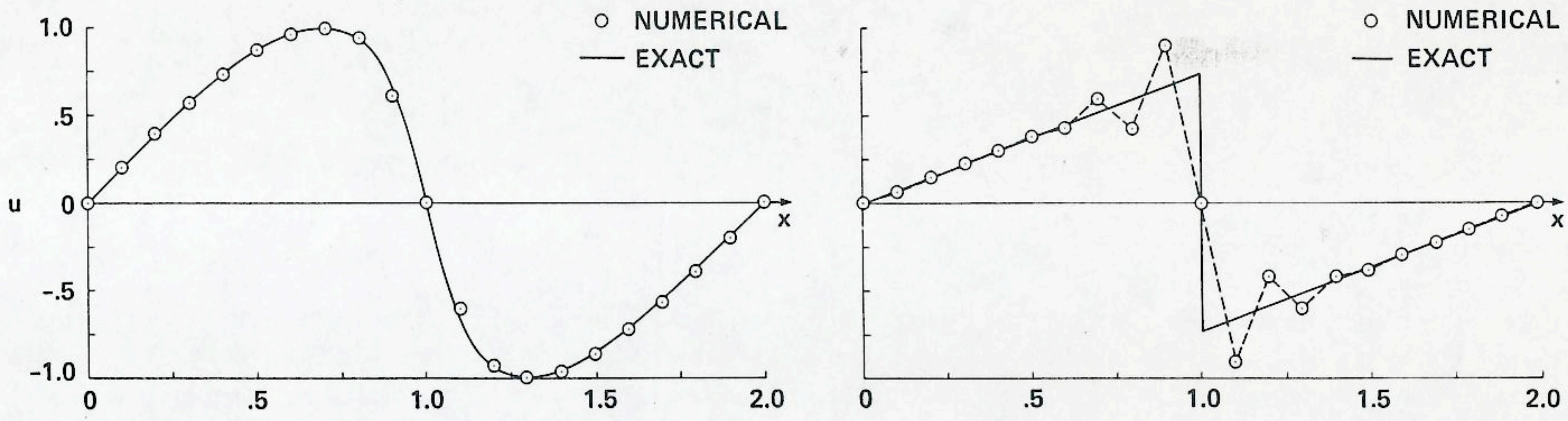

Lax-Wendroff numerical solution of Burger's equation at t=0.2 (left) and t=1.0 (right)

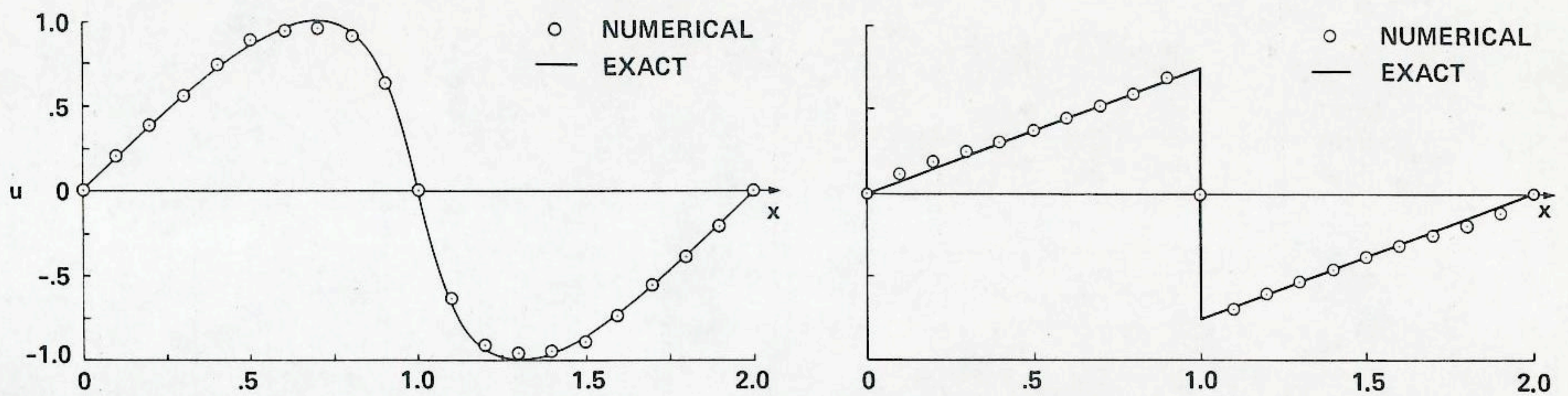

2nd order TVD numerical solution of Burger's equation at t=0.2 (left) and t=1.0 (right) rarefaction wave

shock front

courtesy of L. Rezzolla

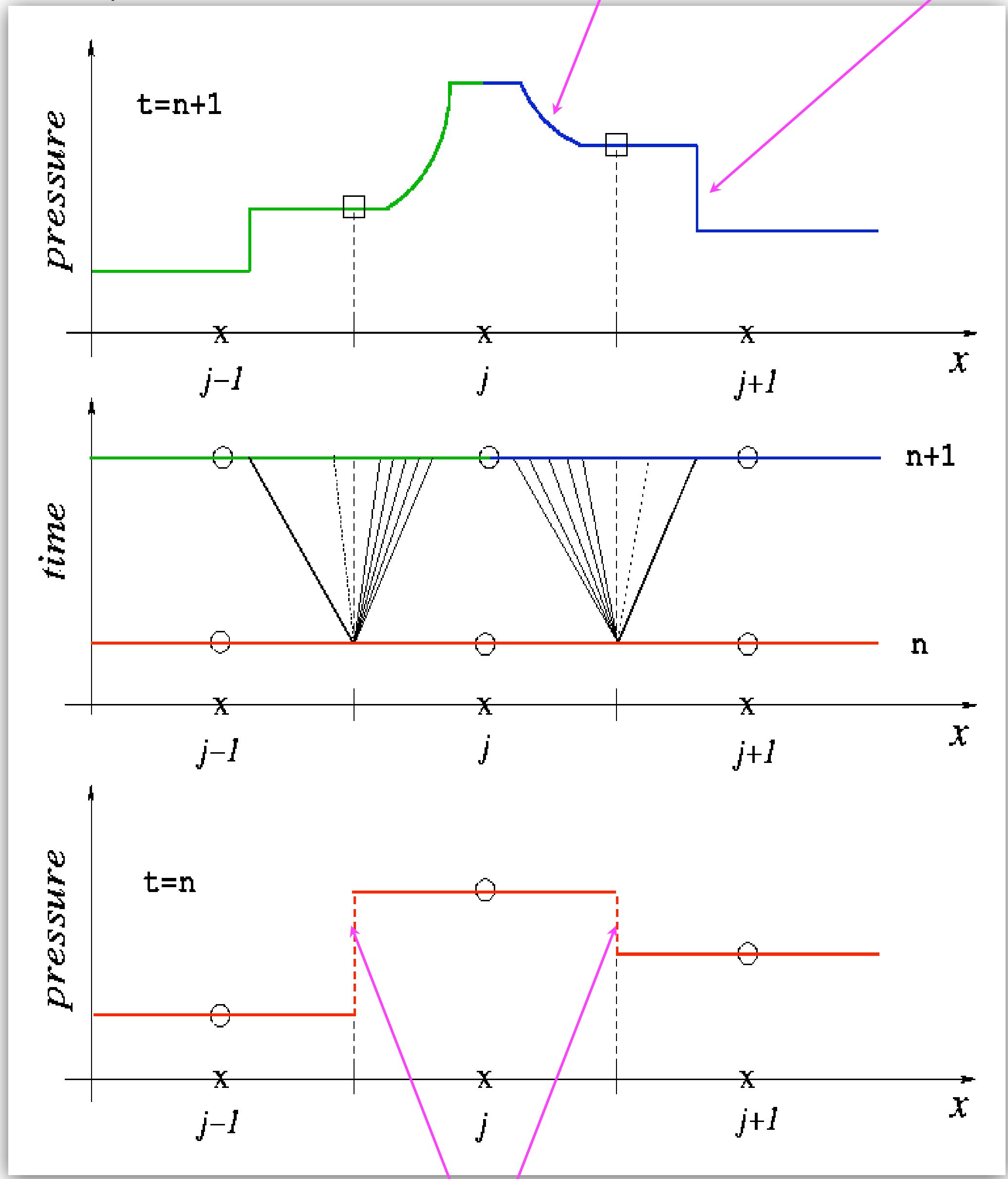

Solution at time n+1 of the two Riemann problems at the cell boundaries $x_{j+1/2}$ and $x_{j-1/2}$

Spacetime evolution of the two Riemann problems at the cell boundaries $x_{j+1/2}$ and $x_{j-1/2}$. Each problem leads to a shock wave and a rarefaction wave moving in opposite directions

Initial data at time n for the two Riemann problems at the cell boundaries $x_{j+1/2}$ and $x_{j-1/2}$

$$\mathbf{u}_j^{n+1} = \mathbf{u}_j^n - \frac{\Delta t}{\Delta x}\left(\hat{\mathbf{f}}^n_{j+\frac{1}{2}} - \hat{\mathbf{f}}^n_{j-\frac{1}{2}}\right)$$

cell boundaries where fluxes are required

Exact solution of the Riemann problem in RHD (sketch)

Derived by Martí & Müller in 1994

- Self-similar solution: $\xi=(x-x_0)/t$
- 5 regions, 3 elementary waves

- State 1: initial left state (with respect to x_0); $x_1=x_0+\xi_1 t$ ($\xi_1<0$)
- State 2 (RW): $v=v_2(\xi)$, $\rho=\rho_2(\xi)$, $p=p_2(\xi)$; $x_2=x_0+\xi_2 t$
- States 3 and 4: constant states separated by a CD; $x_3=x_0+\xi_3 t$
- State 5: initial right state. Its leftmost part is limited by the SW moving with speed ξ_4

- Unknowns: v_3, p_3, ρ_3, v_4, p_4, ρ_4 (constants), $v_2(\xi)$, $p_2(\xi)$, $\rho_2(\xi)$ (functions), and ξ_1, ξ_2, ξ_3, ξ_4 (velocity of points separating the regions).

- Solution procedure:
  First: the RH (jump) conditions across discontinuities provide 6 equations to solve for 6 variables.
  Second: the remaining relations are obtained from the condition of self-similar flow across the RW.

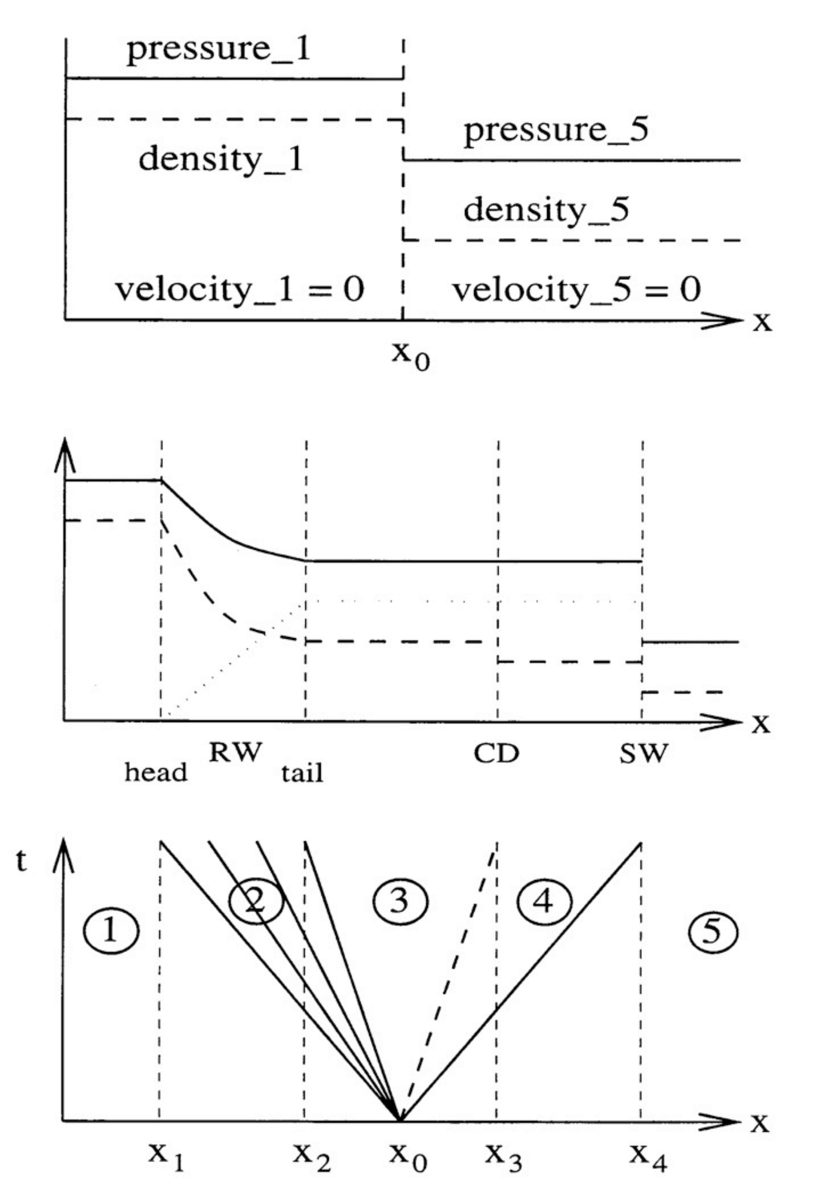

SRH eqs. (1D, Cartesian)

$$\begin{aligned}\frac{\partial(\rho W)}{\partial t}+\frac{\partial(\rho W v)}{\partial x}&=0\\ \frac{\partial(\rho h W^2 v)}{\partial t}+\frac{\partial(\rho h W^2 v^2+p)}{\partial x}&=0\\ \frac{\partial(\rho h W^2-p)}{\partial t}+\frac{\partial(\rho h W^2 v)}{\partial x}&=0\end{aligned}$$

self-similarity

$$\frac{\partial}{\partial x}=\frac{1}{t}\frac{d}{d\xi},\ \frac{\partial}{\partial t}=-\frac{\xi}{t}\frac{d}{d\xi}$$

$$\begin{aligned}(v-\xi)\frac{d\rho}{d\xi}+(1-v\xi)\rho W^2\frac{dv}{d\xi}&=0\\ (v-\xi)W^2\rho h\frac{dv}{d\xi}+(1-v\xi)\frac{dp}{d\xi}&=0\end{aligned}$$

and some algebra lead to

a self-similar flow is isoentropic

$$\frac{dp}{d\xi}=c_s^2 h\frac{d\rho}{d\xi}$$

$$\begin{aligned}(v-\xi)\frac{d\rho}{d\xi}+(1-v\xi)\rho W^2\frac{dv}{d\xi}&=0\\ (v-\xi)\rho W^2\frac{dv}{d\xi}+(1-v\xi)c_s^2\frac{d\rho}{d\xi}&=0\end{aligned}\qquad(*)$$

whose solution is

$$\boxed{\xi=\frac{v\mp c_s}{1\mp v c_s}\quad\text{(I)}}$$

on the other hand $v_1=0\rightarrow\xi_1=-c_{s1}$

solution (I) in Eq. (*) $\rightarrow W^2dv=-\frac{c_s}{\rho}d\rho$ $\longrightarrow$ $\frac{1}{2}\left[\ln\frac{1+v}{1-v}\right]_{v_1}^{v}=-\int_{\rho_1}^{\rho}\frac{c_s}{\rho}d\rho$

adiabatic flow: $p=K\rho^\gamma,\ c_s^2=\frac{\gamma(\gamma-1)p}{\rho(\gamma-1)+\gamma p}$

hence, two arbitrary states are related by: $\rho=\rho_1\left[\frac{c_s^2(\gamma-1-c_{s1}^2)}{c_{s1}^2(\gamma-1-c_s^2)}\right]^{\frac{1}{\gamma-1}}$

$$\rightarrow\frac{1}{2}\left[\ln\frac{1+v}{1-v}\right]_{v_1}^{v}=-\int_{c_{s1}}^{c_s}\frac{2}{\gamma-1-c_s^2}dc_s\rightarrow\boxed{\boxed{c_s=f(\gamma,c_{s1},v_1,v)}\quad\text{(II)}}$$

using the two equations highlighted in red allows to obtain v(x,t) and c_s(x,t) in state 2, and hence ρ and p. Finally, the continuity of the flow guarantees: $v_3=v(\xi_2)$, $p_3=p(\xi_2)$, and $\rho_3=\rho(\xi_2)$.

Exact solution of the Riemann problem in RHD (II)

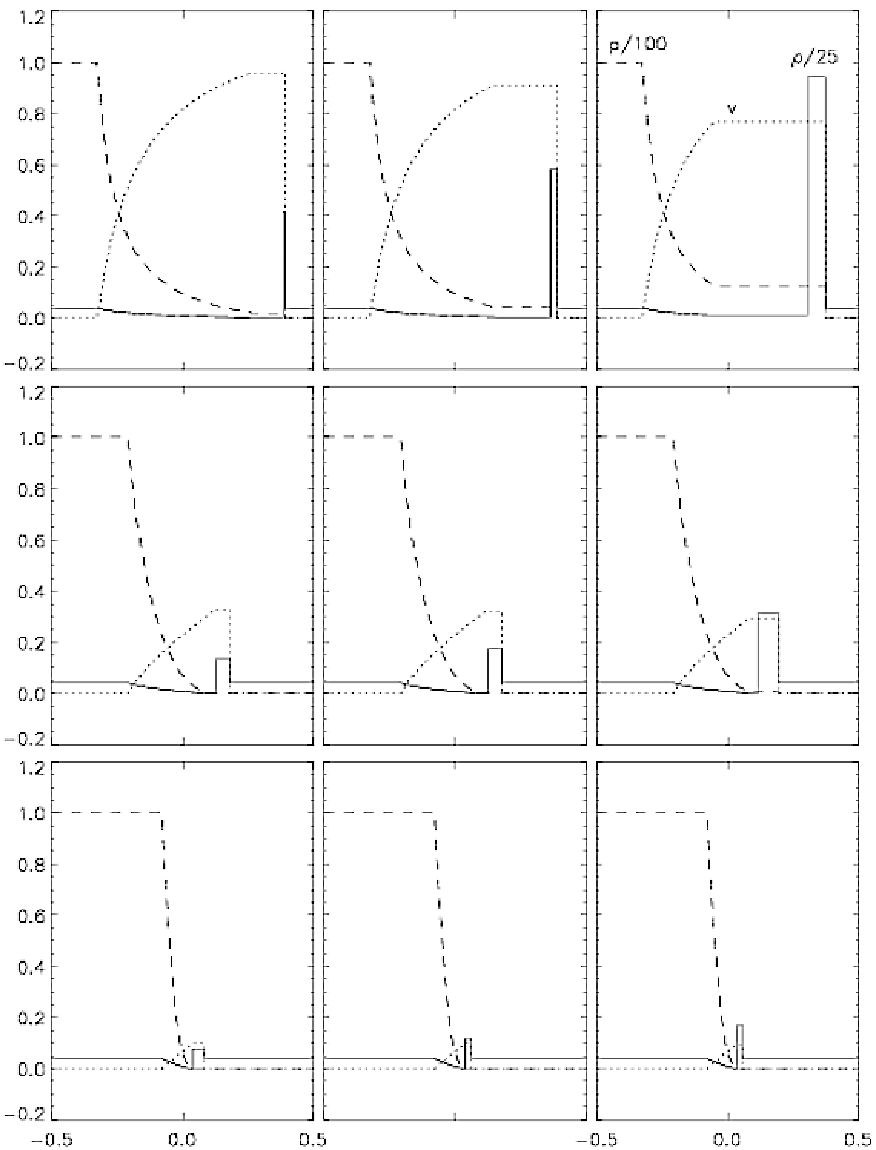

Pons, Martí & Müller 2000

Intrinsic relativistic effects: coupling of tangential velocities.

In RHD all components of the flow velocity are coupled, through the Lorentz factor, in the solution of the Riemann problem.

In addition, the specific enthalpy also couples with the tangential velocity components, which becomes significant in the thermodinamically ultrarelativistic regime.

Two Fortran codes (RIEMANN, RIEMANN-VT) are available in the Living Review Article of Martí & Müller (2003) to compute the exact solution of an arbitrary Riemann problem in SRH for an ideal gas with constant adiabatic index, both with zero and non-zero tangential speeds.

(download and try them!)

Approximate Riemann solvers

In Godunov's method the structure of the Riemann solution is "lost" in the cell averaging process (1st order in space).

The exact solution of a Riemann problem is computationally expensive, particularly in multidimensions and for complicated EoS.

Relativistic multidimensional problems: coupling of all flow velocity components through the Lorentz factor.

- Shocks: increase in the number of algebraic jump (RH) conditions.
- Rarefactions: solving a system of ODEs.

This motivated development of approximate (linearized) Riemann solvers.

They are based in the exact solution of Riemann problems corresponding to a new system of equations obtained by a suitable linearization of the original one (quasi-linear form). The spectral decomposition of the Jacobian matrices is on the basis of all solvers ("extending" ideas used for linear hyperbolic systems).

$$\frac{\partial \vec{u}}{\partial t} + \frac{\partial \vec{f}}{\partial x} = 0 \quad \Rightarrow \quad \frac{\partial \vec{u}}{\partial t} + A\frac{\partial \vec{u}}{\partial x} = 0, \quad A = \frac{\partial \vec{f}}{\partial \vec{u}} \qquad \text{(Jacobian matrix)}$$

Approach followed by an important subset of shock-capturing schemes, the so-called **Godunov-type methods** (Harten & Lax 1983; Einfeldt 1988).

HRSC schemes in Relativistic Hydrodynamics (extended from CFD)

Based on Riemann solvers (upwind methods)

see Martí & Müller 2003, Living Reviews in Relativity **www.livingreviews.org**

- Solvers relying on the exact solution of the Riemann problem (Martí & Müller 1994; Pons, Martí & Müller 2000)
  - **rPPM** (Martí & Müller 1996)
  - **Glimm's random choice method** (Wen et al. 1997)
  - **Two-shock approximation** (Balsara 1994; Dai & Woodward 1997)

- Linearized solvers: based on local linearizations of the Jacobian matrices of the vector of fluxes
  - **Roe-type Riemann solvers** (Roe-Eulderink: Eulderink 1993; LCA: Martí et al. 1991; Font et al 1994)
  - **Falle-Komissarov** (Falle & Komissarov 1996)
  - **Marquina Flux Formula** (Donat & Marquina 96)
  - ...

The exact solution of a Riemann problem is computationally expensive particularly for complex EoS and in multidimensions.

Relativistic multidimensional flows: coupling of all velocity components through the Lorentz factor.

- Shocks: increase in the number of algebraic jump (RH) conditions.
- Rarefactions: solving a system of ODEs.

Symmetric schemes with nonlinear numerical dissipation

- LW scheme with conservative TVD dissipation terms (Koide at al. 1996)
- Del Zanna & Bucciantini 2002: Third-order ENO reconstruction algorithm + spectral-decomposition-avoiding RS (LF, HLL)
- NOCD (Anninos & Fragile 2002)
- Kurganov-Tadmor scheme (Lucas-Serrano et al 2004; Shibata & Font 2005)

High-Resolution Shock-Capturing schemes

(Upwind) HRSC schemes are written in conservation form and use Riemann solvers to compute approximations to $\vec{u}(0;\vec{u}_j^n,\vec{u}_{j+1}^n)$

But, high-order central (symmetric) schemes are currently being extended to relativistic hydrodynamics (avoid use of characteristic information! Computationally cheap; high-order cell reconstruction procedures to counterbalance the inhererent diffusion).

In upwind HRSC schemes high-order of accuracy is achieved in two different ways:

1. Flux limiter methods
2. Slope limiter methods

A remark: **artificial viscosity methods**

- Idea: take a high-order finite difference scheme (e.g. Lax-Wendroff) and add an "artificial viscosity" term Q to the hyperbolic equation. Introduced by von Neumann and Richtmyer (1950) in the classical hydrodynamics equations. Q is a term accompanying the pressure of the form (e.g.):

$$Q = \begin{cases} -\alpha \dfrac{\partial v}{\partial x} & \text{if } \dfrac{\partial v}{\partial x} < 0\,,\ \dfrac{\partial \rho}{\partial t} > 0 \\ 0 & \text{otherwise} \end{cases}$$

  with $\alpha = \rho(k\Delta x)^2 \dfrac{\partial v}{\partial x}$

- <u>Damp spurious oscillations</u> (at shocks)
- Q must vanish as $\Delta t\,,\ \Delta x \rightarrow 0$

<u>Advantages</u>: easy to implement; computationally efficient.

<u>Disadvantages</u>: problem dependent; problematic for ultrarelativistic flows.

MAY & WHITE'S CODE (May & White 1966, 1967)

Spherically symmetric, relativistic, stellar collapse in comoving coordinates:

$$ds^2 = -a^2(m,t)\,dt^2 + b^2(m,t)\,dm^2 + R^2(m,t)\,(d\theta^2 + sin^2\theta\, d\phi^2)$$

m: total (barionic) rest-mass up to radius R

Mass, energy and momentum conservation: $b = \frac{1}{4\pi\rho R^2}$, $\frac{\partial\varepsilon}{\partial t} + p\frac{\partial}{\partial t}(\frac{1}{\rho}) = 0$,

$$\frac{\partial u}{\partial t} = -a(4\pi\frac{\partial p}{\partial m}R^2\frac{\Gamma}{h} + \frac{M}{R^2} + 4\pi p R)$$

Einstein equations: $\frac{\partial p}{\partial m} + \frac{1}{a}\frac{\partial a}{\partial m}\rho h = 0$, $\frac{1}{\rho R^2}\frac{\partial \rho R^2}{\partial t} = -a\frac{\partial u/\partial m}{\partial R/\partial m}$

[$h = 1 + \varepsilon + p/\rho$ (specific enthalpy) , $u = \frac{1}{a}\frac{\partial R}{\partial t}$, $\Gamma^2 = 1 - u^2 - \frac{2M}{R}$, $M = \int_0^m 4\pi R^2\rho(1+\varepsilon)\frac{\partial R}{\partial m}dm$]

EOS: $p = p(\rho, \varepsilon)$

Finite difference scheme + AV (Richtmyer-von Neumann)

$$p \rightarrow p + Q_{AV}$$

$$Q_{AV} = \begin{cases} \rho(\frac{a\Delta m}{R^2})^2\frac{\partial R^2 u}{\partial m}/\Gamma & \text{if } \frac{\partial\rho}{\partial t} > 0 \\ 0 & \text{otherwise} \end{cases}$$

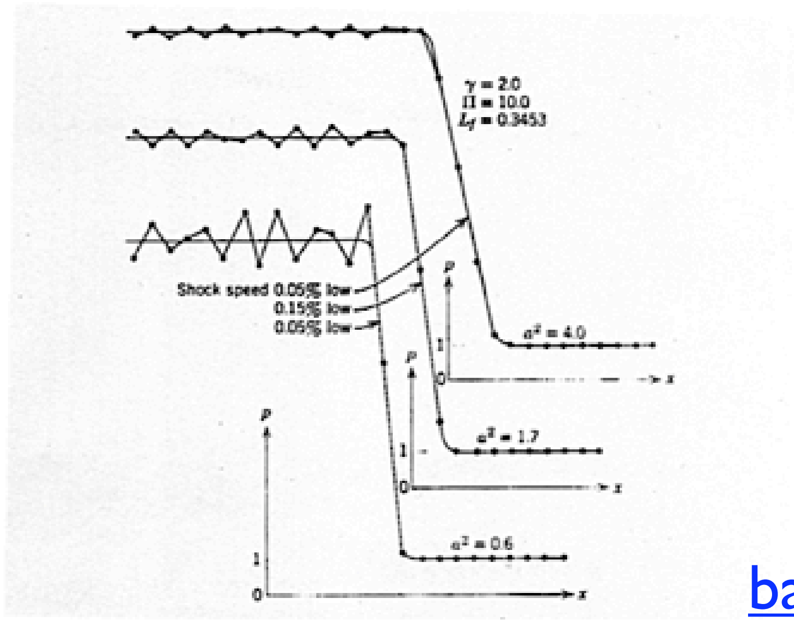

back

Flux limiter schemes vs slope limiter schemes

Flux limiter schemes: the numerical flux is obtained from a high-order flux (e.g. Lax-Wendroff) in the smooth regions and from a low order flux (e.g. the flux from some monotone method) near discontinuities:

$$\hat{f} = \hat{f}_h - (1-\Phi)(\hat{f}_h - \hat{f}_l)$$

with the limiter $\Phi \in [0,1]$ Example: the flux-corrected-transport (FCT) algorithm (Boris & Book 1973), one of the earliest high-resolution methods.

Slope limiter schemes: use of conservative polynomials to interpolate the approximate solutions within the numerical cells. The goal is to produce more accurate left and right states for the Riemann problems by substituting the mean values u_j^n (1st order) for better approximations $u_{j+1/2}^L, u_{j+1/2}^R$

The interpolation algorithms must preserve the TV-stability of the scheme. This can be achieved using monotonic functions which lead to a decrease in the total variation (total-variation-diminishing schemes, TVD, Harten 1984).

The **total variation** of a solution at t=t^n, TV(u^n), is defined as

$$\mathrm{TV}\left(u^n\right) = \sum_{j=0}^{\infty} | u_{j+1}^n - u_j^n |$$

A numerical scheme is TV-stable in TV (u^n) is bounded at all time steps.

If $\tilde{u}(x,t^n)$ is the interpolated function within the cells, satisfying

$$\mathrm{TV}\left(\tilde{u}(x,t^n)\right) \leq \mathrm{TV}\left(u^n\right)$$

then it can be proved that the whole scheme verifies $\mathrm{TV}\left(u^{n+1}\right) \leq \mathrm{TV}\left(u^n\right)$

High-Resolution Shock-Capturing schemes (2)

High-order TVD schemes were first constructed by van Leer (1979) who obtained 2nd order accuracy by using monotonic piecewise linear slopes for cell reconstruction (MUSCL algorithm):

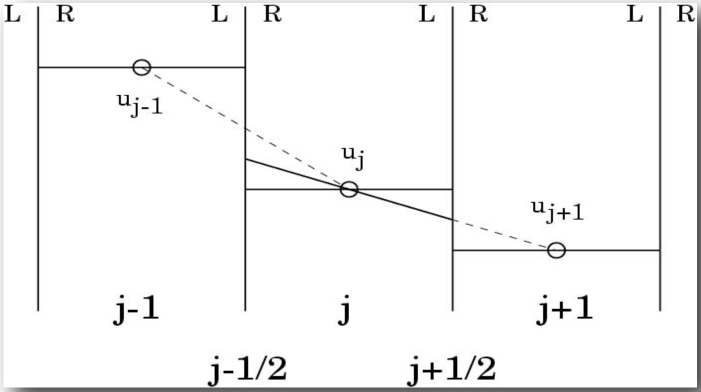

$$\vec{u}_j^{L,R} = \vec{u}_j + s_j\left(x_{j\pm1/2} - x_j\right) \qquad x_j = \frac{1}{2}\left(x_{j+1/2} + x_{j-1/2}\right)$$

$$s_j = \begin{cases} \min\left(\Delta Q_{j+1/2}, \Delta Q_{j-1/2}\right) \times \operatorname{sgn}\left(\Delta Q_{j+1/2}\right) & \text{if } \operatorname{sgn}\left(\Delta Q_{j+1/2}\right) = \operatorname{sgn}\left(\Delta Q_{j-1/2}\right) \\ 0 & \text{otherwise} \end{cases}$$

$$\Delta Q_{j+1/2} = \frac{\vec{u}_{j+1} - \vec{u}_j}{x_{j+1} - x_j}$$

The piecewise parabolic method (PPM) of Colella & Woodward (1984) provides 3rd order accuracy in space.

The TVD property implies TV-stability but can be too restrictive. In fact, TVD schemes degenerate to 1st order accuracy at extreme points (Osher & Chakravarthy 1984).

Other reconstruction alternatives exist in which some growth of the total variation is allowed:

- total-variation-bounded (TVB) schemes (Shu 1987).
- essentially nonoscillatory (ENO) schemes (Harten, Engquist, Osher & Chakravarthy 1987).
- piecewise hyperbolic method (PHM) (Marquina 1994).

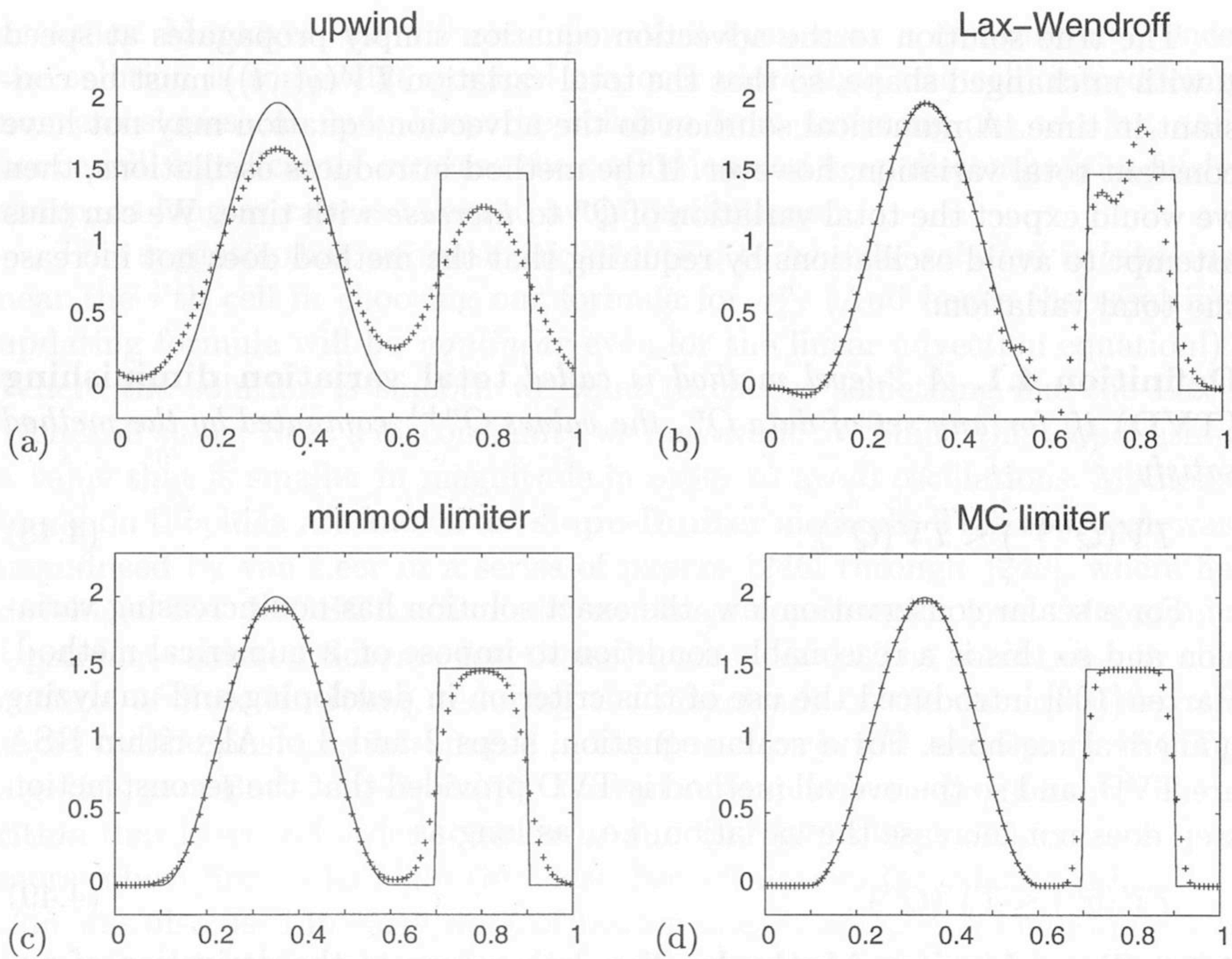

Fig. 4.8. Tests on the advection equation with different limiters. All results are at time $t = 1$, after one revolution with periodic boundary conditions

Relativistic Riemann Solvers and Flux Formulae

• Roe-type SRRS	Martí, Ibáñez & Miralles, 1991
• HLLE SRRS	Schneider et al, 1993
• Exact SRRS	Martí & Müller, 1994; Pons et al, 2000
• Two-shock approx.	Balsara, 1994
• ENO SRRS	Dolezal & Wong, 1995
• Roe GRRS	Eulderink & Mellema, 1995
• Upwind SRRS	Falle & Komissarov, 1996
• Glimm SRRS	Wen, Panaitescu & Laguna, 1997
• Iterative SRRS	Dai & Woodward, 1997
• Marquina's FF	Donat et al, 1998

Martí & Müller, 2003

Living Reviews in Relativity   www.livingreviews.org

Roe's approximate Riemann solver (I)

(P.L. Roe, J. Comput. Phys. **43**, 357-372, 1981)

Idea: determine the approximate solution by solving a quasi-linear system instead of the original nonlinear system.

Solve a modified conservation law with flux: $\vec{f} = \hat{A}\vec{u}$ Then, the linear problem reads:

$$\boxed{\frac{\partial \vec{u}}{\partial t} + \hat{A}(\vec{u}_L, \vec{u}_R)\frac{\partial \vec{u}}{\partial x} = 0}$$

To determine $\hat{A}$ Roe suggested the following conditions:

1. $\hat{A}(\vec{u}_L, \vec{u}_R)(\vec{u}_R - \vec{u}_L) = \vec{f}(\vec{u}_R) - \vec{f}(\vec{u}_L)$
2. $\hat{A}(\vec{u}_L, \vec{u}_R)$ can be diagonalized and has real eigenvalues.
3. $\hat{A}(\vec{u}_L, \vec{u}_R) \rightarrow \hat{A}(<\vec{u}>)$ smoothly as $\vec{u}_L, \vec{u}_R \rightarrow <\vec{u}>$

Condition 1 (provided 2 is fulfilled) ensures that if a single discontinuity is located at the cell interface, then the solution of the linearized problem gives the exact solution to the Riemann problem.

Condition 3 is necessary to recover the linearized algorithm (discussed before) from the nonlinear one smoothly. Once Roe's matrix is obtained for every numerical interface the numerical fluxes are computed by solving locally the linear system.

Roe's approximate Riemann solver (II)

(P.L. Roe, J. Comput. Phys. **43**, 357-372, 1981)

Roe's numerical flux:

$$\hat{\vec{f}} = \frac{1}{2}\left[\vec{f}(\vec{u}_R) + \vec{f}(\vec{u}_L) - \sum_{n=1}^{5} \left|\tilde{\lambda}_n\right| \Delta\tilde{\omega}_n \tilde{R}_n\right], \quad \vec{u}_R - \vec{u}_L = \sum_{n=1}^{5} \Delta\tilde{\omega}_n \tilde{R}_n$$

$\tilde{\lambda}_n, \tilde{R}_n$ are the eigenvalues and eigenvectors of $\hat{A}$. The tilde stands for the "Roe average".

The above expression for the flux of conserved variables is the "natural" extension of the upwind flux for characteristic variables, once the quasi-linear system has been written in diagonal form.

$$\frac{\partial \mathbf{W}}{\partial t} + \hat{\mathbf{\Lambda}} \frac{\partial \mathbf{W}}{\partial x} = 0, \quad \mathbf{W} = \mathbf{R}^{-1}\mathbf{u}, \quad \hat{\mathbf{\Lambda}} = \mathbf{R}^{-1}\mathbf{A}\mathbf{R}, \quad \hat{\mathbf{\Lambda}} = \mathrm{diag}(\hat{\lambda}_1, \hat{\lambda}_2, \cdots)$$

The upwind flux of the characteristic variables across x=x0 is given by:

$$\frac{1}{2}\left(\hat{\lambda}_i W_{iL} + \hat{\lambda}_i W_{iR} - |\hat{\lambda}_i| \Delta W_i\right), \quad \Delta W_i = W_{iR} - W_{iL}$$

which yields the Roe flux when transformed back to the conserved variables.

When computing discontinuous solutions, upwind differencing is an important tool, as the directionality of the flow (wave speeds) is accounted for. Many of the existing methods require solving Riemann problems to accomplish the appropriate splitting between wave propagation to the left and right.

Eulderink's approximate Riemann solver

(Eulderink & Mellema, A&A Supp. Ser. **110**, 587-623, 1995)

Eulderink and Mellema (1995) extended the Roe solver to compute numerical solutions of the general relativistic hydrodynamics equations.

They looked for a local linearization of the Jacobian matrices for the GR system which fulfilled the properties demanded by Roe's matrix.

It is done in terms of the average state:

$$\boxed{\tilde{\vec{w}} = \frac{\vec{w}_L + \vec{w}_R}{k_L + k_R}}$$

with $\vec{w} = \left(ku^0, ku^1, ku^2, ku^3, k\dfrac{p}{\rho h}\right), \quad k^2 = \sqrt{-g}\rho h$

The role played by ρ in the non-relativistic Roe solver as a weight for averaging is now played by k which, apart from geometrical factors, tends to ρ in the non-relativistic limit.

Relaxing condition 1 in Roe's linearization, the Roe/Eulderink solver is no longer exact for shocks but still produces accurate solutions. The main advantage is that the reduced set of conditions is fulfilled by a large number of averages, a typical choice being the arithmetic mean (approach followed in the Roe-type Riemann solvers).

Roe's original idea has been exploited in the so-called local characteristic approach (local linearization of the system by defining at each grid point a set of characteristic variables obeying a system of uncoupled scalar equations). Based on this approach are the methods developed by Marquina (PHM), and by Dolezal and Wong (ENO).

Falle & Komissarov Riemann solver

(Falle & Komissarov, MNRAS **278**, 586, 1996)

Falle and Komissarov proposed several approximate special relativistic Riemann solvers relying on a primitive-variable formulation of the relativistic hydrodynamics equations in quasi-linear form:

$$\frac{\partial \vec{V}}{\partial t} + B\frac{\partial \vec{V}}{\partial x} = 0, \qquad B = B(\vec{V}), \qquad \vec{V} = \left(\rho, v_x, v_y, v_z, p\right)$$

(or any other set of primitive variables)

A local linearization of this system allows to obtain the solution of the Riemann problem, and hence the numerical fluxes.

Relativistic HLL method

(Schneider et al, J. Comput. Phys. **105**, 92, 1993)

Schneider et al proposed to use the method of Harten, Lax, and van Leer (1983) to integrate the equations of SR hydrodynamics. This method avoids the explicit use of the spectral decomposition of the Jacobian matrices. The original Riemann problem is approximated with a single intermediate state:

$$\vec{u}^{\,\mathrm{HLL}}\left(\frac{x}{t};\vec{u}_L,\vec{u}_R\right) = \begin{cases} \vec{u}_L & \text{for } x < a_L t \\ \dfrac{a_R\vec{u}_R - a_L\vec{u}_L - \vec{f}(\vec{u}_R) + \vec{f}(\vec{u}_L)}{a_R - a_L} & \text{for } a_L t \le x \le a_R t \\ \vec{u}_R & \text{for } x > a_R t \end{cases}$$

$$\boxed{\begin{gathered}\hat{\vec{f}}^{\,\mathrm{HLL}} = \frac{a_R^+\vec{f}(\vec{u}_L) - a_L^-\vec{f}(\vec{u}_R) + a_R^+a_L^-(\vec{u}_R - \vec{u}_L)}{a_R^+ - a_L^-} \\ a_L^- = \min(0, a_L), \qquad a_R^+ = \max(0, a_R)\end{gathered}}$$

a_L, a_R are lower and upper bounds for the smallest and largest signal velocities (such good estimates are an essential ingredient of the HLL scheme). Einfeldt proposed calculating them based on the smallest and largest eigenvalues of Roe’s matrix.

Marquina´s flux formula

(Donat & Marquina, J. Comput. Phys. **125**, 42, 1996; Donat et al, *ibid*, **146**, 58, 1998)

Donat & Marquina extended to systems a numerical flux formula first proposed by Shu & Osher for scalar equations.

In the scalar case and for characteristic wave speeds which do not change sign at a given numerical interface, Marquina's flux formula is identical to Roe's flux. Otherwise, the scheme switches to the more viscous, entropy-satisfying local Lax-Friedrichs scheme.

In the case of systems the combination of Roe and local-Lax-Friedrichs solvers is carried out in each characteristic field after the local linearization and decoupling of the equations. However, contrary to Roe's and other linearized methods, Marquina's method is not based on any averaged intermediate state at cell interfaces.

Marquina's numerical flux:

$$\boxed{\hat{\vec{f}}^{\mathrm{M}}(\vec{u}_L,\vec{u}_R)=\sum_p\left(\phi_+^p\vec{r}^{\,p}(\vec{u}_L)+\phi_-^p\vec{r}^{\,p}(\vec{u}_R)\right)}$$

$\vec{r}^{\,p}(\vec{u}_L), \vec{r}^{\,p}(\vec{u}_R)$ are the right-eigenvectors of the Jacobian matrices $A(\vec{u}_L), A(\vec{u}_R)$

The local characteristic fluxes ϕ_+^p, ϕ_-^p are obtained from the sided local characteristic variables and fluxes (and taking into account possible sign changes of the eigenvalues at cell interfaces).

$$\begin{aligned} w_L^p &= \vec{l}^p(\vec{u}_L)\cdot\vec{u}_L, \qquad \Phi_L^p = \vec{l}^p(\vec{u}_L)\cdot\vec{f}(\vec{u}_L) \\ w_R^p &= \vec{l}^p(\vec{u}_R)\cdot\vec{u}_R, \qquad \Phi_R^p = \vec{l}^p(\vec{u}_R)\cdot\vec{f}(\vec{u}_R) \end{aligned}$$

$\vec{l}^p(\vec{u}_L), \vec{l}^p(\vec{u}_R)$ left-eigenvectors

Relativistic Glimm's method

(Wen, Panaitescu, and Laguna, ApJ, **486**, 919, 1997)

Wen, Panaitescu, and Laguna extended Glimm's random choice method to one-dimensional special relativistic hydrodynamics.

In the random choice method, given two adjacent states $\mathbf{u}_j^n$, $\mathbf{u}_{j+1}^n$ at time t^n the value of the numerical solution at time $t^{n+1/2}$ and position $x_{j+1/2}$ is given by the exact solution $\mathbf{u}(x,t)$ of the Riemann problem evaluated at a randomly chosen point inside zone (j,j+1) i.e.:

$$\vec{u}_{j+\frac{1}{2}}^{n+\frac{1}{2}} = \vec{u}\left(\frac{(j+\xi_n)\Delta x}{\left(n+\frac{1}{2}\right)\Delta t}; \vec{u}_j^n, \vec{u}_{j+1}^n\right)$$

where ξ_n is a random number in the interval [0,1].

Besides being conservative (on average), the main advantages of Glimm's method are that it produces both completely sharp shocks and contact discontinuities, and that is free of diffusion.

Extension of the method to 2D via operator splitting investigated by Colella (not fully accomplished).

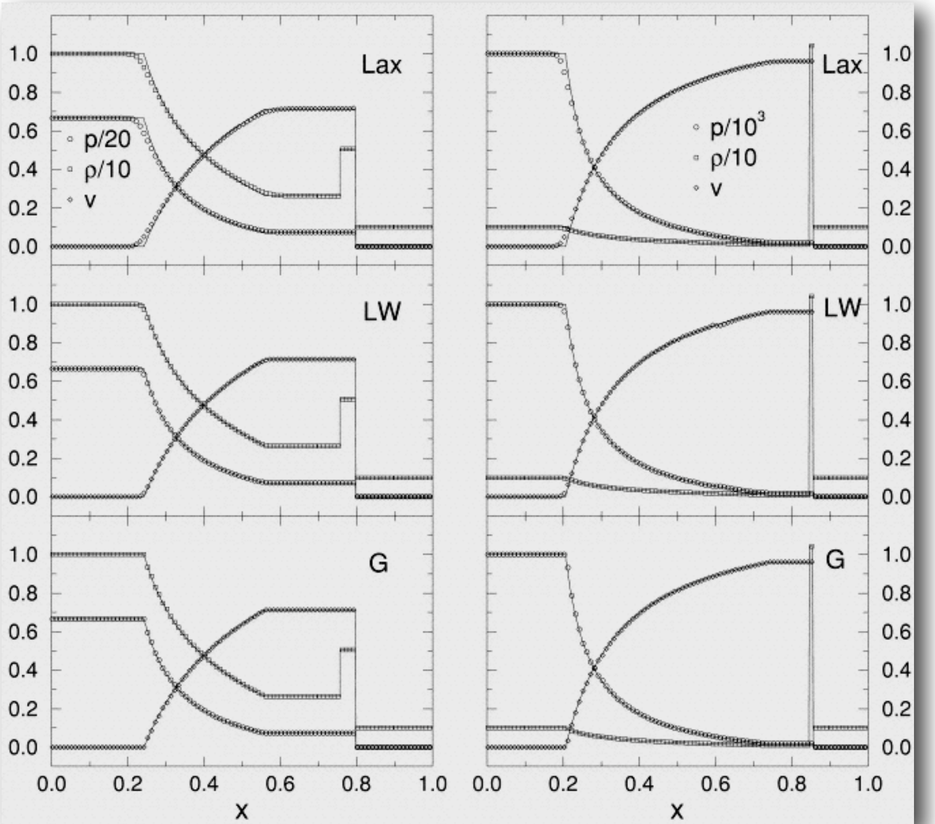

HRSC schemes using characteristic information (lists incomplete)

Code	Basic characteristics
Roe type-l (MI91,RI96,FM99)	Riemann solver of Roe type with arithmetic averaging; monotonicity preserving, linear reconstruction of primitive variables; 2nd order time stepping: predictor-corrector (MI91,RI96); standard scheme (FM99)
Roe-Eulderink (Eu93)	Linearized Riemann solver based on Roe averaging; 2nd order accuracy in space and time
LCA-phm (MM92)	Local linearization and decoupling of the system; PHM reconstruction of characteristic fluxes; 3rd order TVD preserving RK method for time stepping
LCA-eno (DW95)	Local linearization and decoupling of the system; high order ENO reconstruction of characteristic split fluxes; high order TVD preserving RK methods for time stepping
rPPM (MM96)	Exact (ideal gas) Riemann solver; PPM reconstruction of primitive variables; 2nd order accuracy in time by averaging states in the domain of dependence of zone interfaces
Falle-Komissarov (FK96)	Approximate Riemann solver based on local linearizations of the RHD equations in primitive form; monotonic linear reconstruction of p, ρ and u^i; 2nd order predictor-corrector time stepping
MFF-ppm (MM97,AI99)	Marquina's flux formula for numerical flux computation; PPM reconstruction of primitive variables; 2nd and 3rd order TVD preserving RK methods for time stepping
MFF-eno/phm (DF98)	Marquina's flux formula for numerical flux computation; upwind biased ENO/PHM reconstruction of characteristic fluxes; 2nd and 3rd order TVD preserving RK methods for time stepping
MFF-l (FM99)	Marquina's flux formula for numerical flux computation; monotonic linear reconstruction of primitive variables; standard 2nd order finite difference algorithms for time stepping
Flux split (FM99)	TVD flux-split second order method
rGlimm (WP97)	Glimm's method applied to RHD equations in primitive form; 1st order accuracy in space and time
rBS (YC97)	Relativistic beam scheme solving equilibrium limit of relativistic Boltzmann equation; distribution function approximated by discrete beams of particles reproducing appropriate moments; 1st and 2nd order TVD, 2nd and 3rd order ENO schemes

MI91: Martí et al. 1991; MM92: Martí et al. 1992; Eu93: Eulderink 1993; DW95: Dolezal & Wong 1995; MM96: Martí & Müller 1996; FK96: Falle & Komissarov 1996; RI96: Romero et al. 1996; WP97: Wen et al. 1997; YC97: Yang et al. 1997; DF98: Donat et al. 1998; FM99: Font et al . 1999

Martí & Müller 2003, Living Reviews in Relativity www.livingreviews.org

HRSC schemes sidestepping characteristic information

Code	Main features
RHLLE (SK93)	Harten-Lax-van Leer-Einfeldt approximate Riemann solver; monotonic linear reconstruction of conserved/primitive variables; 2nd order accuracy in space and time.
sTVD (KN96)	Davis (1984) symmetric TVD scheme with nonlinear numerical dissipation; 2nd order accuracy in space and time.
rAW (So99)	Global and local (1st order) and differential (2nd order) artificial wind methods.
sCENO (DB02)	Symmetric first order numerical flux (HLL, local Lax-Friedrichs); high-order (convex) ENO interpolation; 2nd and 3rd order TVD-preserving RK methods for time stepping.
NOCD (AF02)	Non-oscillatory central difference scheme; 2nd order accuracy in space (MUSCL-type piecewise linear reconstruction) and time (two step predictor-corrector scheme).
KT (LS04, SF05)	Kurganov-Tadmor semi-discrete central scheme; 2nd & 3rd order accuracy in space (MUSCL & PPM reconstruction) and time (conservative RK methods).

SK93: Schneider et al 1993; KN96: Koide et al 1996; So99: Sokolov 1999; DB02: Del Zanna & Bucciantini 2002; AF02: Anninos & Fragile 2002; LS04: Lucas-Serrano et al 2004; SF05: Shibata & Font 2005.

Other approaches (1)

Code	Main features
	Artificial Viscosity
AV-mono (CW84,HSW84)	Non-conservative formulation of the RHD equations (transport differencing, internal energy equation); AV extra term in the momentum flux; monotonic 2nd order transport differencing; explicit time stepping.
cAV-implicit (NW86)	AV-mono + consistent AV + adaptive mesh + implicit time stepping
cAV-mono (AF02)	AV-mono + consistent bulk scalar and tensorial AV + monotonic 2nd order transport differencing
	Flux Corrected Transport
FCT-Iw (Du91)	Non-conservative formulation of the RHD equations (transport differencing, equation for ρhW); explicit 2nd order LW scheme with FCT algorithm.
SHASTA-c (SK93)	FCT algorithm based on SHASTA (Boris & Book 1973); advection of conserved variables.

CW84: Centrella & Wilson 1984; HSW84: Hawley, Smarr & Wilson 1984; NW86: Norman & Winkler 1986; AF02: Anninos & Fragile 2002; Du91: Dubal 1991; SK93: Schneider et al 1991.

Other approaches (2)

Code	Main features
	van Putten
van Putten (vP93)	RMHD equations in constraint-free divergence form; evolution of integrated variational parts of conserved quantities; smoothing algorithm in numerical differentiation step; leapfrog for time stepping.
	Smoothed Particle Hydrodynamics
SPH-AV-0 (Ma91, LM93)	Specific internal energy equation; AV extra terms in momentum and energy equations; 2nd order time stepping (Ma91: predictor-corrector; LM93: RK)
SPH-AV-1 (Ma91)	Time derivatives in SPH equations include variations in smoothing length and mass per particle; Lorentz factor terms treated more consistently; otherwise same as SPH-AV-0.
SPH-AV-2 (Ma91)	Total energy equation; otherwise same as SPH-AV-1.
SPH-cAV-c (SR99)	RHD equations in conservation form; consistent AV.
SPH-RS-c (CM97)	RHD equations in conservation form; dissipation terms constructed in analogy to terms in Riemann-solver-based methods.

vP93: van Putten 1993; Ma91: Mann 1991; LM93; Laguna et al 1993; SR99: Siegler & Riffert 1999; CM97: Chow & Monaghan 1997.

A standard implementation of a HRSC scheme

1. Time update:

Conservation form algorithm

$$\mathbf{u}_j^{n+1} = \mathbf{u}_j^n - \frac{\Delta t}{\Delta x}\left(\hat{\mathbf{f}}^n_{j+\frac{1}{2}} - \hat{\mathbf{f}}^n_{j-\frac{1}{2}}\right)$$

In practice: 2nd or 3rd order time accurate, conservative Runge-Kutta schemes (Shu & Osher 1989; MoL)

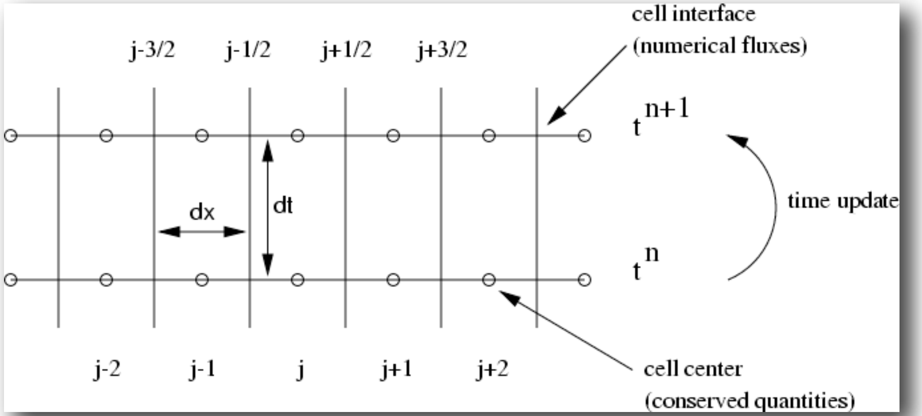

2. Cell reconstruction: Piecewise constant (Godunov), linear (MUSCL, MC, van Leer), parabolic (PPM, Colella & Woodward) interpolation procedures of state-vector variables from cell centers to cell interfaces.

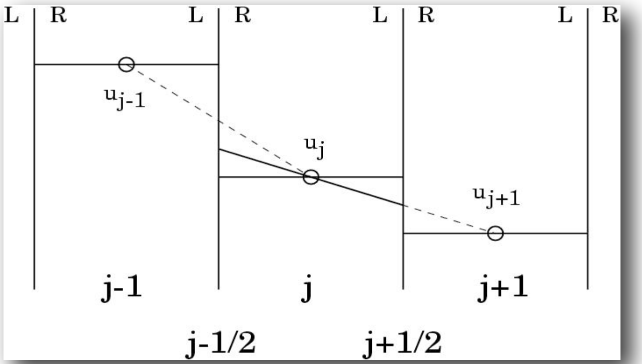

MUSCL minmod reconstruction (piecewise linear)

3. Numerical fluxes: Approximate Riemann solvers (Roe, HLLE, Marquina). Explicit use of the spectral information of the system

$$\hat{\vec{f}}_i = \frac{1}{2}\left[\vec{f}_i(w_R) + \vec{f}_i(w_L) - \sum_{n=1}^{5} \left|\widetilde{\lambda}_n\right| \Delta\widetilde{\omega}_n \widetilde{R}_n\right]$$

$$\mathrm{U}(w_R) - \mathrm{U}(w_L) = \sum_{n=1}^{5} \Delta\widetilde{\omega}_n \widetilde{R}_n$$

Source terms

Most "conservation laws" include source terms (e.g. relativistic hydrodynamics equations)

$$\frac{\partial \vec{u}}{\partial t} + \frac{\partial \vec{f}(\vec{u})}{\partial x} = \vec{s}(\vec{u})$$

Two basic ways to handle source terms:

1. Unsplit methods: a single formula advances the full equation over one time step

$$\mathbf{u}_j^{n+1} = \mathbf{u}_j^n - \frac{\Delta t}{\Delta x}\left(\hat{\mathbf{f}}^n_{j+\frac{1}{2}} - \hat{\mathbf{f}}^n_{j-\frac{1}{2}}\right) + \Delta t \mathbf{s}_j$$

This algorithm can be improved by introducing succesive substeps for the time update (e.g. predictor-corrector, conservative high-order RK schemes, …)

2. Fractional step (splitting methods): split equation into different pieces (transport + sources) and apply appropriate methods for each independent piece: $\vec{u}^{n+1} = L_s^{\Delta t} L_f^{\Delta t} \vec{u}^n$ (Godunov splitting, 1st order)

(a) First step (PDE): $\dfrac{\partial \vec{u}}{\partial t} + \dfrac{\partial \vec{f}(\vec{u})}{\partial x} = 0 \;\rightarrow\; \vec{u}^*$

(b) Second step (ODE): $\dfrac{\partial \vec{u}^*}{\partial t} = \vec{s}(\vec{u}^*) \;\rightarrow\; \vec{u}^{n+1}$

2nd order accuracy (assuming each method is 2nd order) can be obtained using the Strang splitting:

$$\vec{u}^{n+1} = L_s^{\Delta t/2} L_f^{\Delta t} L_s^{\Delta t/2} \vec{u}^n$$

$$\vec{u}^n \xrightarrow[\text{source}]{\frac{\Delta t}{2}} \vec{u}^* \xrightarrow[\text{transport}]{\Delta t} \vec{u}^{**} \xrightarrow[\text{source}]{\frac{\Delta t}{2}} \vec{u}^{n+1}$$

Multidimensional problems

$$\frac{\partial \vec{u}}{\partial t} + \frac{\partial \vec{f}(\vec{u})}{\partial x} + \frac{\partial \vec{g}(\vec{u})}{\partial y} + \frac{\partial \vec{h}(\vec{u})}{\partial z} = \vec{s}(\vec{u})$$

- Dimensional splitting $\vec{u}^{\,n+1}_{i,j,k} = L_s^{\Delta t/2} L_h^{\Delta t} L_g^{\Delta t} L_f^{\Delta t} L_s^{\Delta t/2} \vec{u}^{\,n}_{i,j,k}$

where L_f, L_g, and L_h stand for the operators associated, respectively, with the 1D systems (PDEs): $\frac{\partial \vec{u}}{\partial t} + \frac{\partial \vec{f}(\vec{u})}{\partial x} = 0 \qquad \frac{\partial \vec{u}}{\partial t} + \frac{\partial \vec{g}(\vec{u})}{\partial y} = 0 \qquad \frac{\partial \vec{u}}{\partial t} + \frac{\partial \vec{h}(\vec{u})}{\partial z} = 0$

and L_s is the operator which solves a system of ODEs of the form:

$$\frac{\partial \vec{u}}{\partial t} = \vec{s}(\vec{u})$$

- Method of lines

$$\frac{d\vec{u}_{i,j,k}(t)}{dt} = -\frac{\hat{\vec{f}}_{i+1/2,j,k} - \hat{\vec{f}}_{i-1/2,j,k}}{\Delta x} - \frac{\hat{\vec{g}}_{i,j+1/2,k} - \hat{\vec{g}}_{i,j-1/2,k}}{\Delta y} - \frac{\hat{\vec{h}}_{i,j,k+1/2} - \hat{\vec{h}}_{i,j,k-1/2}}{\Delta z} + \vec{s}_{i,j,k}$$

where the numerical fluxes are given by

$$\hat{\vec{f}}_{i+1/2,j,k} = \vec{f}(\vec{u}_{i-p,j,k}, \vec{u}_{i-p+1,j,k}, \cdots, \vec{u}_{i+p,j,k})$$

$$\hat{\vec{g}}_{i,j+1/2,k} = \vec{g}(\vec{u}_{i,j-p,k}, \vec{u}_{i,j-p+1,k}, \cdots, \vec{u}_{i,j+p,k})$$

$$\hat{\vec{h}}_{i,j,k+1/2} = \vec{h}(\vec{u}_{i,j,k-p}, \vec{u}_{i,j,k-p+1}, \cdots, \vec{u}_{i,j,k+p})$$

Solution procedure of the GRMHD equations

$$\frac{1}{\sqrt{-g}}\left(\frac{\partial\sqrt{\gamma}\mathbf{U}}{\partial t}+\frac{\partial\sqrt{-g}\mathbf{F}^i}{\partial x^i}\right)=\mathbf{S}$$

- Same HRSC as for the GRHD equations
- Wave structure information obtained
- Primitive variable recovery more involved

Details: Antón, Zanotti, Miralles, Martí, Ibáñez, Font & Pons, ApJ (2006)

$$\frac{\partial\sqrt{\gamma}\,B^i}{\partial x^i}=0$$

The divergence-free constraint is not guaranteed to be satisfied numerically when updating the B-field with a HRSC scheme in conservation form.

An ad-hoc scheme has to be used to update the magnetic field components.

Main physical implication of divergence constraint is that the magnetic flux through a closed surface is zero: essential to the constrained transport (CT) scheme (Evans & Hawley 1988, Tóth 2000).

$$\Phi_{\mathrm{T}}=\oint_{\hat{S}=\partial\hat{V}}\vec{B}^*\cdot d\vec{\hat{S}}=\int_{\hat{V}}\vec{\hat{\nabla}}\cdot\vec{B}^* d\hat{V}=0$$

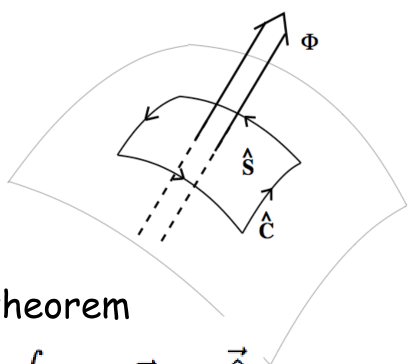

For any given surface, the time variation of the magnetic flux across the surface is:

Stokes theorem

$$\frac{\partial\Phi}{\partial t}=\frac{\partial}{\partial t}\int_{\hat{S}}\vec{B}^*\cdot d\vec{\hat{S}}=\int_{\hat{S}}\left(\vec{\hat{\nabla}}\times\vec{v}^*\times\vec{B}^*\right)\cdot d\vec{\hat{S}}=-\int_{\hat{S}}\left(\vec{\hat{\nabla}}\times\vec{E}^*\right)\cdot d\vec{\hat{S}}=-\oint_{\hat{C}=\partial\hat{S}}\vec{E}^*\cdot d\vec{l}$$

Induction equation

The magnetic flux through a surface can be calculated as the line integral of the electric field along its boundary.

Magnetic field evolution: flux-CT (1)

Numerical implementation (e.g. in axisymmetry):

Assumption: B-field components constant at each cell surface
E-field components constant along each cell edge

$$\frac{\partial \Phi_r}{\partial t} = \Delta \hat{S}_r \frac{\partial}{\partial t} B^{*r} = [E^*_\varphi \Delta \hat{l}_\varphi]_a - [E^*_\varphi \Delta \hat{l}_\varphi]_c$$

$$\frac{\partial \Phi_\theta}{\partial t} = \Delta \hat{S}_\theta \frac{\partial}{\partial t} B^{*\theta} = [E^*_\varphi \Delta \hat{l}_\varphi]_c - [E^*_\varphi \Delta \hat{l}_\varphi]_a$$

$$\frac{\partial \Phi_\varphi}{\partial t} = \Delta \hat{S}_\varphi \frac{\partial}{\partial t} B^{*\varphi} = [E^*_r \Delta \hat{l}_r]_c - [E^*_r \Delta \hat{l}_r]_a + [E^*_\theta \Delta \hat{l}_\theta]_d - [E^*_\theta \Delta \hat{l}_\theta]_b$$

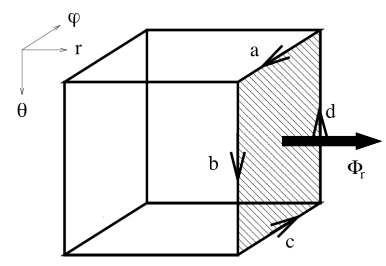

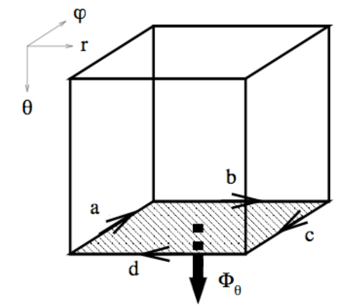

$$[E^*_\theta \Delta \hat{l}_\theta]_b = [E^*_\theta \Delta \hat{l}_\theta]_d$$

$$[E^*_r \Delta \hat{l}_r]_b = [E^*_r \Delta \hat{l}_r]_d$$

(axisymmetry condition)

Evolution equations for the B-field (CT scheme)

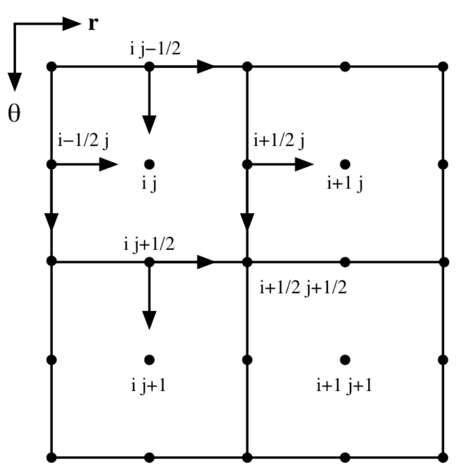

The polodial (r and θ) B-field components are defined at cell interfaces (staggered grid)

The total magnetic flux through the cell interfaces is given by:

$$\Phi_{\mathrm{T}\ i\ j} = \Phi_{r\ i+\frac{1}{2}\ j} - \Phi_{r\ i-\frac{1}{2}\ j} + \Phi_{\theta\ i\ j+\frac{1}{2}} - \Phi_{\theta\ i\ j-\frac{1}{2}}$$

$$\left.\frac{\partial \Phi_\mathrm{T}}{\partial t}\right|_{i\ j} = 0$$

If the initial data satisfy the divergence constraint, it will be preserved during the evolution

Magnetic field evolution: flux-CT (2)

Discretisation:

$$\left.\frac{\partial B^{*r}}{\partial t}\right|_{i+\frac{1}{2}\ j} = \frac{\sin\theta_{j+\frac{1}{2}}\ E^*_{\varphi\ i+\frac{1}{2}\ j+\frac{1}{2}} - \sin\theta_{j-\frac{1}{2}}\ E^*_{\varphi\ i+\frac{1}{2}\ j-\frac{1}{2}}}{r_{i+\frac{1}{2}\ j}\ \Delta(\cos\theta)_j}$$

$$\left.\frac{\partial B^{*\theta}}{\partial t}\right|_{i\ j+\frac{1}{2}} = 2\ \frac{r_{i+\frac{1}{2}}\ E^*_{\varphi\ i+\frac{1}{2}\ j+\frac{1}{2}} - r_{i-\frac{1}{2}}\ E^*_{\varphi\ i-\frac{1}{2}\ j+\frac{1}{2}}}{\Delta r_i^2}$$

$$\left.\frac{\partial B^{*\varphi}}{\partial t}\right|_{i\ j} = \frac{2\Delta r_i}{\Delta\theta_j \Delta r_i^2}\left[E^*_{r\ i\ j+\frac{1}{2}} - E^*_{r\ i\ j-\frac{1}{2}}\right] - \frac{2}{\Delta r_i^2}\left[r_{i+\frac{1}{2}}\ E^*_{\theta\ i+\frac{1}{2}\ j} - r_{i-\frac{1}{2}}\ E^*_{\theta\ i-\frac{1}{2}\ j}\right]$$

Equations used by the code to update the B-field.

The only remaining aspect is an explicit expression for the E-field.

The E-field components can be calculated from the numerical fluxes of the conservation equations for the B-field. Done solving Riemann problems at cell interfaces (characteristic information of the flux-vector Jacobians incorporated in the B-field evolution).

This procedure is only valid for r and θ E-field components.

$$E^*_{r\ i\ j+\frac{1}{2}} = -\left[v^{*\theta}B^{*\varphi} - v^{*\varphi}B^{*\theta}\right]_{i\ j+\frac{1}{2}} = (\boldsymbol{F}^\theta)^\varphi_{i\ j+\frac{1}{2}}$$

$$E^*_{\theta\ i+\frac{1}{2}\ j} = -\left[v^{*\varphi}B^{*r} - v^{*r}B^{*\varphi}\right]_{i+\frac{1}{2}\ j} = -(\boldsymbol{F}^r)^\varphi_{i+\frac{1}{2}\ j}$$

$$E^*_{\varphi\ i+\frac{1}{2}\ j+\frac{1}{2}} = -\left[v^{*r}B^{*\theta} - v^{*\theta}B^{*r}\right]_{i+\frac{1}{2}\ j+\frac{1}{2}}$$

Balsara & Spicer (1999) proposed a practical way to compute the φ component of the E-field from the numerical fluxes in adjacent interfaces.

<u>Resulting scheme</u>

$$E^*_{\varphi\ i+\frac{1}{2}\ j+\frac{1}{2}} = -\frac{1}{4}\left[(\boldsymbol{F}^r)^\theta_{i\ j+\frac{1}{2}} + (\boldsymbol{F}^r)^\theta_{i+1\ j+\frac{1}{2}} - (\boldsymbol{F}^\theta)^r_{i+\frac{1}{2}\ j} - (\boldsymbol{F}^\theta)^r_{i+\frac{1}{2}\ j+1}\right]$$

flux-CT

Current status numerical RMHD

Riemann Solver - HRSC

Komissarov 1999, 2005	Extension of FK96 to RMHD; right-eigenvectors in primitive variables; no left eigenvectors; eigenvector sets for degenerate/non-degenerate states; extra artificial viscosity and resistivity; 2nd order in space and time; extension to test GRMHD following Pons et al (1998).
Balsara 2001	Left eigenvectors from numerical inversion of right eigenvectors matrix; TVD interpolation on characteristic fields; 2nd order accuracy in space and time; 1D.
Koldoba et al. 2002	Right and left eigenvectors in covariant variables directly used to obtain the fluxes of conserved variables; 1D.
Antón et al. 2006	Right and left eigenvectors in conserved variables from covariant ones; single (consistent) set of left/right eigenvectors for both degenerate and non-degenerate states; 2nd order in space (minmod) and time (RK); extension to test GRMHD following Pons et al (1998).

Symmetric - HRSC

Koide et al. 1996	Symmetric TVD scheme with nonlinear numerical dissipation; 2nd order accuracy in space and time; (test) GRMHD.
Del Zanna et al. 2002	HLL scheme for numerical fluxes; point-value representation of variables (instead of cell averaged); 3rd order accuracy in space (CENO) and time (RK).
Gammie et al. 2003	HLL scheme for numerical fluxes; 2nd order in space and time; (test) GRMHD.
Leisman et al. 2005	HLL scheme for numerical fluxes; 2nd order in space (minmod) and time (RK).
Duez et al. 2005	HLL scheme for numerical fluxes; 2nd order in space (MC, CENO, minmod) and time; full GRMHD
Shibata & Sekiguchi 2005	Kurganov-Tadmor TVD scheme with nonlinear numerical dissipation; 2nd order in space and time; full GRMHD

Artificial Viscosity approach: Yokosawa 1993, De Villiers & Hawley 2003.

All codes (but AV-approach-based) use a conservative formulation of the RMHD equations. All codes reconstruct primitive variables (but Balsara's).

Part 4
Tests and applications in astrophysics

HRSC schemes: numerical assessment

- Stable and sharp discrete shock profiles
- Accurate propagation speed of discontinuities
- Accurate resolution of multiple nonlinear structures: discontinuities, rarefaction waves, vortices, etc

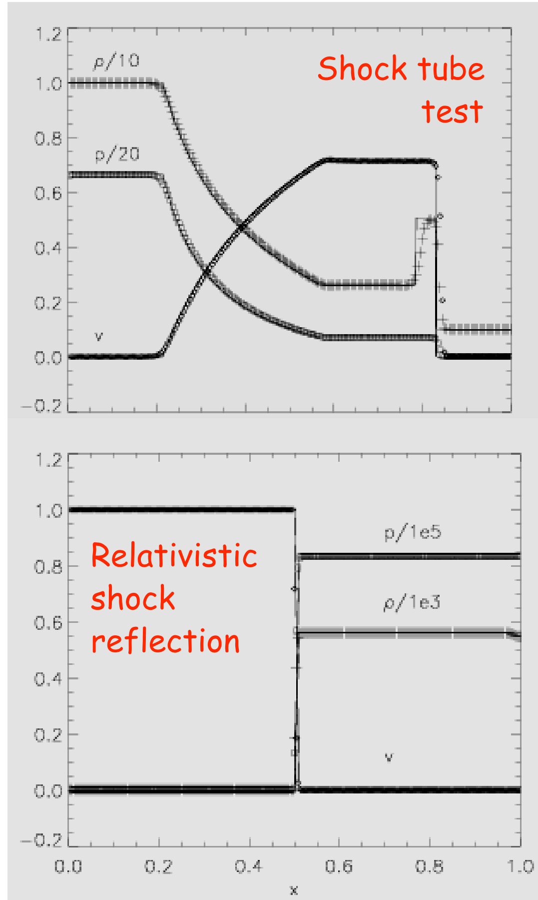

V=0.99999c
(W=224)

Propagation of a relativistic blast wave (Martí & Müller, movie from LRR)

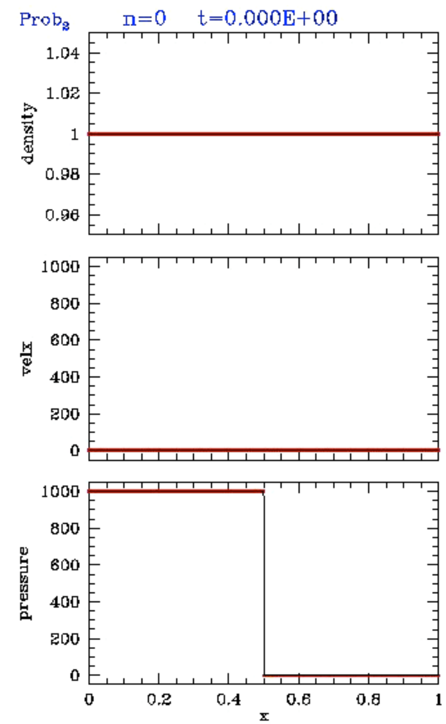

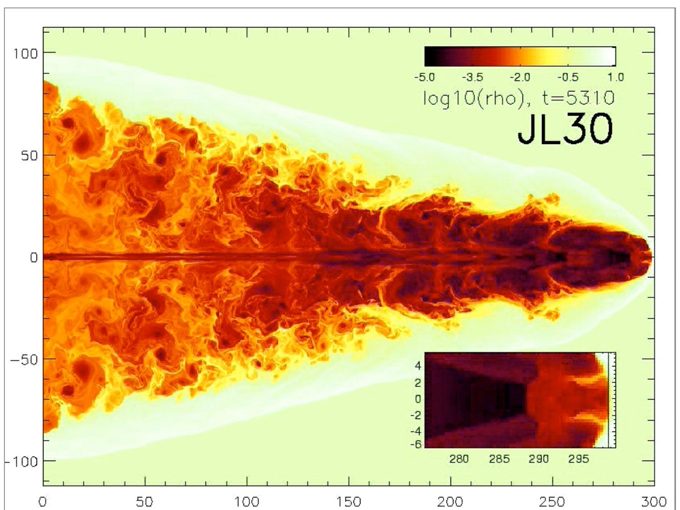

Simulation of a extragalactic relativistic jet

Scheck et al, MNRAS, 331, 615 (2002)

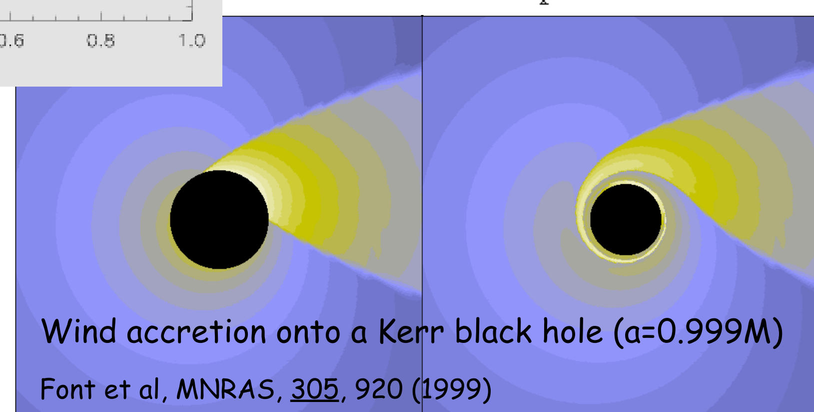

Wind accretion onto a Kerr black hole (a=0.999M)

Font et al, MNRAS, 305, 920 (1999)

Relativistic shock tube test

Shock tube test

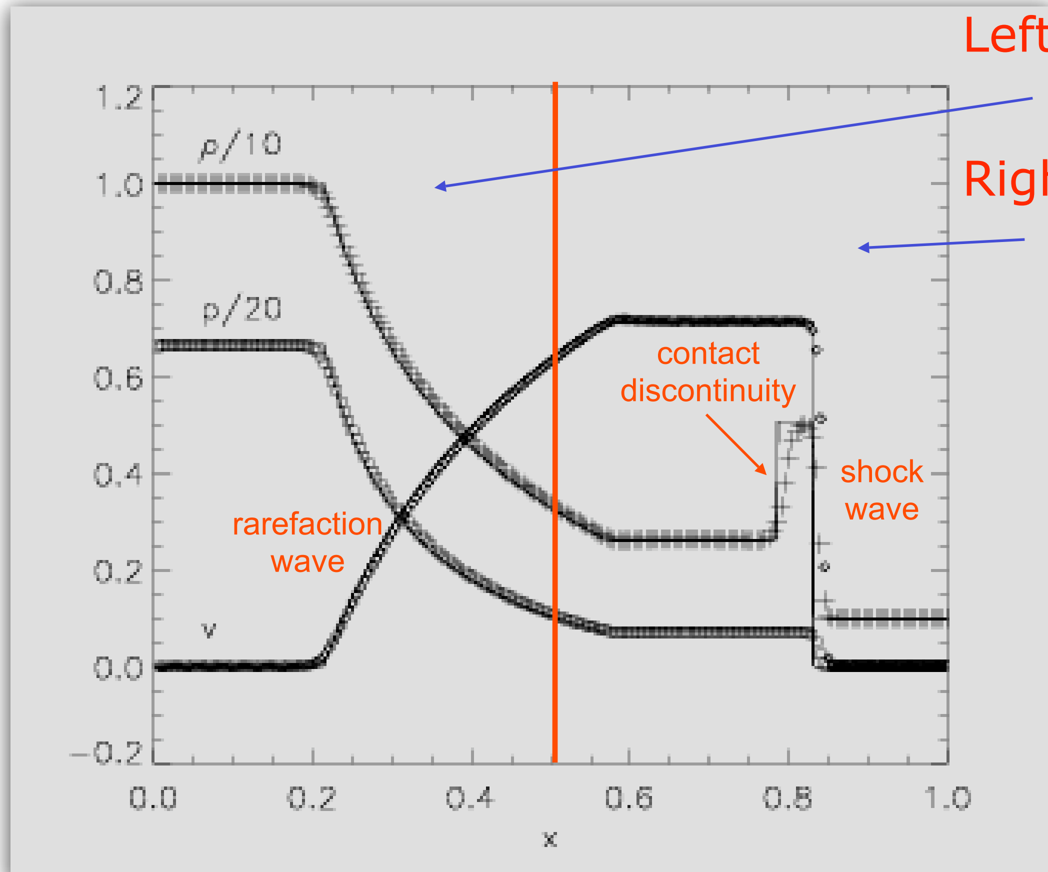

Final configuration at t=0.4

<u>Initial configuration</u>(t=0):

Left state: hot gas, high pressure.
$P=13.3$, $\rho=10$, $v=0$

Right state: cold gas, low pressure.
$P=0$, $\rho=1$, $v=0$

- Stable and sharp discrete shock profiles.
- Accurate propagation speed of discontinuities

3rd order scheme (PPM), perfect fluid EoS ($\gamma=5/3$), $\Delta x=1/200$

Relativistic shock reflection

Problem setup

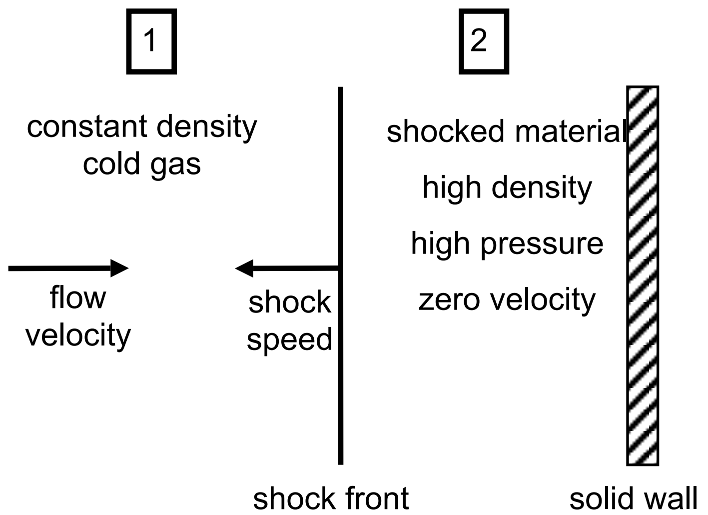

Analytic solution:

$$\frac{\rho_2}{\rho_1} = \frac{\gamma + 1}{\gamma - 1} + \frac{\gamma}{\gamma - 1}\varepsilon_2, \quad \varepsilon_2 = W_1 - 1$$

Relativistic shock reflection

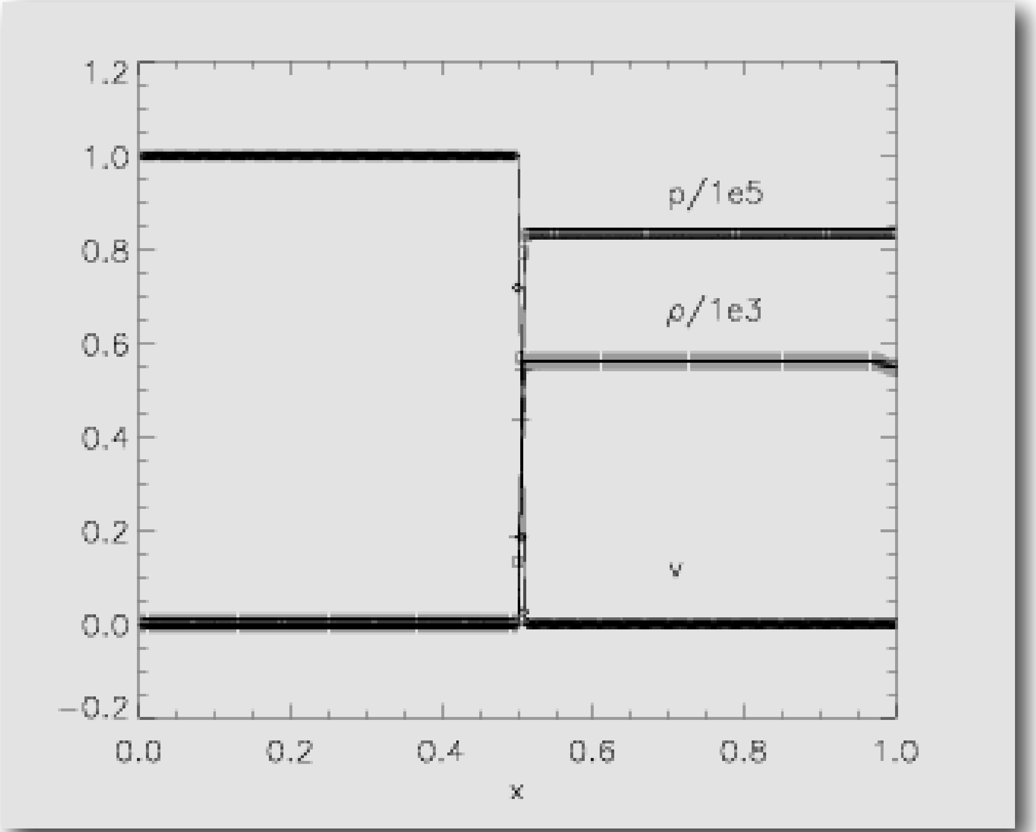

v=0.99999c (W=224)

3rd order scheme (PPM)
perfect fluid EoS (γ=5/3), Δx=1/400

Blast wave test

Initial configuration

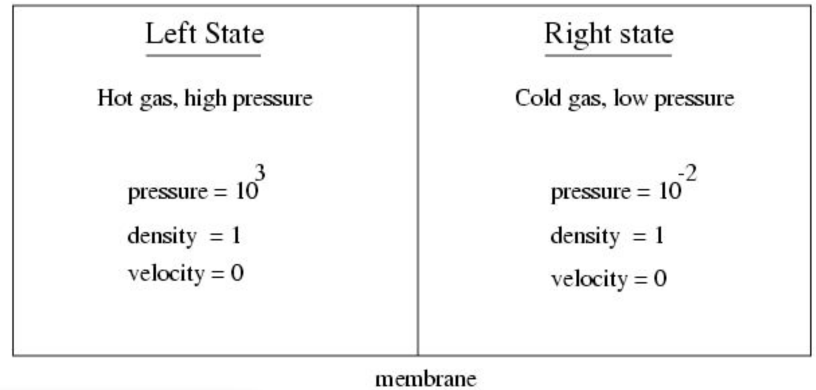

Final configuration, t=0.35

Perfect fluid EoS, γ=5/3, Δx=1/400

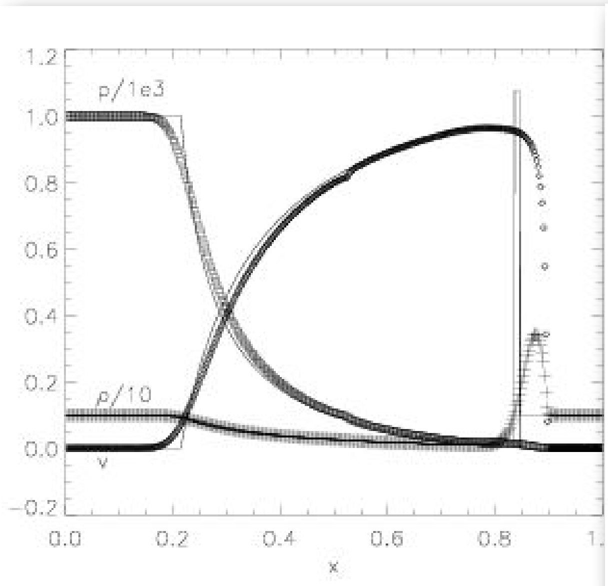

First-order scheme

(Godunov)

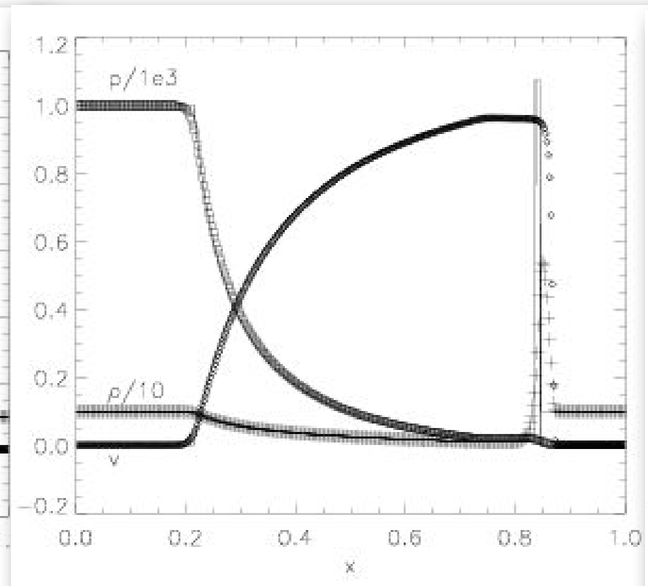

Second-order scheme

(MUSCL)

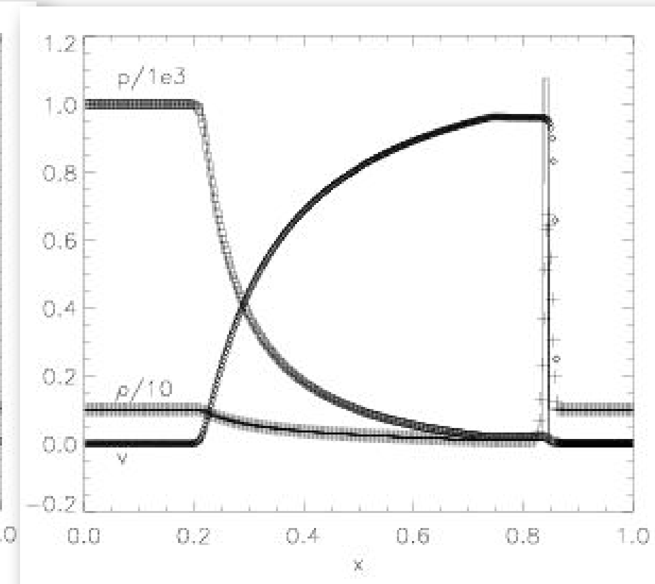

Third-order scheme

(ENO-3)

Spherical accretion onto a Schwarzshild black hole

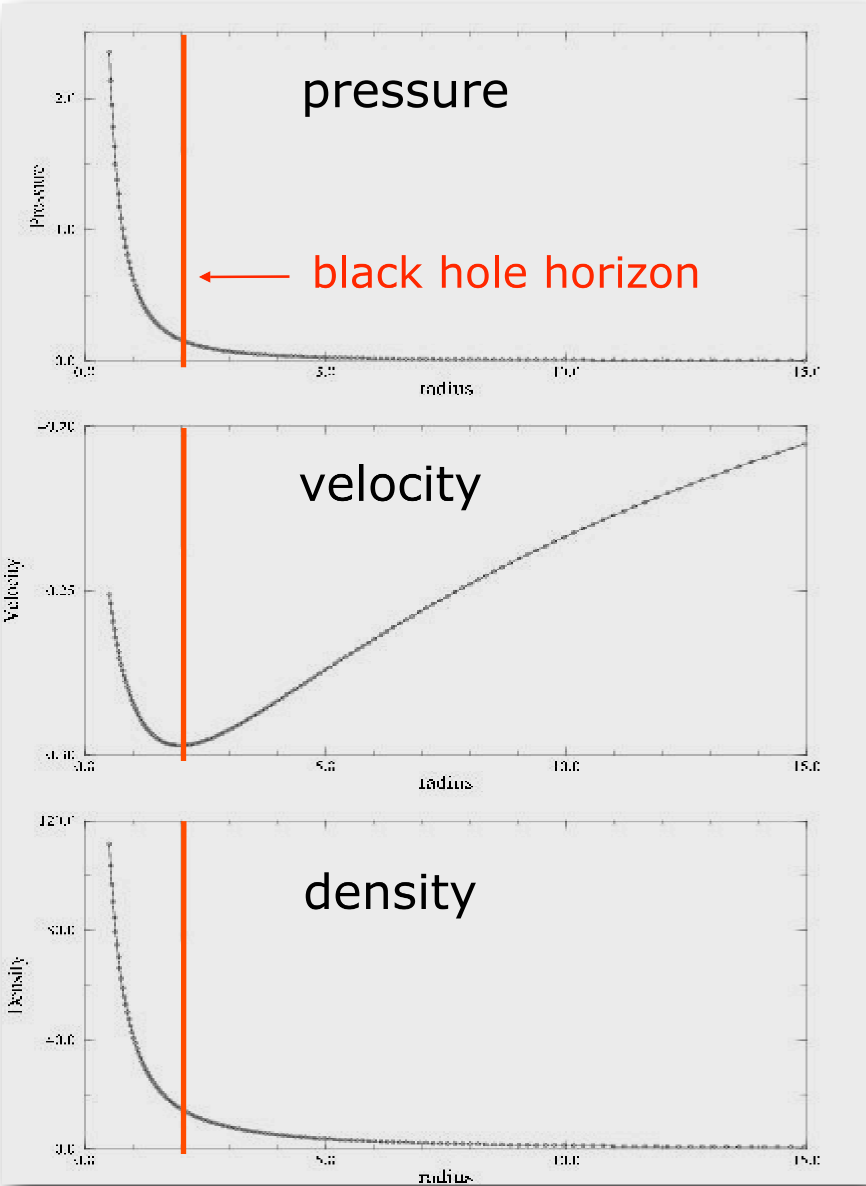

Stationary analytic solution which permits to calibrate hydrodynamics relativistic codes in the presence of strong gravitational fields.

Solid line: analytic solution
Symbols: numerical solution

Eddington-Finkelstein (horizon-adapted) coordinates allow to place the innermost grid point inside the event horizon.

This removes the ambiguity in the location of the innermost radial grid point when using Boyer-Lindquist coordinates (for which the Lorentz factor diverges at the horizon leading to the code crash).

Papadopoulos & Font, Phys. Rev. D 58, 024005 (1998).

Wind tunnel with flat-faced step

Isocontours of rest-mass density at selected frames during the evolution.

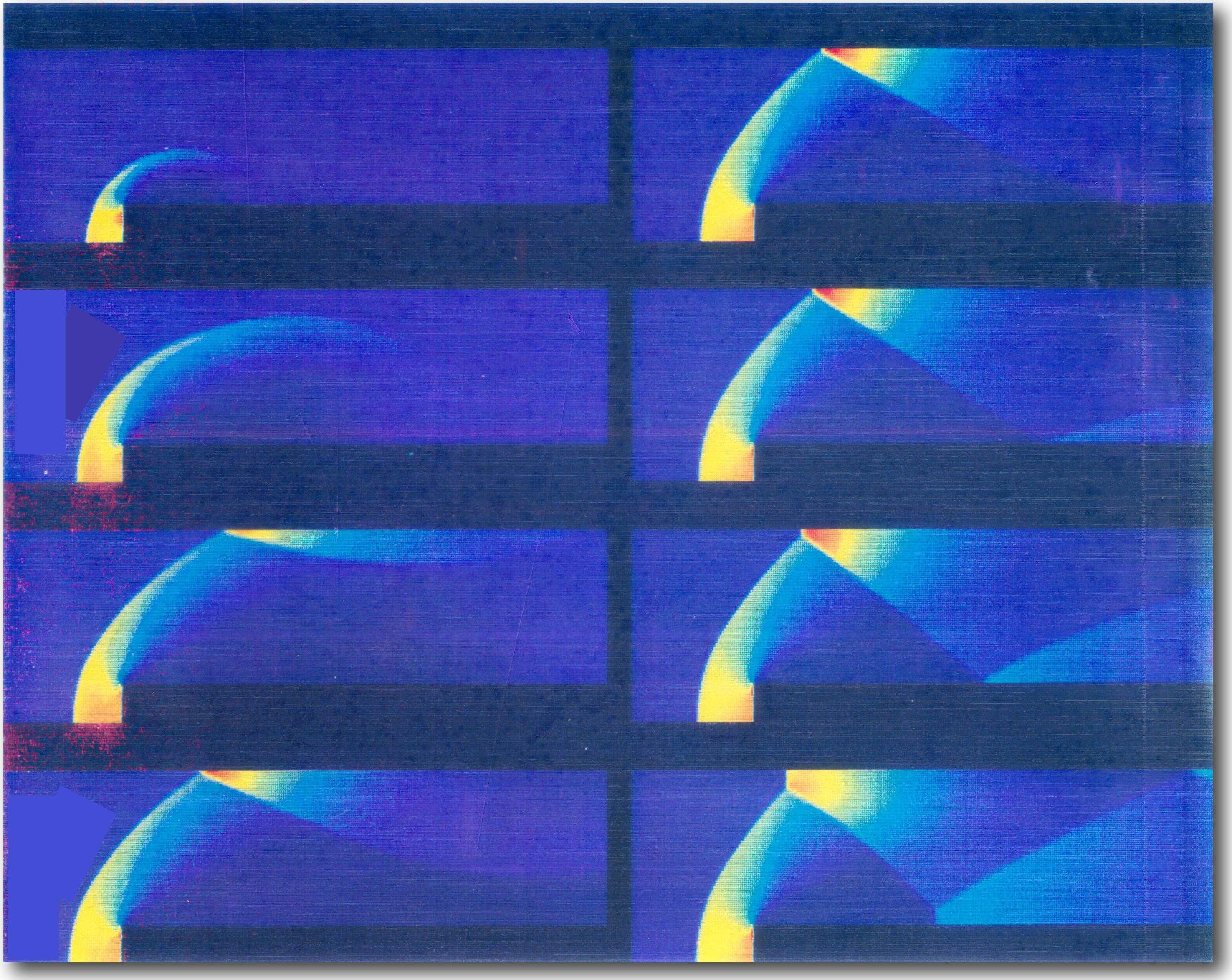

GRMHD equations: shock tube tests

1D Relativistic Brio-Wu shock tube test (van Putten 1993, Balsara 2001)

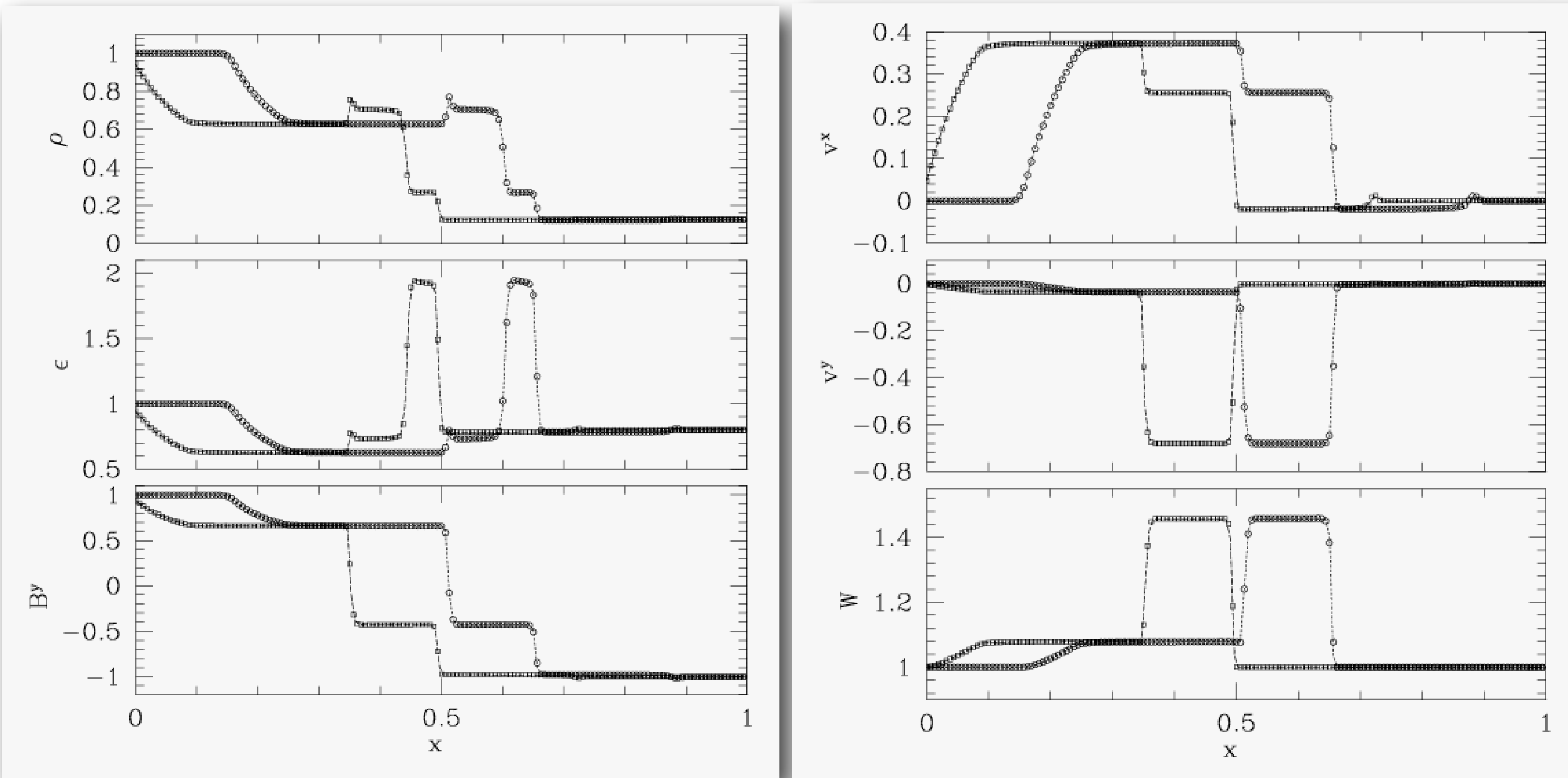

Dashed line: wave structure in Minkowski spacetime at time t=0.4
Open circles: non vanishing lapse function (2), at time t=0.2
Open squares: non vanishing shift vector (0.4), at time t=0.16

HLL solver
1600 zones
CFL 0.5

Agreement with previous authors (Balsara 2001) regarding wave locations, maximum Lorentz factor achieved, and numerical smearing of the solution.

Magnetised spherical accretion onto a Schwarzschild BH

Test difficulty: keep stationarity of the solution.

Used in the literature (Gammie et al 2003, De Villiers & Hawley 2003)

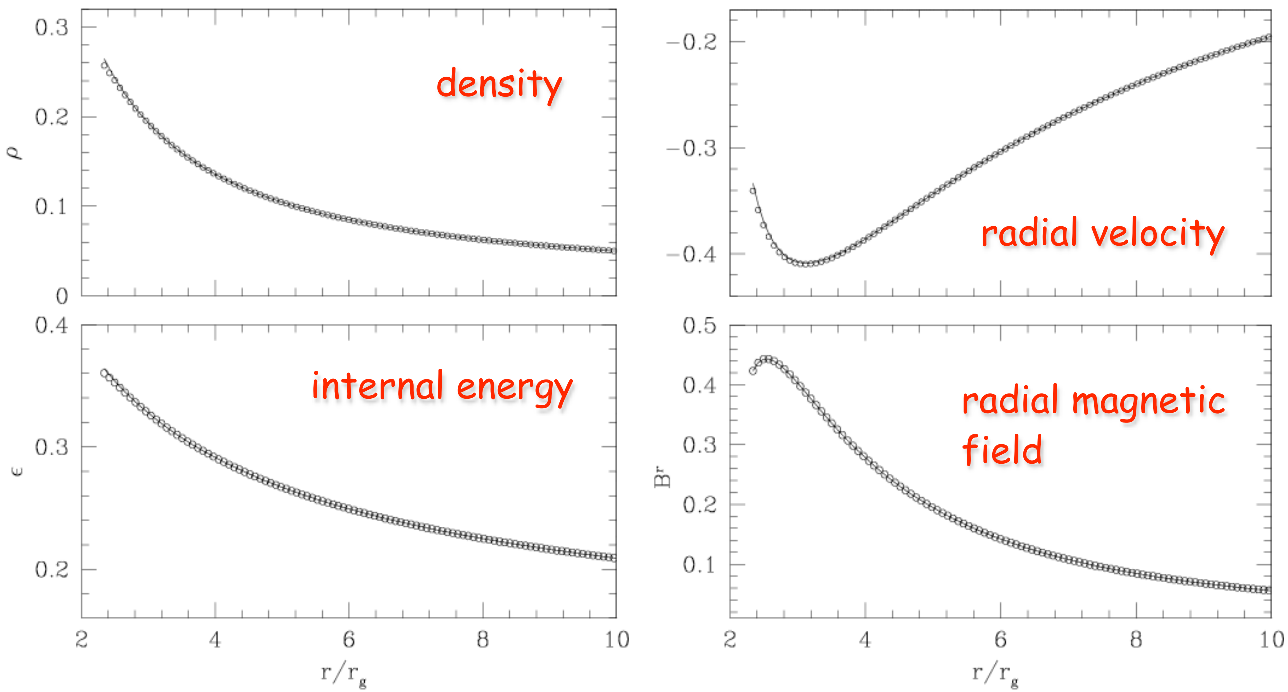

Antón et al (2006)

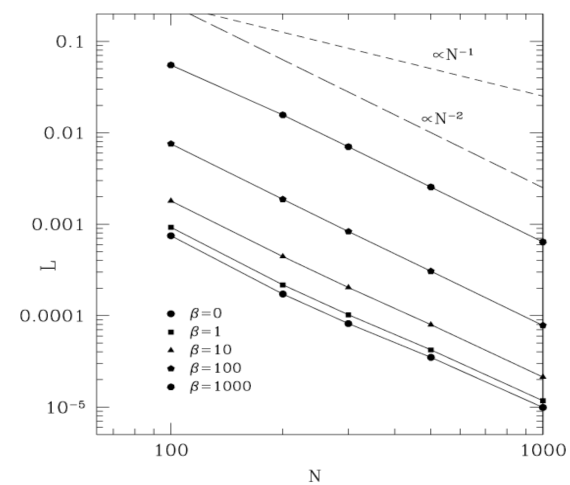

2nd order convergence

Magnetised spherical accretion onto a Kerr BH

Magnetised equatorial Kerr accretion (Takahashi et al 1990, Gammie 1999)

Test difficulty: keep stationarity of the solution (algebraic complexity augmented, Kerr metric)

Used in the literature (Gammie et al 2003, De Villiers & Hawley 2003)

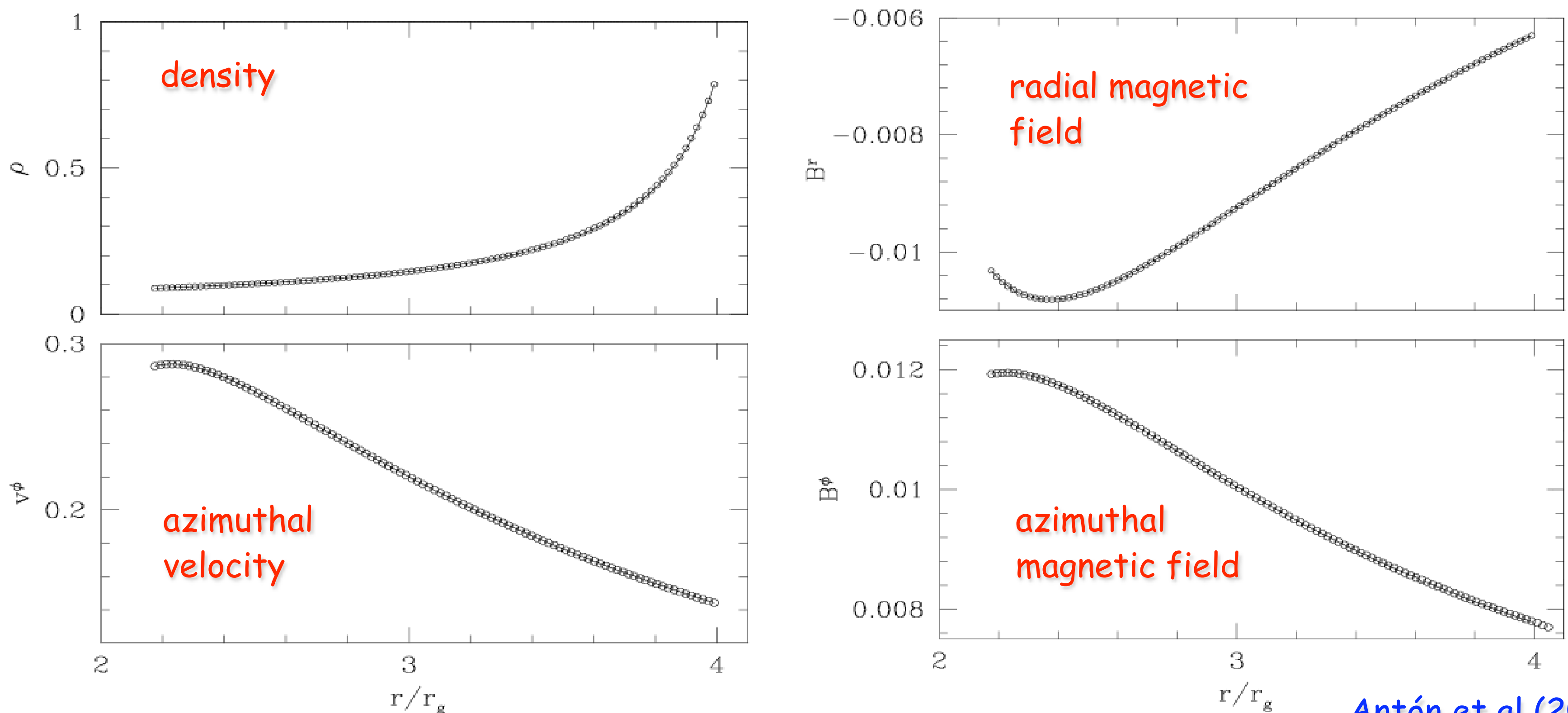

Antón et al (2006)

Numerical HD/MHD simulations are nowadays an essential tool in theoretical astrophysics, both to model classical and relativistic sources. Some examples include:

1. Heavy ion collisions (SR limit): Clare & Strottman 1986, Wilson & Mathews 1989, Rischke et al 1995a,b.
2. Simulations of relativistic jets (SR limit): Martí et al 1994, 1995, 1997, Gómez et al 1995, 1997, 1998, Aloy et al 1999, 2003, Scheck et al 2002, Leismann et al 2005, ….
3. GRB models: Aloy et al 2000, Zhang, Woosley & MacFadyen 2003, Aloy, Janka & Müller 2004, ….
4. Gravitational stellar core collapse: Dimmelmeier, Font & Müller 2001, 2002a,b, Dimmelmeier et al 2004, Cerdá-Durán et al 2004, Shibata & Sekiguchi 2004, 2005, ….
5. Gravitational collapse and black hole formation: Wilson 1979, Dykema 1980, Nakamura et al 1980, Nakamura 1981, Nakamura & Sato 1982, Bardeen & Piran 1983, Evans 1984, 1986, Stark & Piran 1985, Piran & Stark 1986, Shibata 2000, Shibata & Shapiro 2002, Baiotti et al 2005, Zink et al 2005, ….
6. Pulsations and instabilities of rotating relativistic stars: Shibata, Baumgarte & Shapiro, 2000; Stergioulas & Font 2001, Font, Stergioulas & Kokkotas 2000, Font et al 2001, 2002, Stergioulas, Apostolatos & Font 2004, Shibata & Sekiguchi 2003, Dimmelmeier, Stergioulas & Font 2006, ….
7. Accretion on to black holes: Font & Ibáñez 1998a,b, Font, Ibáñez & Papadopoulos 1999, Brandt et al 1998, Papadopoulos & Font 1998a,b, Nagar et al 2004, Hawley, Smarr & Wilson 1984, Petrich et al 1989, Hawley 1991, …
8. Disk accretion: Font & Daigne 2002a,b, Daigne & Font 2004, Zanotti, Rezzolla & Font 2003, Rezzolla, Zanotti & Font 2003, Zanotti et al 2005, …
9. GRMHD simulations of BH accretion disks: Yokosawa 1993, 1995, Igumenshchev & Belodorov 1997, De Villiers & Hawley 2003, Hirose et al 2004. Gammie et al 2003, Fragile 2004, ….
10. Jet formation: Koide et al 1998,…, 2006, McKinney & Gammie 2004, Komissarov 2005, Hawley et al 2005, ….
11. Binary neutron star mergers: Miller, Suen & Tobias 2001, Shibata, Taniguchi & Uryu 2003, Evans et al 2003, Miller, Gressman & Suen 2004, Wilson, Mathews & Marronetti 1995, 1996, 2000, Nakamura & Oohara 1998, Shibata 1999, …, Shibata & Uryu 2000, 2002, …

Example: Long-term evolution of a relativistic, hot, leptonic (e^+/e^-) jet up to 6.3×10^6 years (Scheck et al. MNRAS, 331, 615-634, 2002)

Jets are relativistic collimated ejections of thermal (e+/e-, e-/p) plasma + ultrarelativistic electrons/positrons + magnetic fields + radiation, generated in the vicinity of SMBH

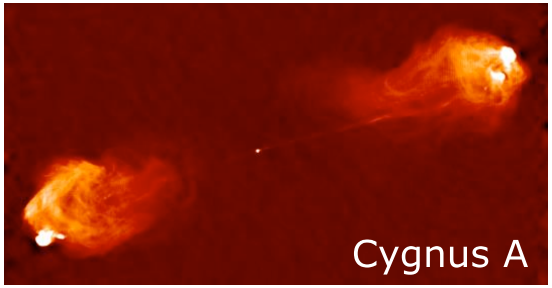

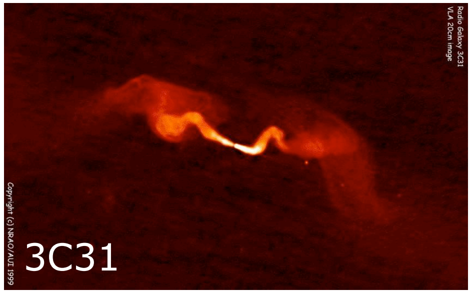

Relativistic jets are a common ingredient of radio-loud AGNs.

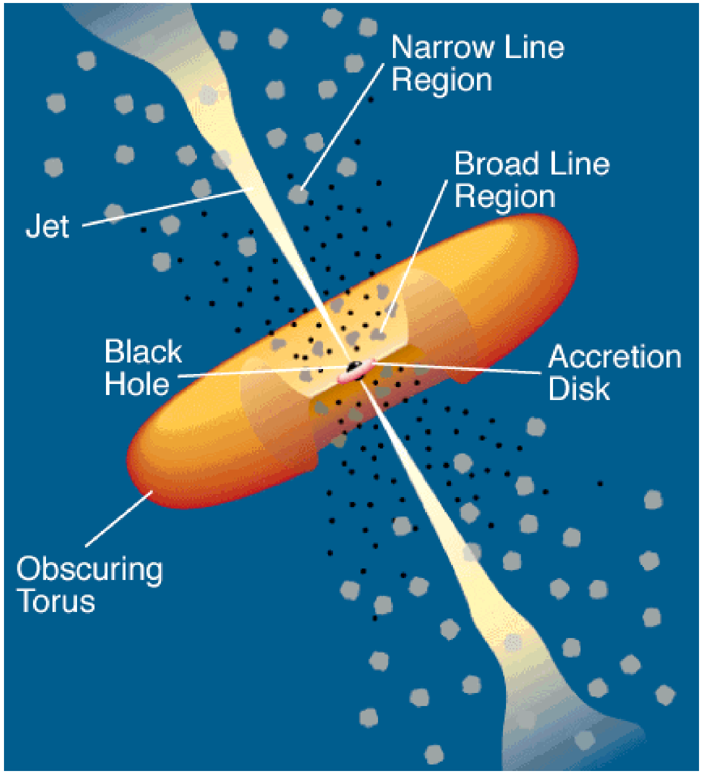

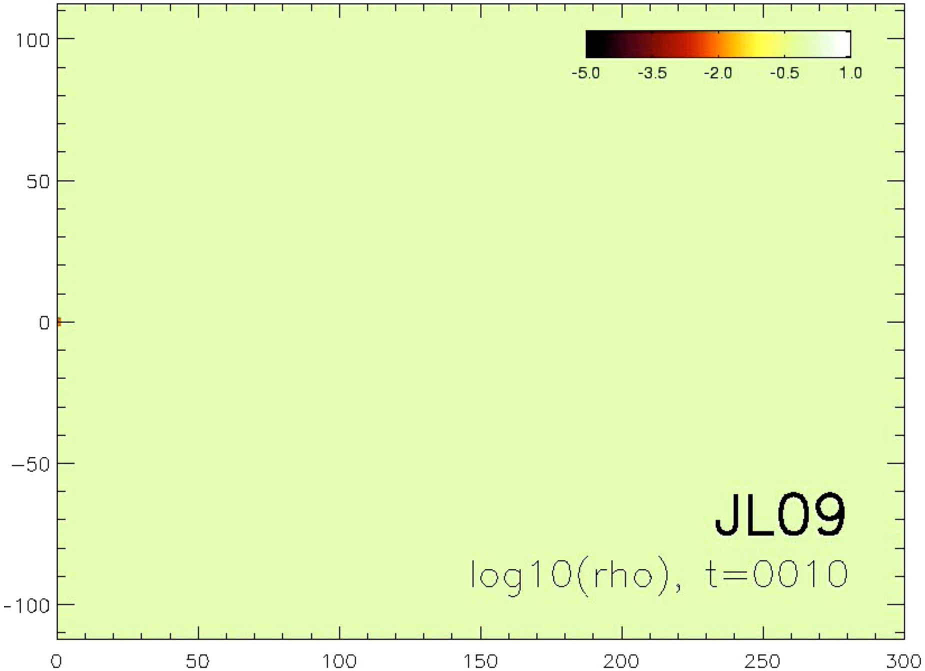

Since the mid 1990s, relativistic simulations have helped to improve our understanding of their formation and propagation.

Example: Nonlinear instabilities in relativistic jets

Perucho et al. ApJ (2004)

2D "slab jet" Cartesian coordinates. Lorentz factor 5. Periodic boundary conditions. 256 zones per beam radius.

Initial model perturbed with 4 symmetric perturbations and 4 antisymmetric perturbations.

Initial location of the beam →

The evolution of the linear phase agrees with analytic results from perturbation theory.

Development of nonlinearities visible (Kelvin-Helmholtz instability). Once they saturate a quasi-equilibrium (turbulent) state is reached.

Time evolution of the jet mass fraction

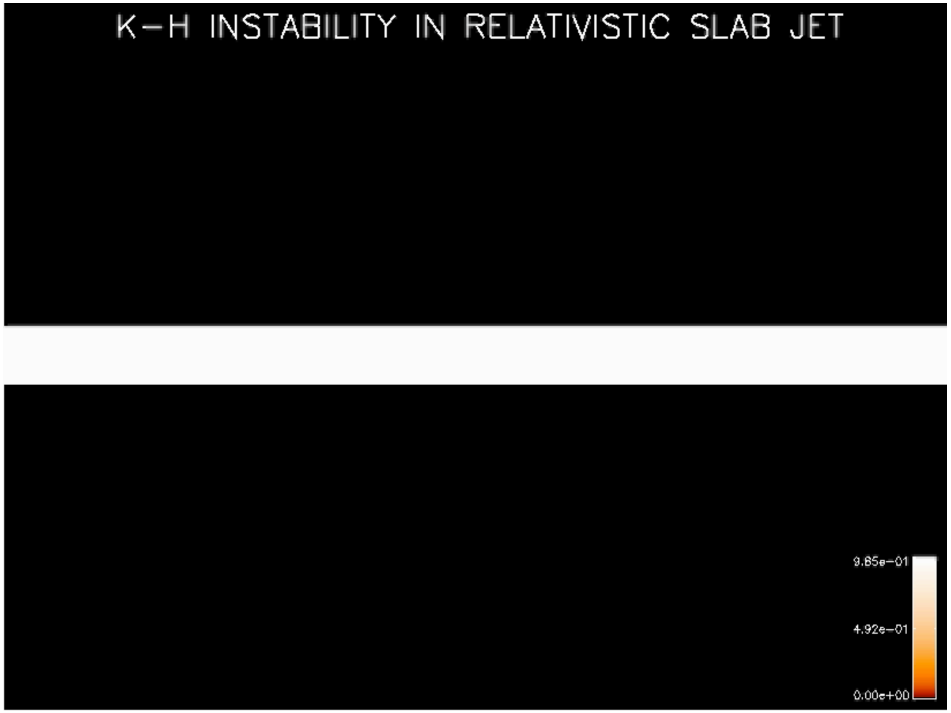

Black: external medium. White: jet

Example: Relativistic wind accretion onto a Kerr black hole

- Binary system: black hole + giant star (O,B spectral type). Strong stellar wind. No Roche lobe overflow (common envelope evolution, Thorne-Zytkow objects).
- Isolated compact objects accreting from the interstellar medium.
- Compact objects in stellar clusters, AGNs and QSOs.

Wind (Bondi-Hoyle-Lyttleton) accretion onto black holes: hydrodynamics in GR.

Difficulties: 1) Strong gravitational fields, 2) Ultra relativistic flows and shock waves.

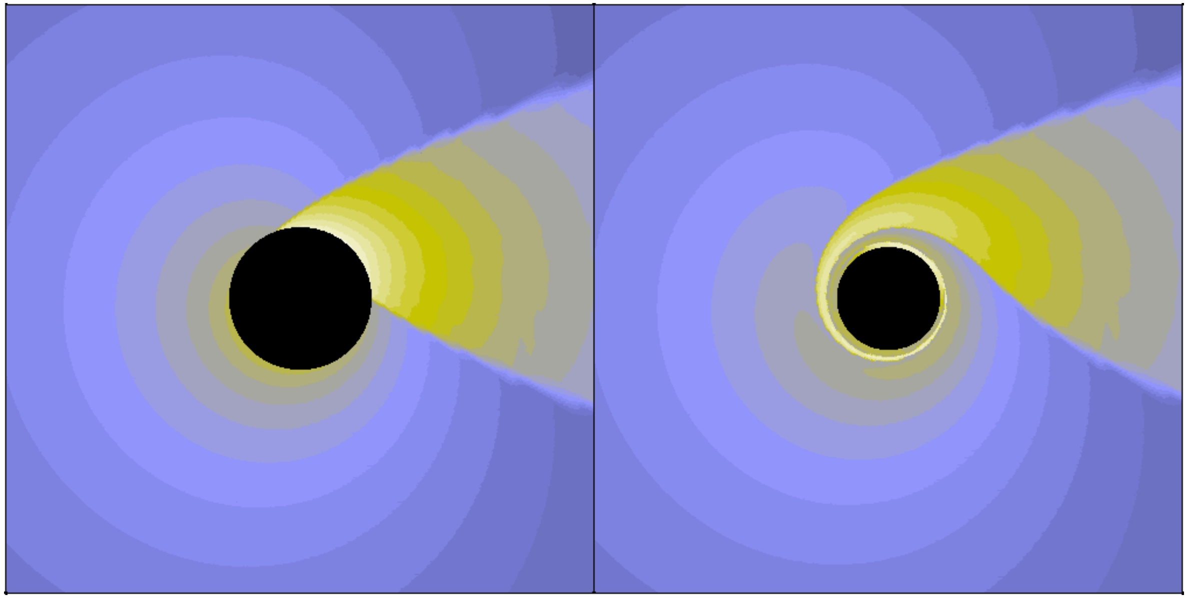

Kerr-Schild　　Boyer-Lindquist

Wind accretion on to a Kerr black hole

(a=0.999M)

Font et al, MNRAS, 305, 920 (1999)

Roe's Riemann solver.

Isocontours of the log of density.

Relativistic wind from left to right.

Black hole spinning counter-clockwise.

Example: Evolution of a magnetised accretion torus around a Schwarzschild black hole (De Villiers & Hawley 2003; Antón et al 2006)

Development of the <u>magneto-rotational instability</u>.

Magnetic field + differentially rotating Keplerian disk → MRI : generation of effective viscosity and angular momentum transport outwards through MHD turbulence.

Central engines of gamma-ray bursts

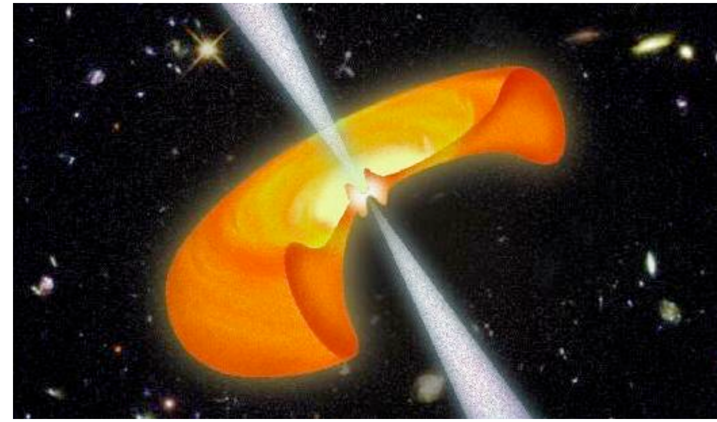

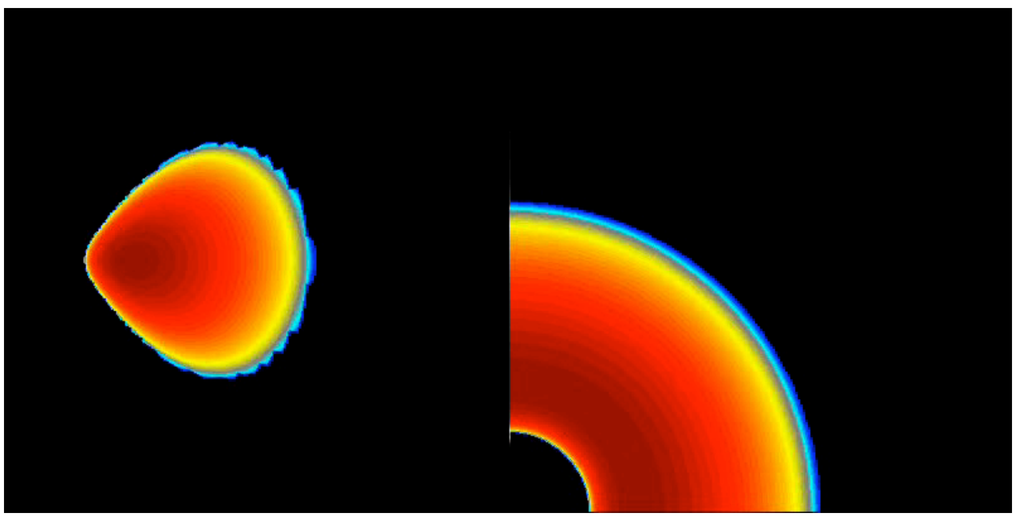

De Villiers & Hawley (2003)

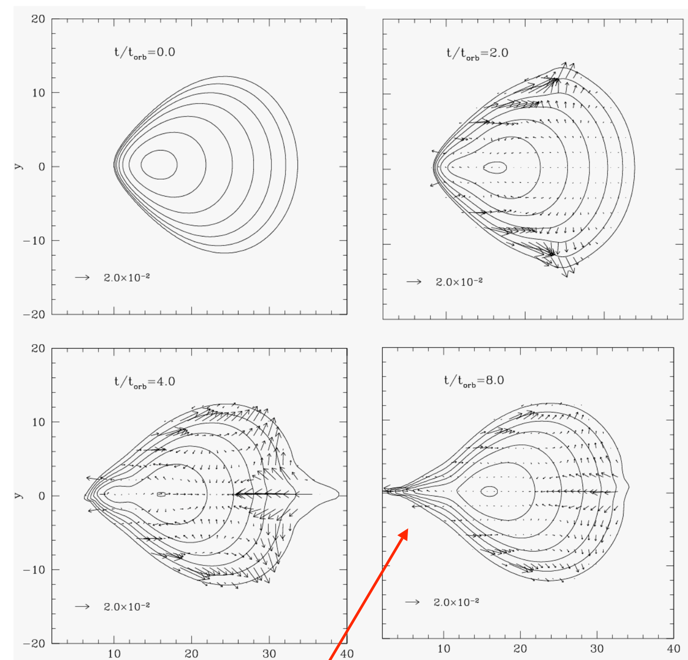

"channel solution"

(De Villiers & Hawley 2003)

For further animations visit: www.astro.virginia.edu/~jd5v/

Example: Relativistic rotating core collapse simulation

For movies of additional models visit:

www.mpa-garching.mpg.de/rel_hydro/axi_core_collapse/movies.shtml

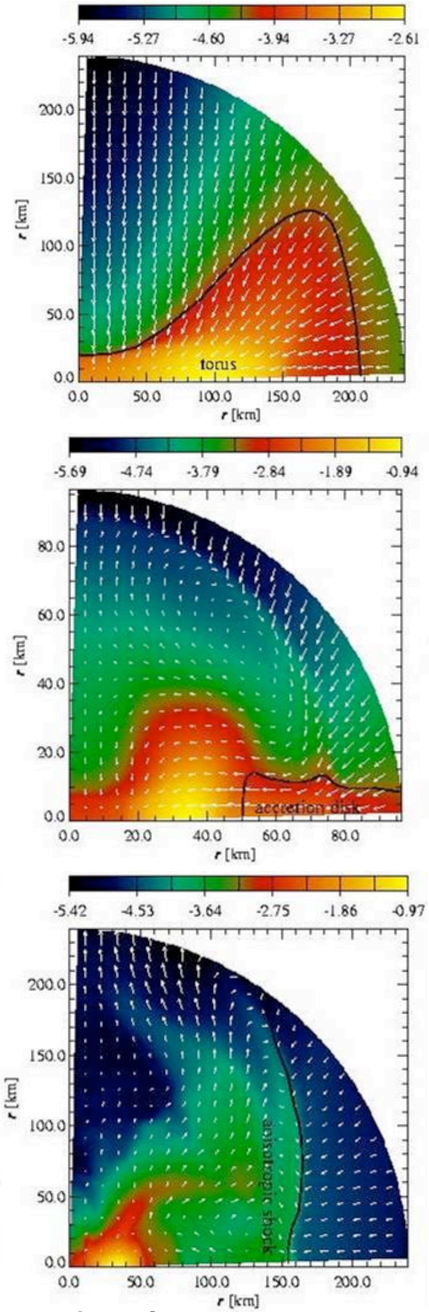

MAX PLANCK INSTITUTE FOR ASTROPHYSICS
GARCHING, GERMANY

http://www.mpa-garching.mpg.de

General Relativistic Collapse of Rotating Stellar Cores in Axisymmetry

Harald Dimmelmeier
José A. Font
Ewald Müller

References:

- Dimmelmeier, H., Font, J. A., and Müller, E., *Astron. Astrophys.*, 388, 917–935 (2002), astro-ph/0204288.
- Dimmelmeier, H., Font, J. A., and Müller, E., *Astron. Astrophys.*, submitted (2002), astro-ph/0220489.

Larger central densities in relativistic models
Similar gravitational radiation amplitudes (or smaller in the GR case)

GR effects do not improve the chances for detection (at least in axisymmetry): Only a Galactic supernova (10 kpc) would be detectable by the first generation of gravitational wave laser interferometers.

Waveform catalogue: www.mpa-garching.mpg.de/rel_hydro/wave_catalogue.shtml

Core collapse and gravitational waves

Numerical simulations of stellar core collapse are highly motivated by the prospects of direct detection of the gravitational waves emitted.

International network of resonant bar detectors

International network of interferometers

Do GR & MHD effects modify the existing GW signals from Newtonian rotational core collapse?

GRAVITATIONAL WAVE ASTRONOMY: NEW WINDOW TO THE UNIVERSE

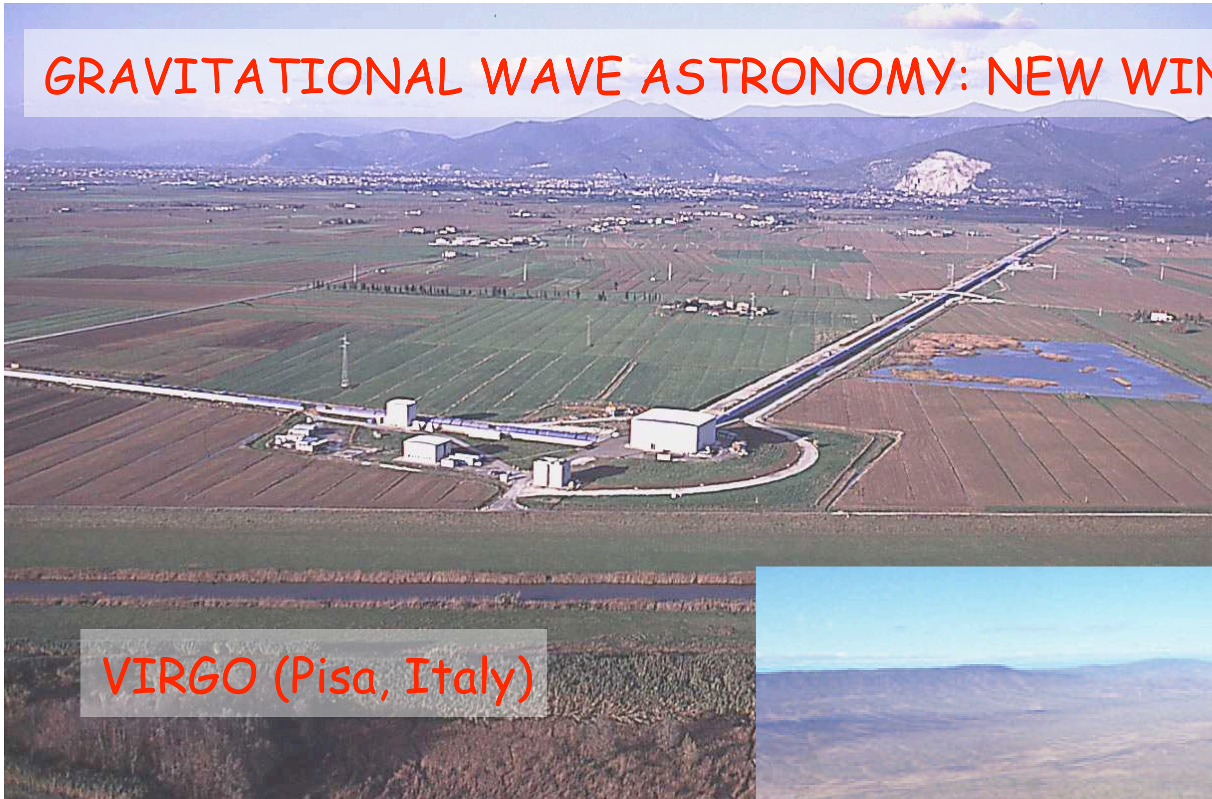

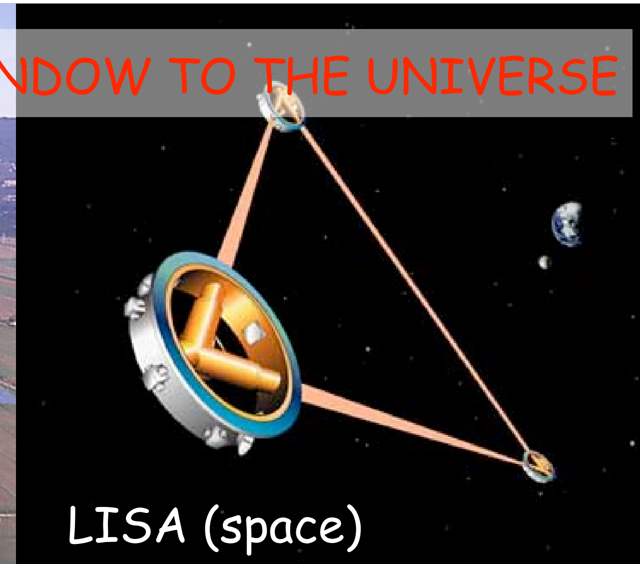

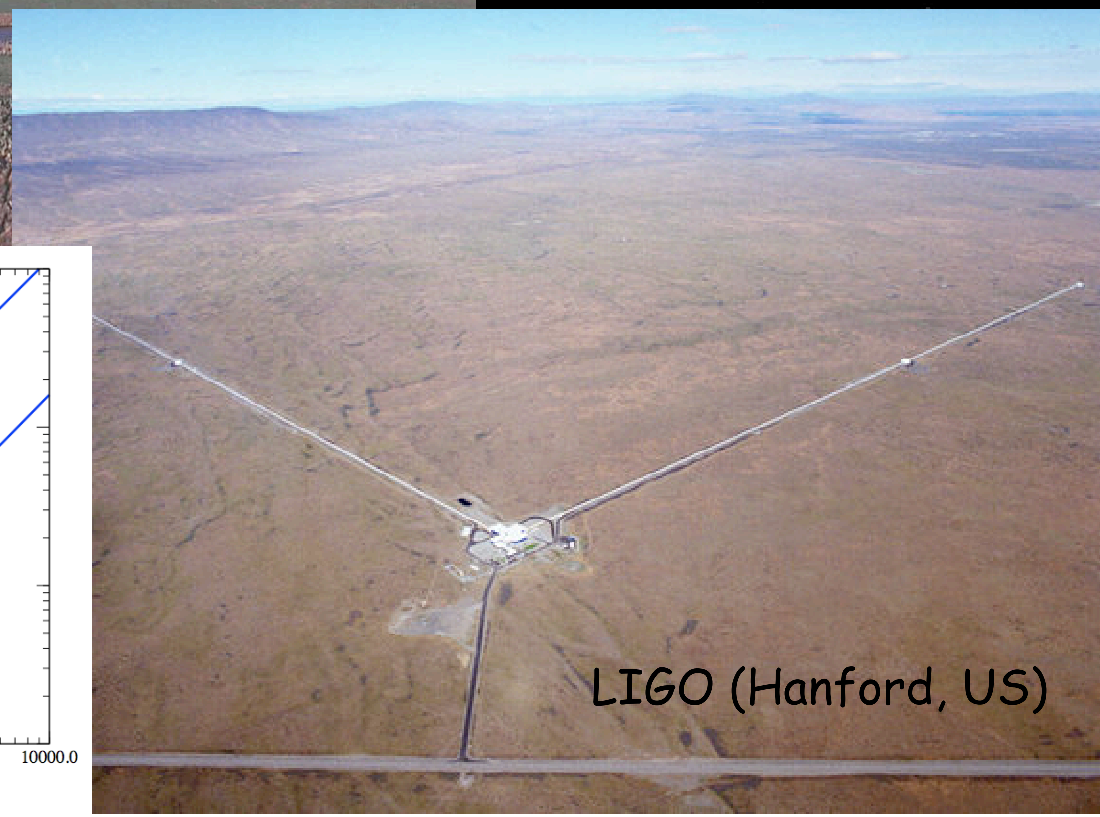

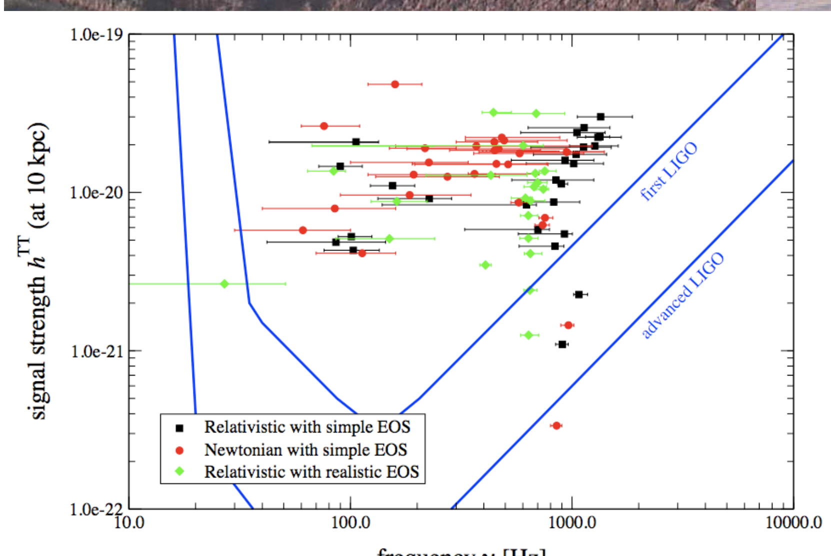

Simulation results

CFC (unmagnetized) core collapse - simple EOS

<u>HRSC scheme:</u> PPM + Marquina solver

<u>Solid line:</u> (CFC) relativistic simulation

<u>Dashed line:</u> Newtonian

Larger central density in relativistic models (more compact PNS)

Similar gravitational radiation amplitudes

Multiple bounce collapse suppressed in GR

Axisymmetric simulations:

Dimmelmeier, Font & Müller (2002) [CFC]
Cerdá-Durán et al (2005) [CFC+]
Shibata & Sekiguchi (2005) [BSSN]

Excellent agreement

Extensions to realistic EoS and 3D available

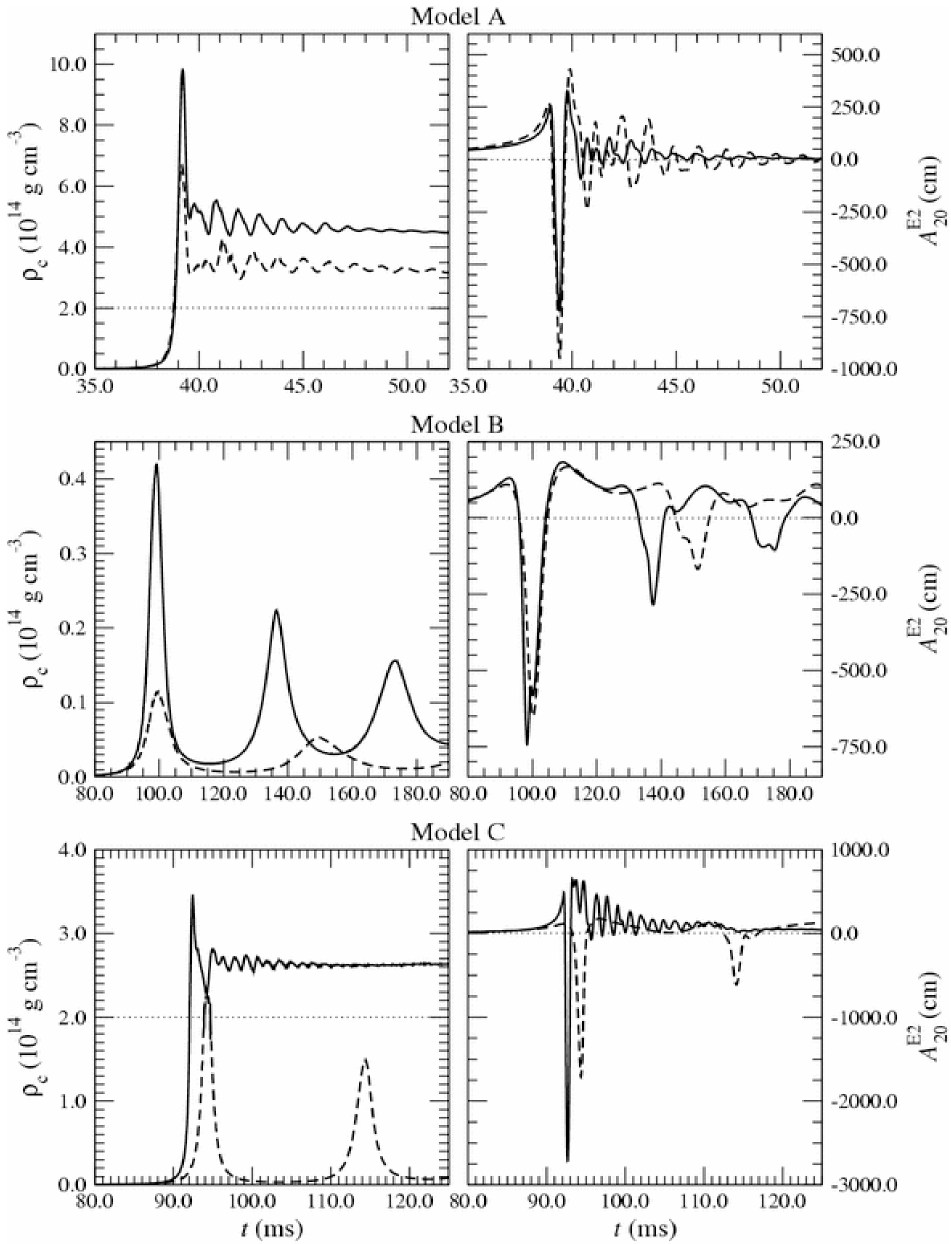

Gravitational Wave Signals (CFC and simple EOS)

www.mpa-garching.mpg.de/Hydro/RGRAV/index.html

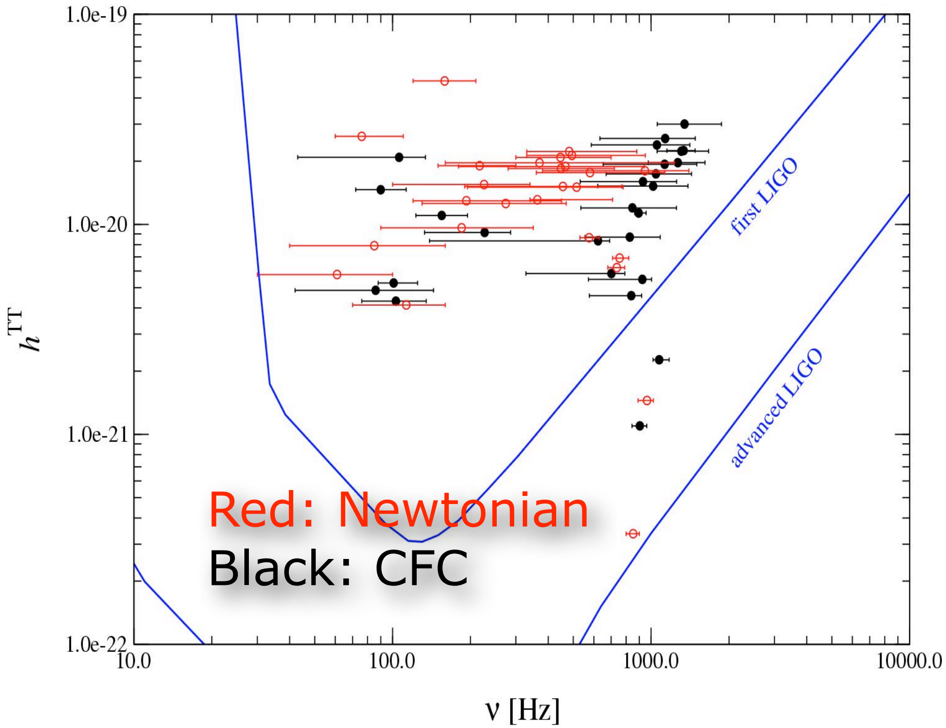

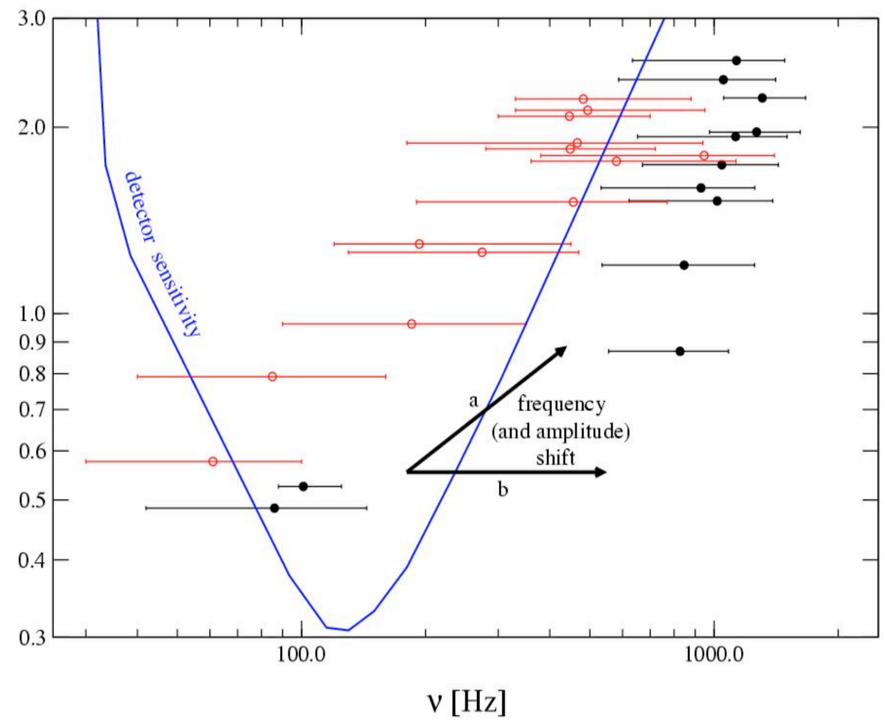

Spread of all DFM models vs ZM models does not change much

Signal of a galactic supernova detectable by first generation detectors
(signal recycling in next generation detectors maybe needed for successful detection of more distant events, e.g. Virgo cluster).

On average: Amplitude → Frequency ↑

If close to detection threshold signal could fall out of sensitivity window!

Gravitational waves from convection

Even for non-rotating models, anisotropic instabilities can develop.

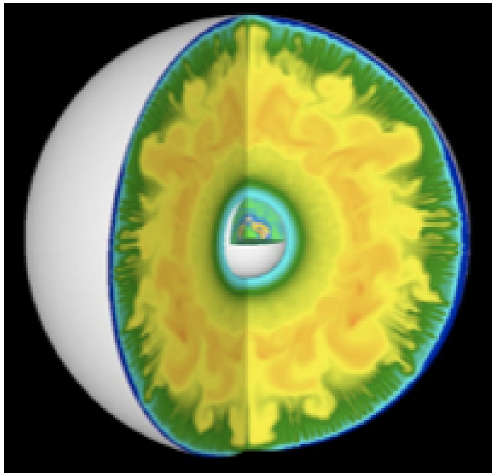

Additional to burst signal, signal from PNS convection.

- Convective boiling of neutron star ("rest mass" quadrupole moment)
- Anistotropic neutrino emission/absorption (neutrino "energy mass" quadrupole moment)

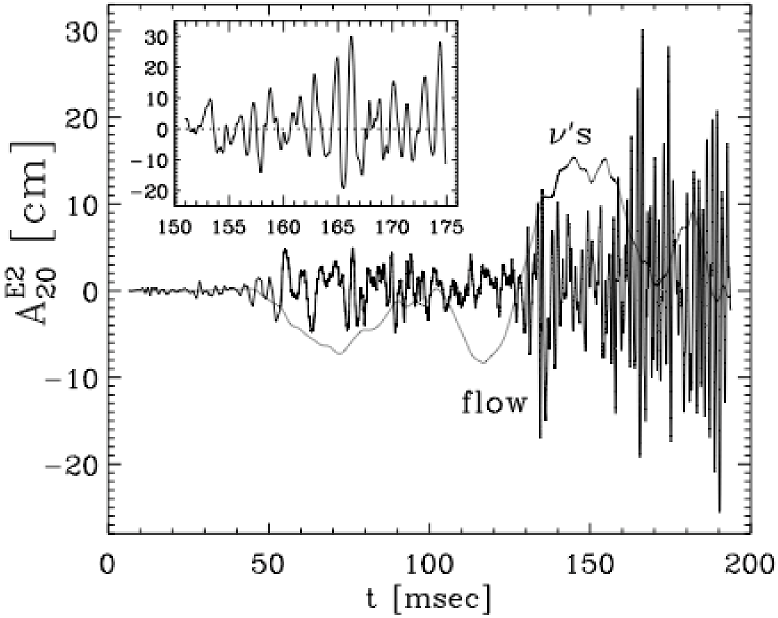

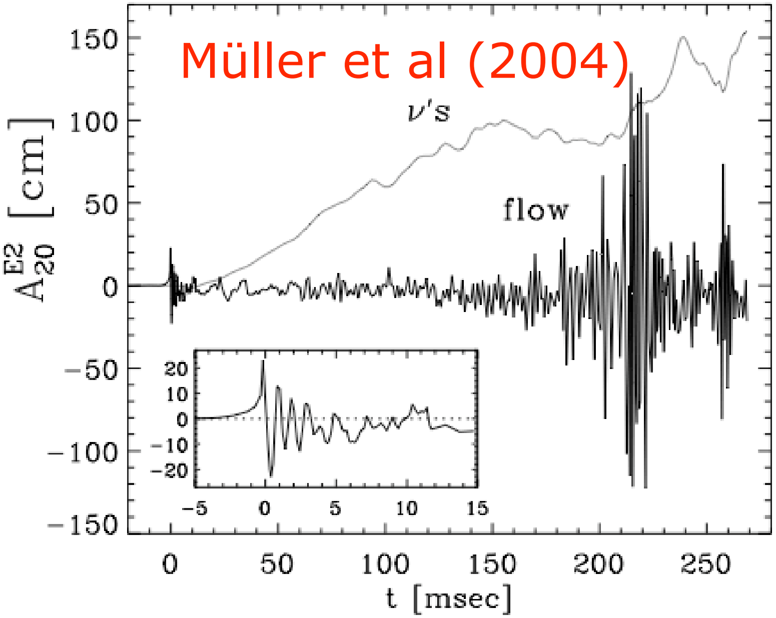

Long emission timescale can yield high energy for continuous signal.

Example: nonlinear pulsations of rotating neutron stars (Asteroseismology)

Pulsations of rotating neutron stars are a potential source of detectable (high-frequency) GWs. They are excited in a number of astrophysical scenarios:

- rotating core collapse.
- accretion-induced collapse.
- core quakes due to phase transitions in EOS (strange stars).
- hypermassive neutron star formation in NS/NS mergers.

Para ver esta película, debe disponer de QuickTime™ y de un descompresor .

Nonlinear evolutions (hydrodynamics + spacetime): promising new approach introduced in recent years for computing mode frequencies (Font et al 2000, 2001, 2002; Stergioulas et al 2001, 2004; Dimmelmeier et al 2005).

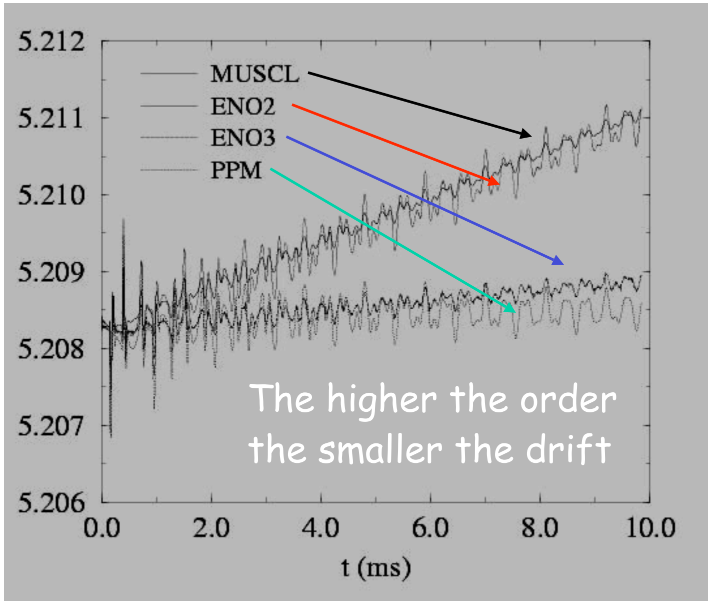

GRHD simulations show the appearance of linear pulsation modes, harmonics (overtones) and nonlinear harmonics.

Fourier transform of evolution data

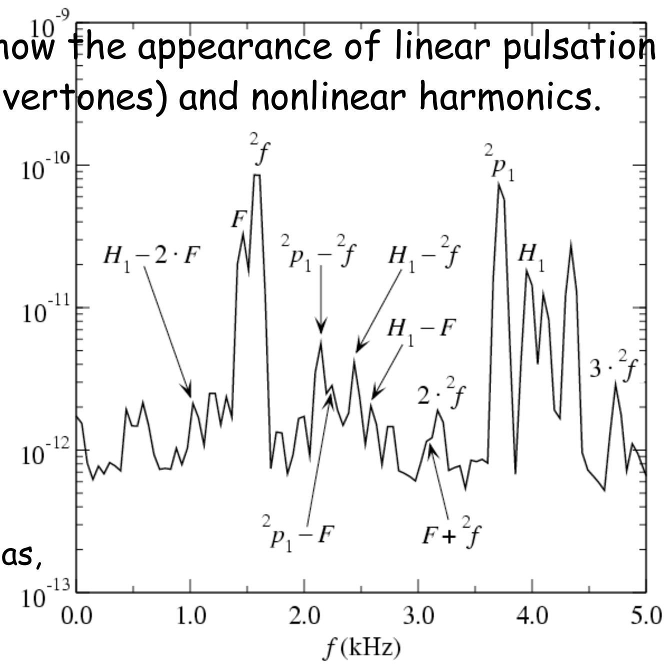

Dimmelmeier, Stergioulas, Font (2006)

Gravitational waves from NS pulsations

(Quasi)-radial NS pulsations easily excited after core collapse (but also accretion from companion star, NS quakes and phase transitions, NS/NS mergers, etc)

The study of pulsations of relativistic rotating stars currently possible with nonlinear numerical hydro codes (complements/extends perturbative approaches).

Evolution of axisymmetric pulsations using CFC (Dimmelmeier, Stergioulas & Font 2006).

Relations between GW detectability and required pulsation amplitudes can be obtained.

See talk by Kostas Kokkotas on instabilities and pulsations in NS.

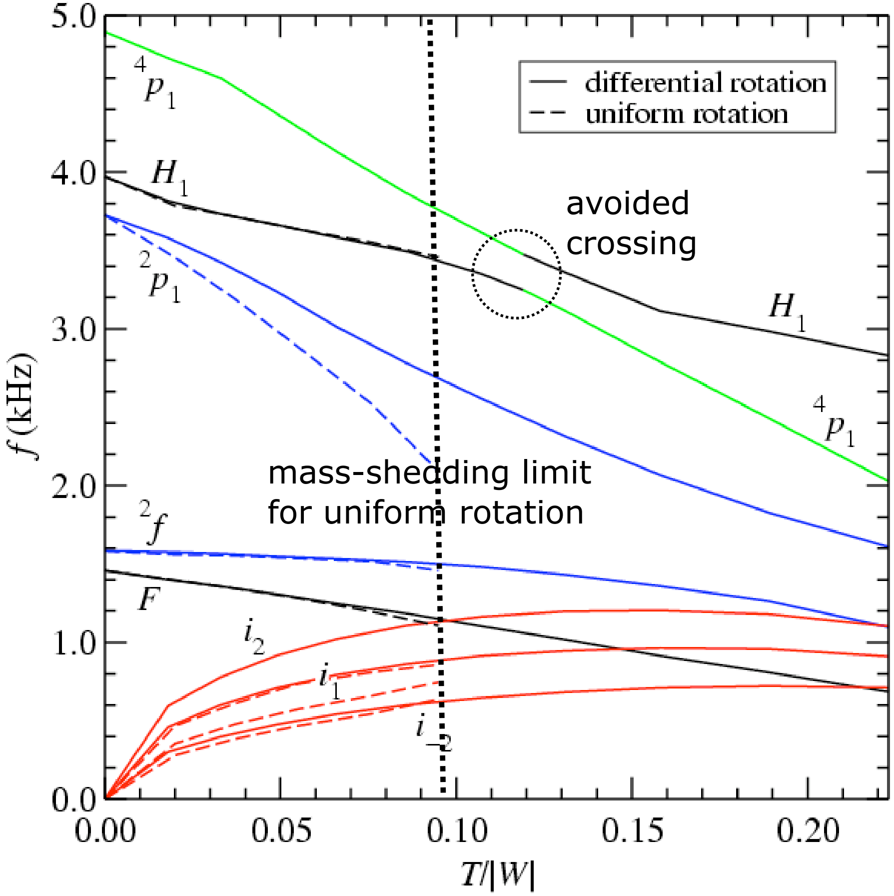

Strong rotation dependence of mode frequencies!

Example: 3D relativistic simulations of rotating NS collapse to a Kerr black hole

Baiotti, Hawke, Montero, Löffler, Rezzolla, Stergioulas, Font & Seidel, Phys. Rev. D, 2005, **75**, 024035

Simulation code Whisky developed at AEI, SISSA, AUTH, UV (www.eu-network.org)

Gravitational mass of secularly and dynamically unstable initial models vs central energy density

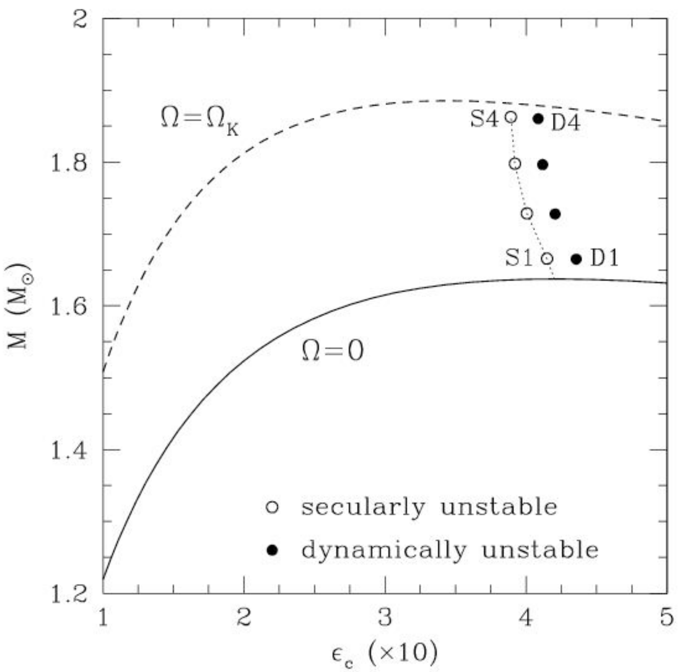

Evolution of model D4

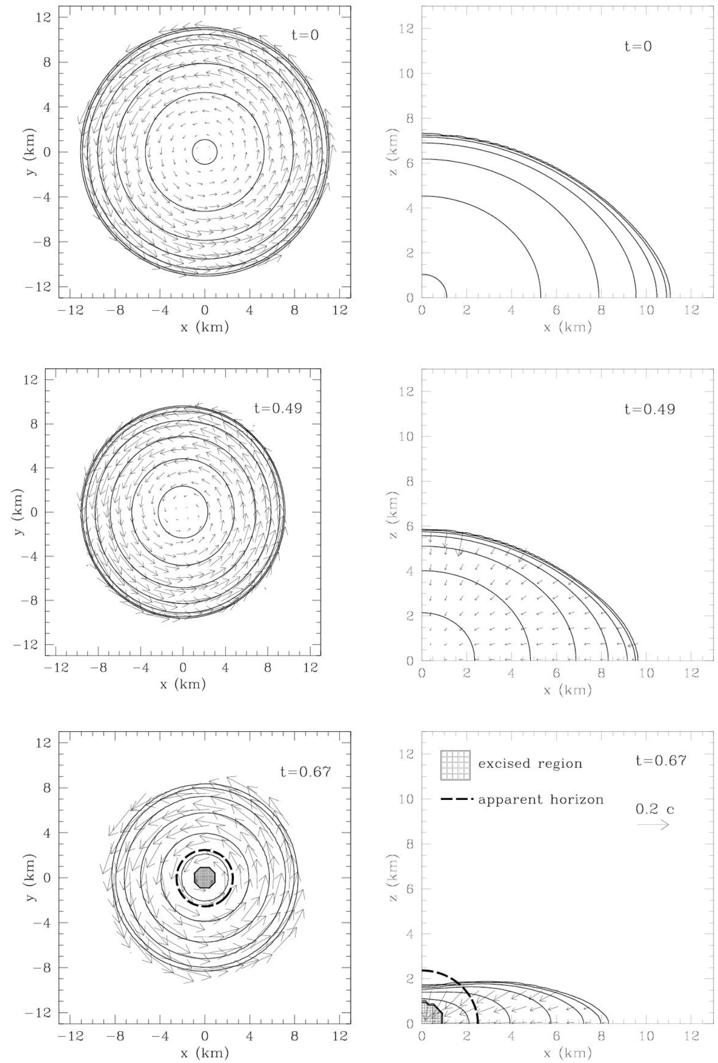

Solid line: sequence of non rotating models

Dashed line: models rotating at the mass-shedding limit

Dotted line: sequence of models at the onset of secular instability to axisymmetric perturbations

Calculating apparent and event horizons

Grey surface: event horizon. White surface: apparent horizon. Circles: horizon generators

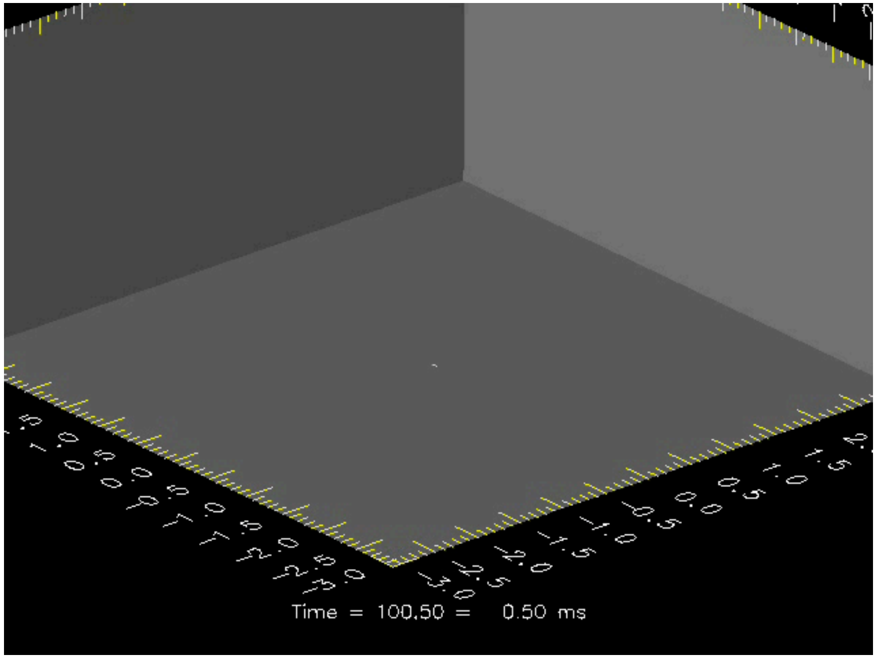

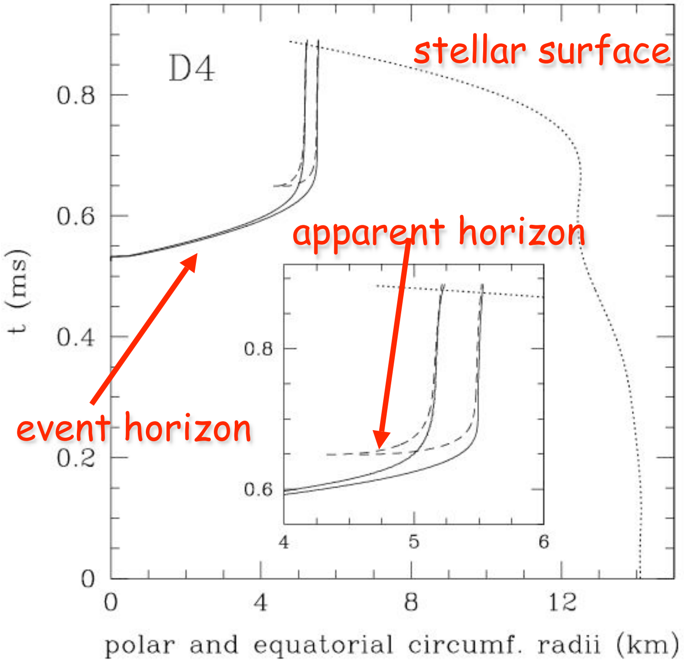

Calculations and visualization by P. Diener (AEI/LSU)

- As the collapse proceeds, trapped surfaces form (photons cannot leave).
- Most relevant surfaces are the apparent horizon (outermost of the trapped surfaces) and the event horizon (global null surface).
- AH can be computed at any time (zero expansion of a photon congruence). EH requires the construction of the whole spacetime.